C.1

LOS ALAMOS SCIENTIFIC LABORATORY
of the
University of California

LOS ALAMOS • NEW MEXICO

Description of the Kiwi-TNT Excursion and Related Experiments

(Title Unclassified)

[redacted]

This document [illegible] Atomic Energy Act of 1954. Its trans-
mittal or the disclosure of its [illegible] to an unauthorized person is prohibited.

[redacted]

[redacted]

All LA...MS reports are informal documents, usually prepared for a special purpose and primarily prepared for use within the Laboratory rather than for general distribution. This report has not been edited, reviewed, or verified for accuracy. All LA...MS reports express the views of the authors as of the time they were written and do not necessarily reflect the opinions of the Los Alamos Scientific Laboratory or the final opinion of the authors on the subject.

Printed in USA. Charge $3.45. Available from the U. S. Atomic Energy Commission, Technical Information Service Extension, P. O. Box 1001, Oak Ridge, Tennessee. Please direct to the same address inquiries covering the procurement of other classified AEC reports.

APPROVED FOR PUBLIC RELEASE

[redacted] LA-3350-MS
C-91, NUCLEAR REACTORS FOR ROCKET PROPULSION
M-3679 (45th Ed.)

LOS ALAMOS SCIENTIFIC LABORATORY
of the
University of California
LOS ALAMOS • NEW MEXICO

Report written: July 1966

Report distributed: August 19, 1966

Description of the Kiwi-TNT Excursion and Related Experiments

(Title Unclassified)

Compiled by

L. D. P. King
Donald Ackworth
W. U. Geer
C. A. Fenstermacher
B. W. Washburn
J. F. Weinbrecht

UNITED STATES
ATOMIC ENERGY COMMISSION
CONTRACT W-7405-ENG. 36

[redacted]

[redacted]

[redacted]

Abstract

A detailed description of the Kiwi Transient Nuclear Test (Kiwi-TNT) is presented in this report. Background information and the objectives of the test are discussed in Chapter 1. A discussion of the operations and test procedures at the Nuclear Rocket Development Station (NRDS) employed prior to, during, and after the excursion is presented in Chapter 2. A complete description of the Kiwi-TNT reactor is presented in Chapter 3 with an emphasis on the modifications used in the Kiwi-TNT reactor as compared with the normal Kiwi-B-4 design. A summary of all the test results is presented in Chapter 4. A large number of auxilary external experiments are described briefly in Chapter 5. These experiments were carried out to make use of the very large, short neutron and gamma ray burst. A number of power reactor fuels including numerous types of Rover "beaded" fuels were tested in this way in a flux region previously unattainable.

[redacted]

Acknowledgments

The material covered in this report represents the efforts of a large number of people associated with N, J, CMB, and H Divisions, and the Rover Flight Safety Office of the Los Alamos Scientific Laboratory. Support functions were performed by Pan American World Airways; Reynolds Electrical and Engineering Co., Inc.; ACF Industries, Inc.; Edgerton, Germeshausen and Grier, Inc.; Catalytic Construction Company; the U. S. Public Health Service; and the U. S. Weather Bureau.

Particular people associated with the preparation of this report are:

Chapter 1 and overall compilation and editing - L. D. P. King, Rover Flight Safety Office;

Chapter 2, "Operations and Test Description" - D. A. Ackworth, Group J-17;

Chapter 3, "Reactor Description" - John F. Weinbrecht, Group N-3;

Chapter 4, "Results of the Kiwi-TNT Experiment" - C. A. Fenstermacher, Group J-18, Beverly Washburn, Group J-18, and L. D. P. King, Rover Flight Safety Office;

Chapter 5, "Additional External Experiments" - W. U. Geer, Group N-2.

Table of Contents

[redacted]

[redacted]

[redacted]

Figures

[redacted]

Tables

UNCLASSIFIED

[redacted]

APPROVED FOR PUBLIC RELEASE

Chapter 1

INTRODUCTION

This report describes a full scale destructive excursion experiment using the Kiwi type of reactor which is being developed for the nuclear rocket propulsion program. The experiment was performed as a part of the Rover Flight Safety program of the Los Alamos Scientific Laboratory. The name chosen for this experiment was Kiwi-TNT which is an acronym for Transient Nuclear Test. Some preliminary reports have been prepared.[1,2]

A. Rover Flight Safety

Los Alamos has been engaged for several years in providing information which will contribute to an understanding of some of the nuclear rocket flight safety problems. An answer to the following questions was desired. (1) What is the probability, magnitude, and consequence of various types of potential launch pad accidents? (2) What is a satisfactory method of reactor disposal after operation in space?

The answer to the first question requires a complete understanding of the behavior of a Kiwi type reactor under abnormal or transient operating conditions as well as the determination of the resulting release and dispersion of fission products. An answer to the second question would be the complete fragmentation and dispersal of the core in space in a manner which would produce no public hazard on reentry of any particulate matter. The use of a nuclear excursion for such a purpose requires a detailed knowledge of fuel breakup during a large reactor excursion.

An extensive experimental and calculational program has been in progress at Los Alamos for several years which has sought to understand the reactor shutdown mechanisms and supply answers to these problem areas. Accidental excursions which have been studied include inadvertent control drum rotation, liquid propellant or water flooding of the core, core impact on the launch pad, and core implosion from a booster explosion. Several

[redacted]

calculational schemes are in progress to understand the detailed fragmentational behavior of Kiwi "beaded" fuel. Numerous fuel samples have been exposed to reactor burst facilities to obtain experimental data on the properties of such fuel in rapid transients. Only threshold data have been obtained by such means so far, since no facilities exist which can provide an adequate neutron flux in a sufficiently short time.

B. Why Kiwi-TNT

Sooner or later in all reactor programs which can involve the safety of the general public, government agencies seek to pin down the accuracy with which calculations can predict various types of accidents. Typical questions asked about any particular type of excursion are: (1) What is the total energy produced? (2) What fission products escape and how are they dispersed? (3) What is the kinetic or explosive energy release?

An analysis of the accuracy in the estimation of potential accidents at Los Alamos showed that the principal uncertainty lay in the lack of knowledge of the physical properties of the core materials under accidental conditions.

The Kiwi type of reactor is designed to run normally at temperatures in excess of 2200°C (4000°F). Under accidental conditions temperatures are expected to be in the 4000-4500°C region. Such temperatures are reached because a destructive shutdown mechanism requires the production of a substantial internal pressure. The Kiwi core materials will not produce disruptive vapor pressures without such extreme temperatures. Little was known about the physical properties and equation of state of graphite under the time-temperature-pressure conditions which are present in a large nuclear excursion. It has furthermore been impossible to achieve such conditions within the laboratory. The molecular species of the vapor produced from high temperature graphite systems is not well known. Vapor forms ranging from C_1 to C_{10} have been observed in experiments. Since the latent heat of vaporization varies considerably between molecular forms, it is evident that it is difficult in a rapid reactor excursion to predict accurately the fraction of the core vaporized and the kinetic energy released.

The only means of obtaining the necessary information on the reactor behavior under transient conditions is through a full scale reactor excursion. The well instrumented, carefully controlled Kiwi-TNT experiment was therefore carried out. It is only through such a test that a high confidence level can be attained in calculational estimates of potential accidents.

C. The Magnitude of the Kiwi-TNT Excursion

The size of the excursion desired was determined in advance as about

[redacted]

10^{21} fissions. This energy release was chosen to assure that there would be adequate energy available to vaporize at least a portion of the core, that sufficient fission products would be produced to permit refined fission product dispersion measurements to 25 miles, and that the total energy release would simulate reasonably well that of a maximum accident excursion.

D. Objectives

1. Primary

To supply experimental information on the total energy produced, the kinetic or explosive energy release, and the fission product dispersal from a maximum type of accidental reactor excursion. This information is of great importance to the Rover Flight Safety program since these results can be directly compared with theoretical predictions. Suitable parameters in such calculations can then be adjusted so that they match the experimental results. The prediction of any other type of accident can then be made with confidence since extrapolations and uncertain assumptions are eliminated.

2. Secondary

a. To supply experimental information on core fragmentation which is of interest to the Self Destruct Concept[3] of reactor disposal in space.

b. To supply information on decontamination problems, potential missile damage, and reactor component dispersal from an accidental excursion.

c. To supply a large short burst of neutrons to external sample experiments. This was of particular importance to power reactor and Rover type fuel studies since experimental results could be extended into a transient flux region hitherto unattainable by any other means.

E. Analysis of the Kiwi-TNT Results

The experimental results from the Kiwi-TNT excursion have provided the basic experimental information required for the general analysis of potential accidents of interest to the Rover Flight Safety program. A report, LA-3358-MS, "Safety Neutronics for Rover Reactors," describes a analysis and application of the Kiwi-TNT results to potential nuclear rocket accidents.[4]

Chapter 2

OPERATIONS AND TEST DESCRIPTION

A. Test Planning

1. Facilities Descriptions

The Kiwi-TNT was conducted on January 12, 1965, at a point 630 feet from the face of Test Cell C (TCC) at the Nuclear Reactor Development Center (NRDS). Figure 2-1 shows the general area. The reactor was mounted on a test cart positioned at the test point. The test point was located on top of a railway fill which crosses a dry wash near TCC, approximately 10,000 feet from the Control Point (CP). A concrete pad, 50 feet long by 30 feet wide, allowed working space around the cart. Instrumentation was routed through a bunker at the base of the fill, and data acquisition was performed with TCC equipment.

2. Reactor Cart

The TNT reactor cart was of special design to accommodate the reactor, the test equipment, and auxiliary irradiation experiments. The rod motion for the TNT excursion was provided by modified rod drive actuators supplied by two hydraulic accumulators mounted beneath the reactor. A 5 horsepower hydraulic pump mounted on the cart supplied the accumulators.

3. Reactor (at NRDS)

The TNT reactor (Figure 2-2) was composed of Kiwi-B-4D type fuel and was shimmed to provide a shutdown margin of approximately 0.60$. Additional shutdown margin was obtained by the use of two boral safing vanes inserted from above the reactor into the annular region between the reflector cylinder and the reflector. These vanes, covering 120° of the reactor perimeter, could be withdrawn remotely from

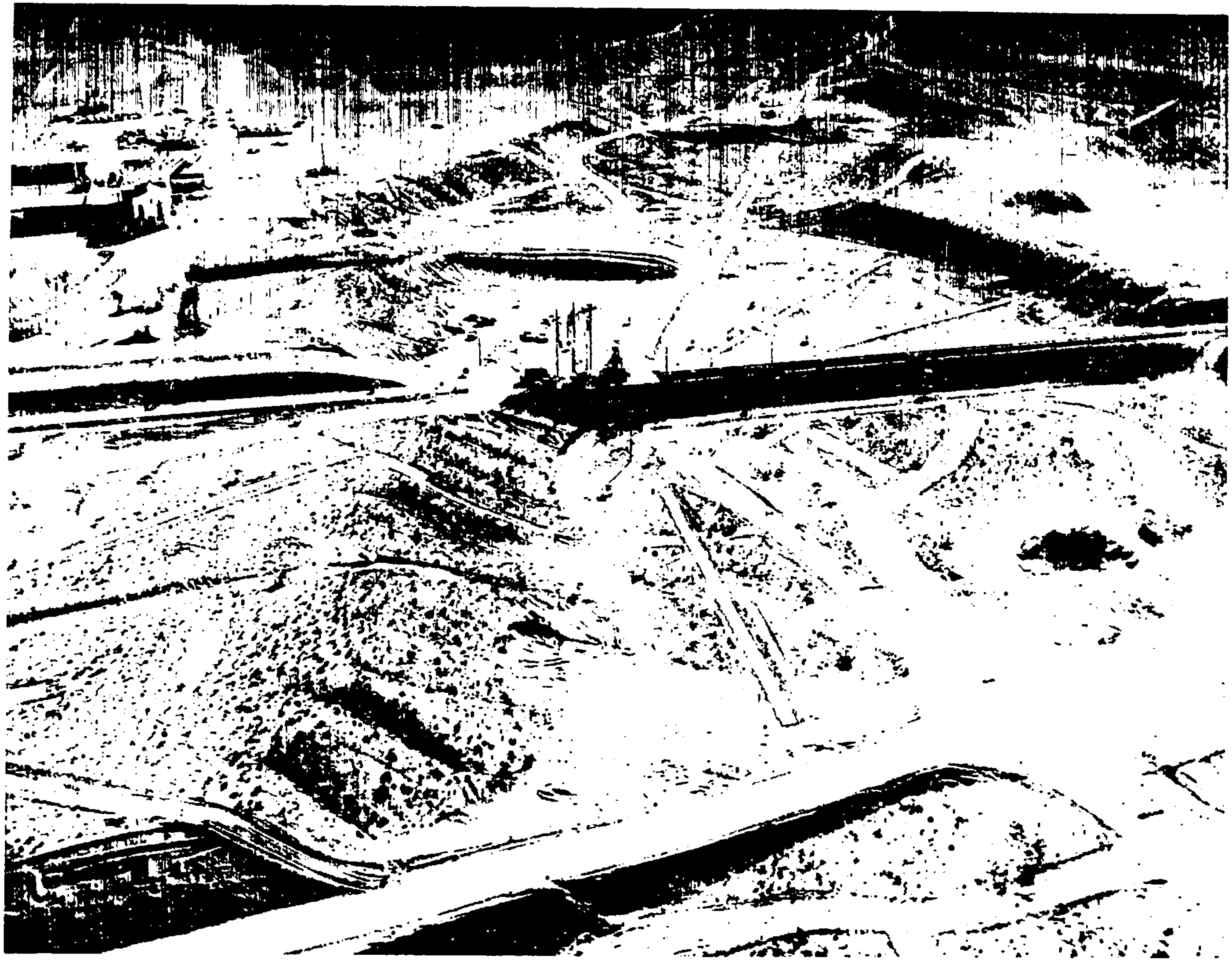

Figure 2-1. General Test Area Before Excursion

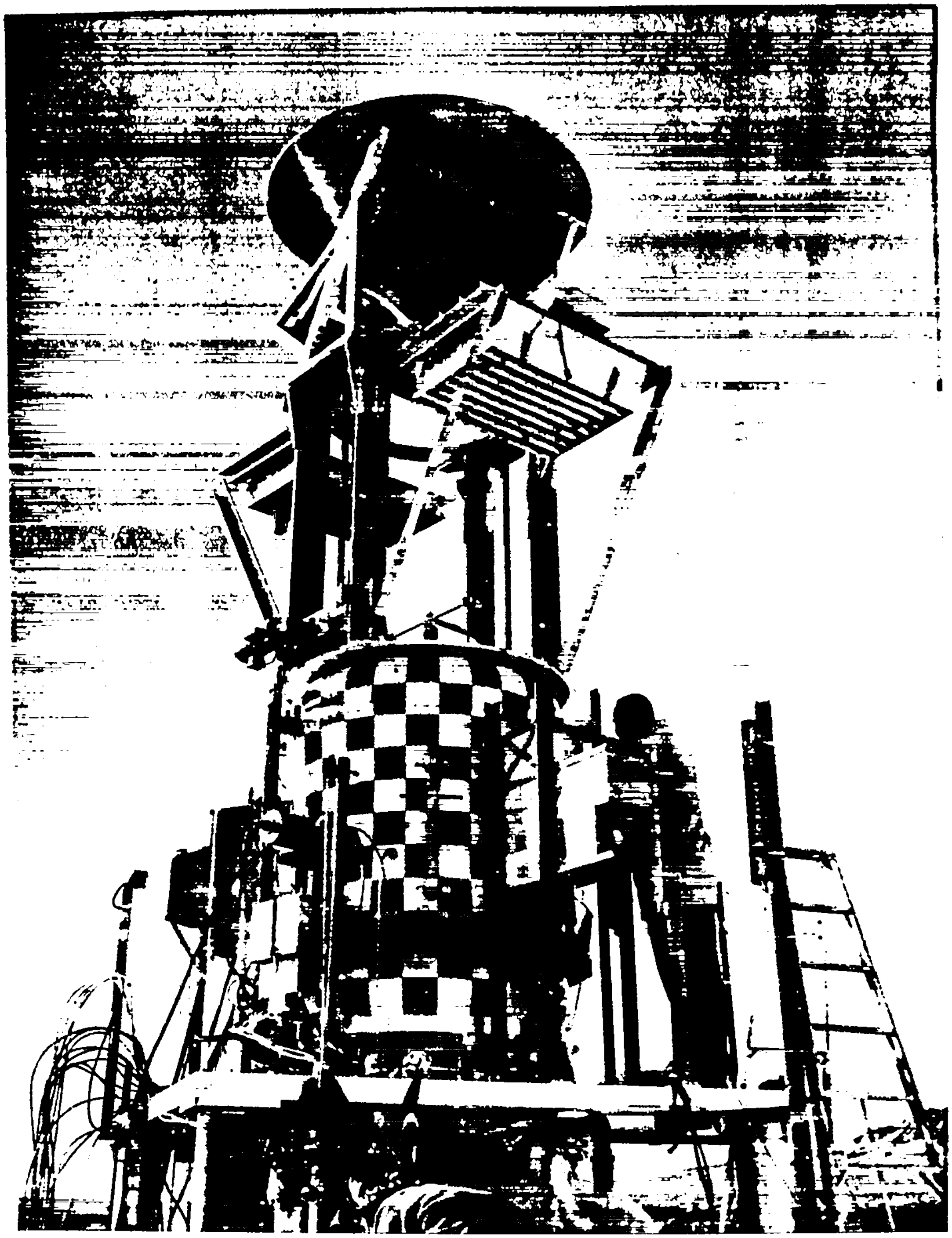

Figure 2-2. Reactor at Pad

UNCLASSIFIED

APPROVED FOR PUBLIC RELEASE

the CP. Until shortly before the test, additional safety was provided by cadmium strips in the remaining 240° sector.

4. Operational Procedures

The operational philosophy for the TNT was quite similar to that used on Kiwi tests, the salient points of which are covered here.

Pre-test setup calibration was performed using a written checklist. Each participating group was required to submit a written checklist to the test group for review well in advance of test days. These checklists were also used for preparing systems for the dry runs preceding the test.

All operations during the setup day preceding each test were formally controlled by a status board which consisted of members of the test group. In addition to approving the start of checklist items and deviations from submitted checklists, the status board controlled access to the test area.

Control room operations proceeded according to a written checklist prepared by members of the test group. All operations and monitoring functions, which were performed at the CP during the test, were coordinated by the test group by incorporation into the control room checklist. Control room operations fell into three major phases. The first involved checkout of the equipment by operation from the CP or by remote calibration. The second involved the arming of systems prior to the test. The final phase was the activation of the timing and firing sequencer with the appropriate Go/No-Go inputs activated. The completion of the timing and firing sequence resulted in the Kiwi-TNT control rod induced excursion.

B. Controls

1. Description of Chassis

Control of the TNT experiment was centered in the arming and firing chassis (Figure 2-3) which were mounted in the TNT control console. Commands from these chassis and responses to them were interchanged directly with some end item of equipment, and indirectly with others via one of three subcenters. The data confirm chassis, the photo distribution chassis (Figure 2-4), and the neutronics control chassis (Figure 2-5) served as subcenters for the various systems, distributing commands to the end items involved and collecting responses which were subsequently returned to the arming and firing chassis. Figure 2-6 is a signal flow diagram of the control system.

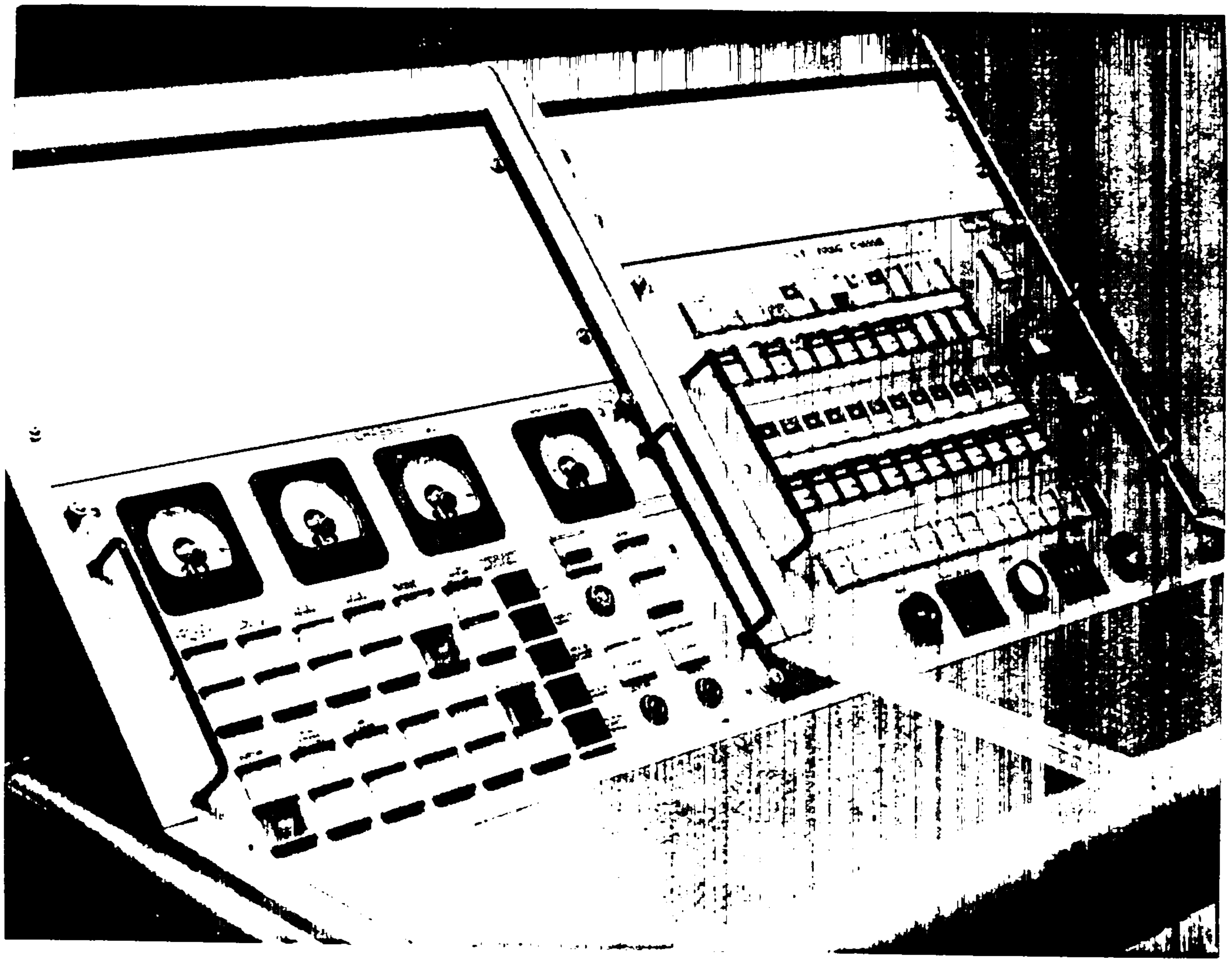

Figure 2-3. TNT Control Console

UNCLASSIFIED
APPROVED FOR PUBLIC RELEASE

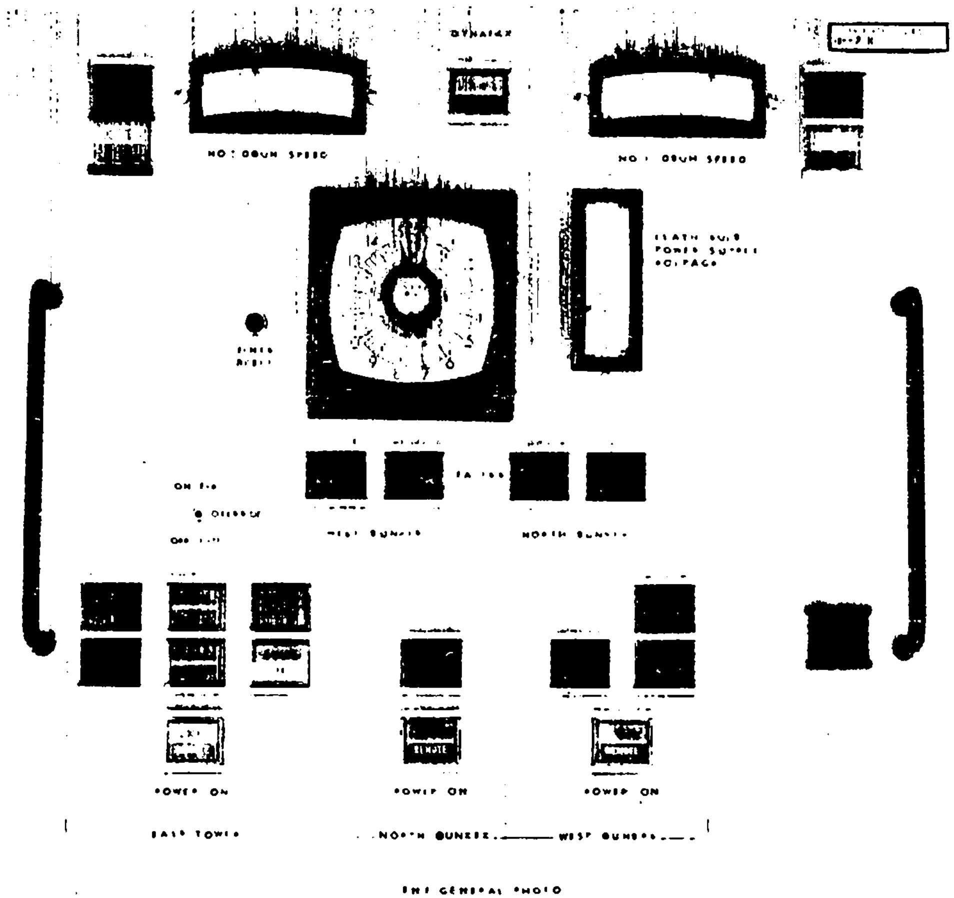

Figure 2-4. General Photo Panel

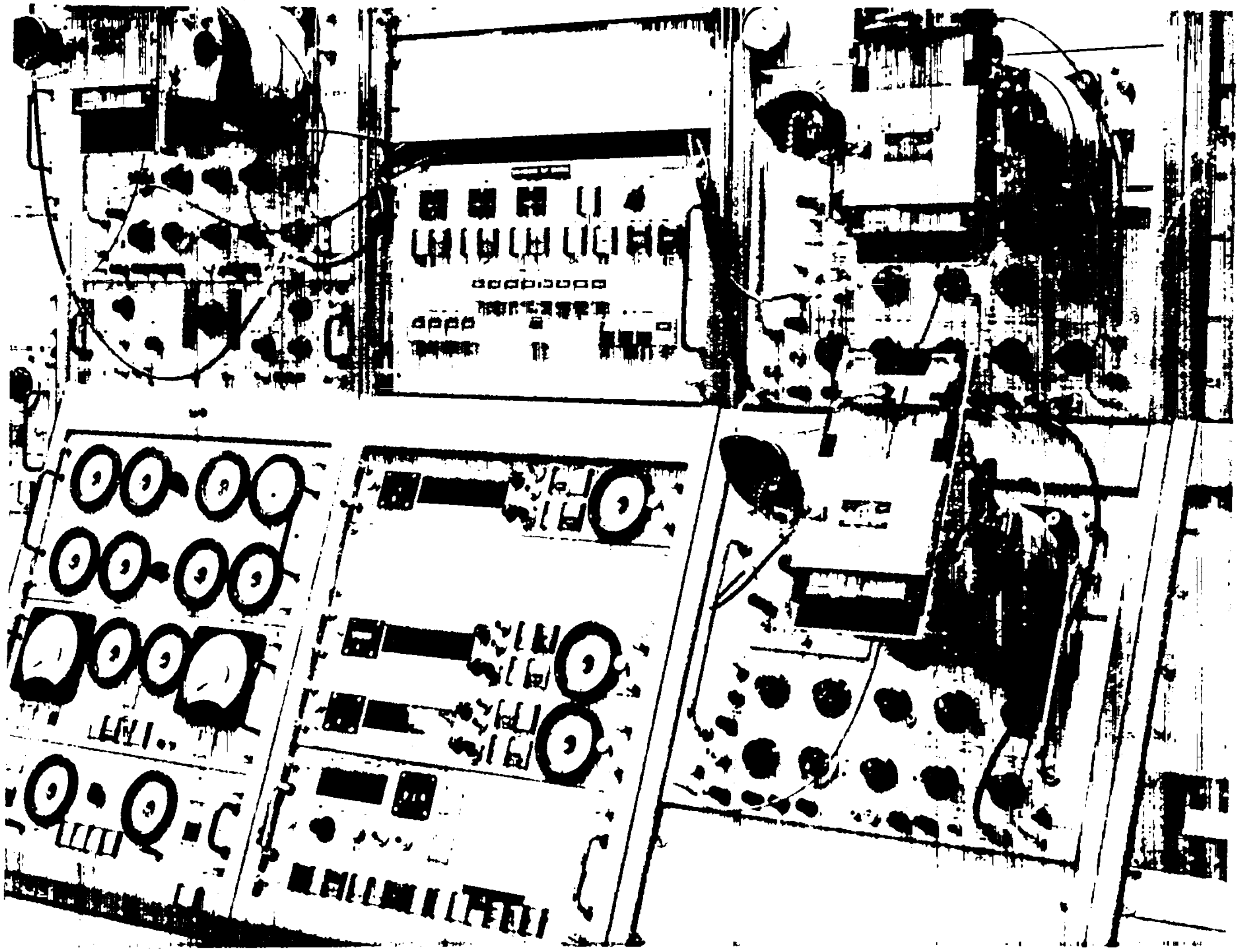

Figure 2-5. Neutronics CP Equipment

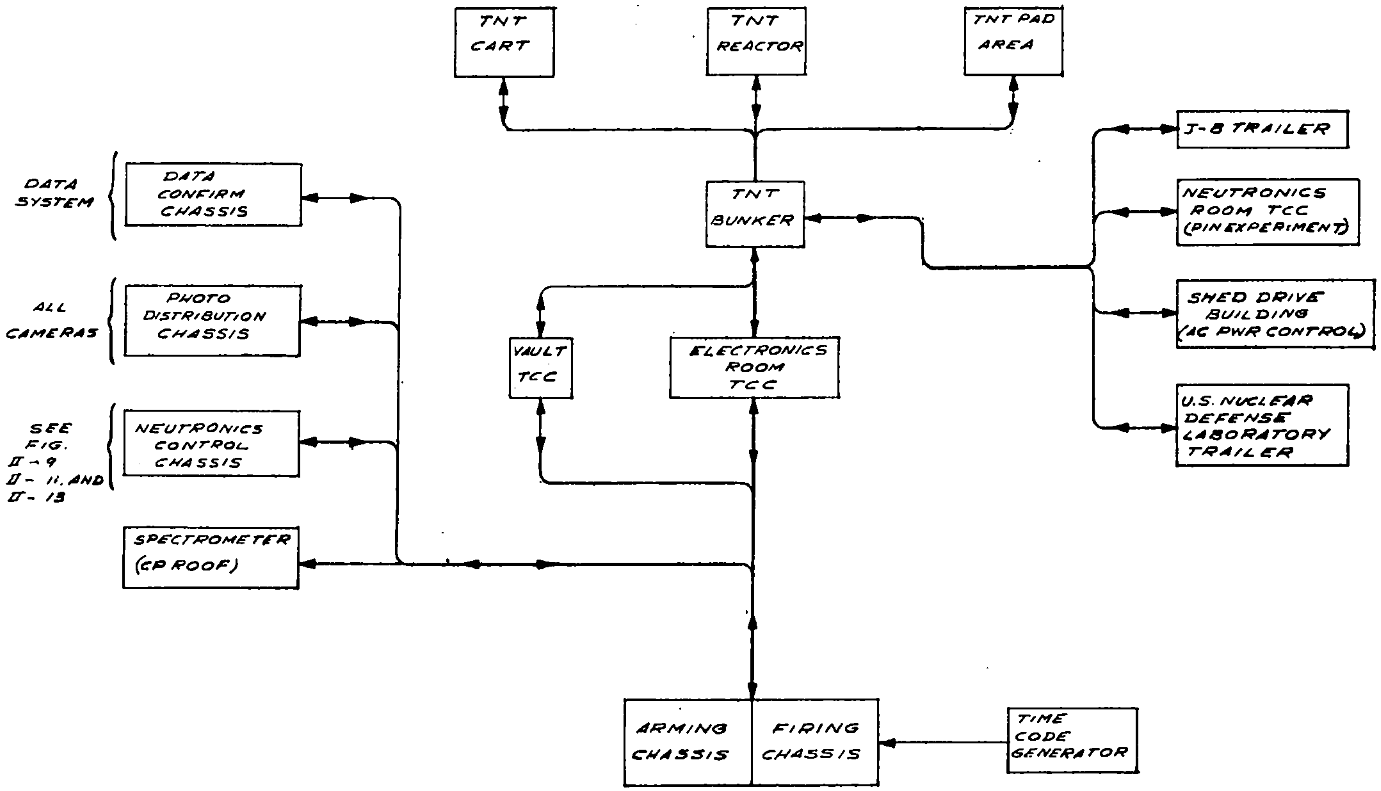

Figure 2-6. Control System Signal Flow Diagram

a. Arming Chassis

Functions which had to be handled prior to F-1 minute were, in general, assigned to the arming chassis. These functions were not extremely critical with respect to when they were executed or with respect to the allowable hold time. Push buttons which would illuminate to indicate the status of the item being controlled were used.

Meters were incorporated in the chassis to indicate the value of the following critical parameters: hydraulic sump level, hydraulic pressure, firing battery voltage, and poison vane position. Lights were used to indicate when the five master control switches had been thrown to transfer control of the experiment to the CP.

Key locks were inserted in the command lines for the poison vanes, cable cutter, and test fire circuit, to preclude inadvertent operation.

b. Firing Chassis

To initiate the firing sequence, the Chief Test Operator (CTO) depressed the Run button on the firing chassis. This started the sequencer which generated all commands from F-1 minute through firing (F-0) to F+1 second. The sequencer was designed to lock in with the base time system, thus placing the excursion at a time which simplified data reduction. Progress of the sequencer was indicated by 13 countdown lights, one of which illuminated at the end of each 5 second interval, and by a mechanical countdown timer which registered seconds to F-0.

As a prerequisite to initiating the countdown sequence, Go signals had to be received from nine critical areas. These signals were fed into relay logic circuits which inhibited the operation of the sequencer. Loss of any one of these Go signals, even momentarily, would cause the sequencer to stop before it issued the next command. The operation of the sequencer could be resumed from this hold position by depressing the Run button again. At any point in the countdown the CTO could stop the sequencer by depressing the manual Hold button.

A mechanical hold-time read-out was provided which indicated in seconds the length of time the sequencer had been in a hold condition. This was necessary because some items, once started, were operational for a very limited period of time.

Twelve countdown command lights were provided. Transmission of each command from the firing chassis was indicated by illumination of the appropriate light. Upon receipt of the command and execution of the required function, each end item returned a Go signal to the firing chassis. Receipt of these signals was also indicated by lights. Relay logic evaluated the Go signals received, and the sequencer automatically went into a hold condition when a required Go signal was not present or was lost. Table 2-1 is a list of firing instructions and Go/No-Go inputs.

Bypass switches were provided for each of the inhibit and countdown inputs. When an input was bypassed, the Go/No-Go logic was satisfied; and a Go input was not required from that specific end item.

Failure of either AC or DC power to the chassis was indicated by lights, and the system would automatically revert to a hold condition.

Key switches were provided in the fire and high speed camera command lines to prevent inadvertent operation.

2. Operational Capability and Flexibility

The equipment just described provided a wide range of operational flexibility. Separation of the arming and firing functions permitted extensive hold time for such things as weather, after the system had been placed in a state of readiness.

Incorporation of complete bypass capability permitted the CTO to proceed with the experiment even though a malfunction had been detected in some area. This judgment capability proved quite useful.

Even though the last 1 minute of the sequence was completely automatic, the CTO retained his ability to control the experiment through the use of the Run, Hold, and Abort circuits.

During the actual experiment it was deemed desirable to bypass certain noncritical countdown inputs. However, all equipment performed flawlessly.

TABLE 2-1

Firing Instructions and Go/No-Go Inputs

Item	Time	Command	Prerequisite
1	F-60 sec	Start tape recorders	Run button has been depressed. Hydraulic pressure within tolerance. Voltage of firing battery within tolerance. Neutronics oscilloscopes not fired. Gamma discriminator not triggered. All rod solenoids activated and rod position power supplies on. Neutronics power supplies on. Transducer excitation oscillator operating. 10 kc oscillator operating. Pin DC power applied. All 12 pneumatic pins are withdrawn.
2	F-60 sec	Start group I cameras	Same as #1
3	F-60 sec	Start tape recorders, (J-8)	Same as #1
4	F-60 sec	Start tape recorders, (J-12)	Same as #1
5	F-55 sec	---	
6	F-50 sec	Continue operation	Same as #1 plus data tape recorders running. J-8 tape recorders running.
7	F-45 sec	Continue operation	Same as #6 plus J-12 tape recorders running.
8	F-40 sec	---	
9	F-35 sec	---	
10	F-30 sec	Start group II cameras	Same as #7
11	F-25 sec	---	

TABLE 2-1, continued

Item	Time	Command	Prerequisite
12	F-20 sec	Continue operation	Same as #7 plus core Dynafax camera motors (2) running at proper speed and core flash bulb voltage within tolerance. Pin Dynafax camera motors running at proper speed.
13	F-15 sec	Continue operation	Same as #12 plus AC power line to bunker open.
14	F-10 sec	Start Milliken cameras	Same as #13 plus cloud cameras running, group I cameras running, group II cameras running.
15	F-10 sec	Start CEC tape recorders	Same as #14
16	F-5 sec	Continue operation	Same as #14 plus Milliken cameras running, CEC recorders running.
17	F-5 sec	Fire timing flash	Same as #16
18	F-1 sec	Open pin scope camera shutter	Same as #16
19	F-1 sec	Open neutronics scope camera shutter	Same as #16
20	F-1 sec	Turn N-1 heaters off	Same as #16
21	F-700 msec	Start Fastax cameras	Same as #16 plus neutronics oscilloscope camera shutter, pin Dynafax shutters open.
22	F-700 msec	Arm pin scopes	Same as #21
23	F-0	Command to open valves to rod actuators	Same as #21 plus Fastax cameras running. Pin scopes armed.
24	F-0	Fire hash mark	Same as #23
25	F-0	Timing and simulation	Same as #23
26	F-0	Timing (data)	Same as #23

[redacted]

TABLE 2-1, continued

Item	Time	Command	Prerequisite
27	F-0	Timing (J-8)	Same as #23
28	F-0	Timing (J-12)	Same as #23
29	F+1 sec	Close neutronics scope camera shutter	None
30	F+1 sec	Close pin scope camera shutter	None

[redacted]

C. Neutronics

1. System Description

a. Uncollimated Gamma Detectors

The majority of gamma profile data was obtained from six uncollimated photofluor detectors, two of which were located at pressure vessel contact (Figure 2-7), two at 24 feet (Figure 2-8), and two at 800 feet from the reactor. The two detectors at each location covered the same three to four decade range giving complete redundancy.

These detectors were modified Edgerton, Germeshausen and Grier, Inc. L24 detectors. Each canister contained a 6 inch cube of MEL 510 plastic fluor and two FW 127 photodiodes. The diodes were operated at 1,500 volts and were connected to the test cell recording system through approximately 800 feet of RG 8/U coaxial cable.

Power supplies for the detectors were located in the TCC penthouse. Additional capacitors on each detector were used to supply the charge necessary to maintain detector voltage. Total capacity for each detector was 16 millifarads.

The detector canisters were fitted with a section containing 23 photoflash bulbs. The bulbs were used to light the fluor and simulate a signal on dry run. Flash bulbs were selected by a stepping relay. Advance and fire commands came from the CP. Figure 2-9 shows a block diagram of the signal flow in the uncollimated gamma detector system.

The four close-in detectors covered a dynamic range of three decades each, and the two far out detectors covered a range of four decades each. Overall system coverage was from 10^{16} to slightly more than 10^{25} fissions per second.

The output of each detector developed a voltage across a 50 ohm terminating resistance. This voltage was routed to three or four inputs (one per decade) of an FM tape recording system using two Ampex FR 600 recorders. Amplifiers and attenuators were used to condition the signal to the 0.5 volt full scale channel level used. Diode clamps prevented the voltage controlled oscillators from deviating outside acceptable limits.

A total of 20 channels were used for the six uncollimated detectors. These data were recorded on two 14-track tape recorders. The voltage controlled oscillators and signal

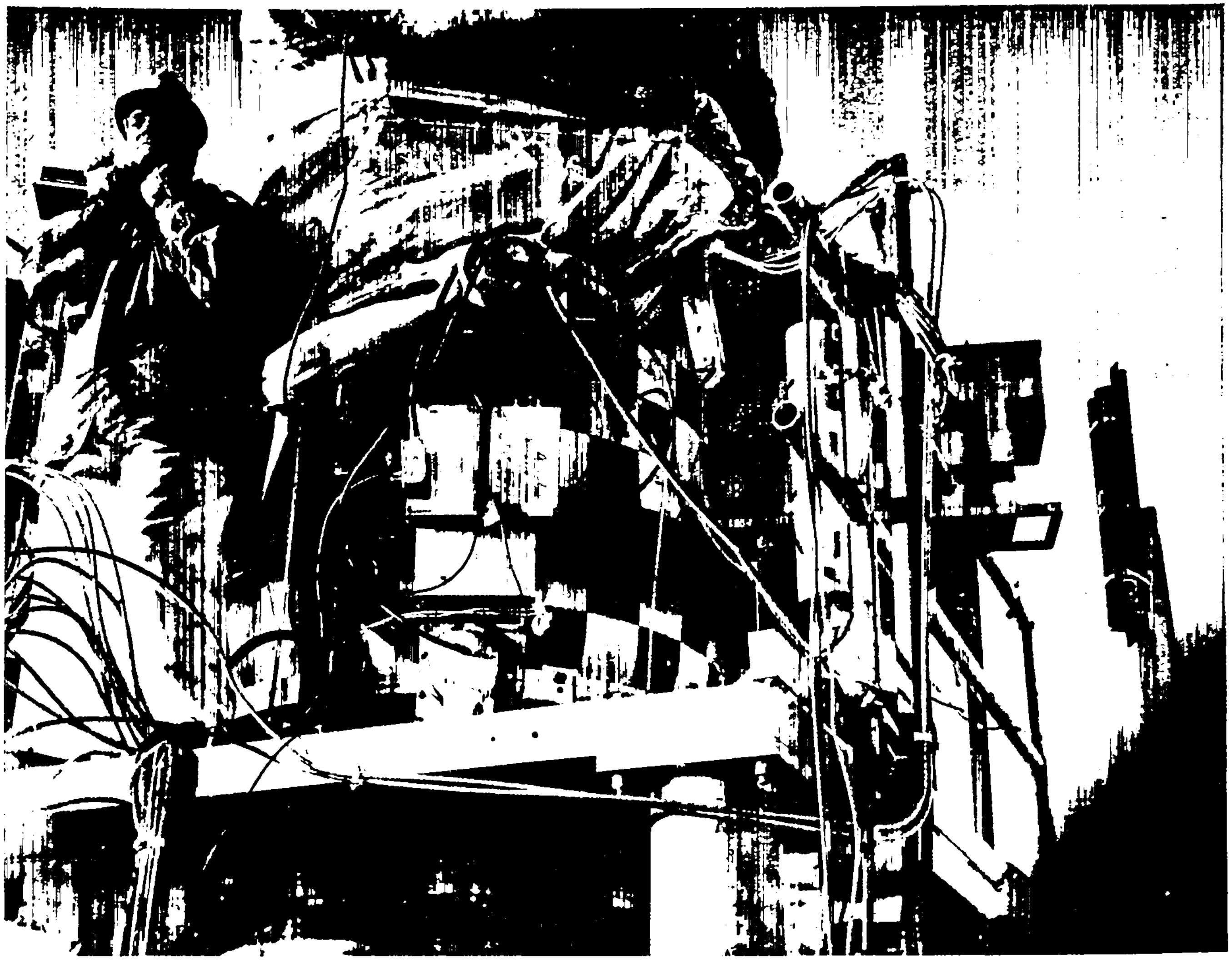

Figure 2-7. Gamma Detectors on Reactor

UNCLASSIFIED

APPROVED FOR PUBLIC RELEASE

[redacted]

SIFIED

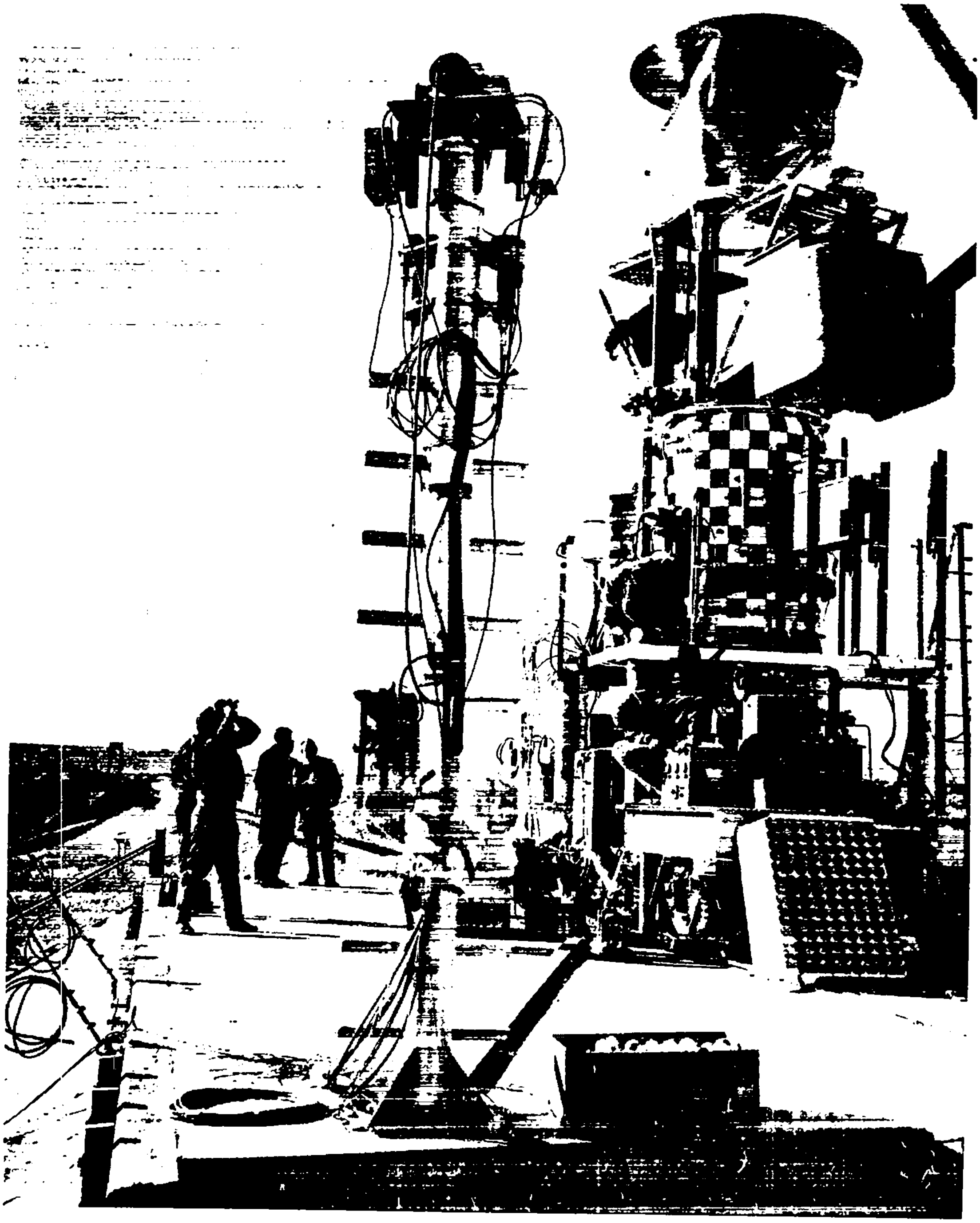

Figure 2-8. Gamma Detectors Twenty Four Feet from Reactor

[redacted]

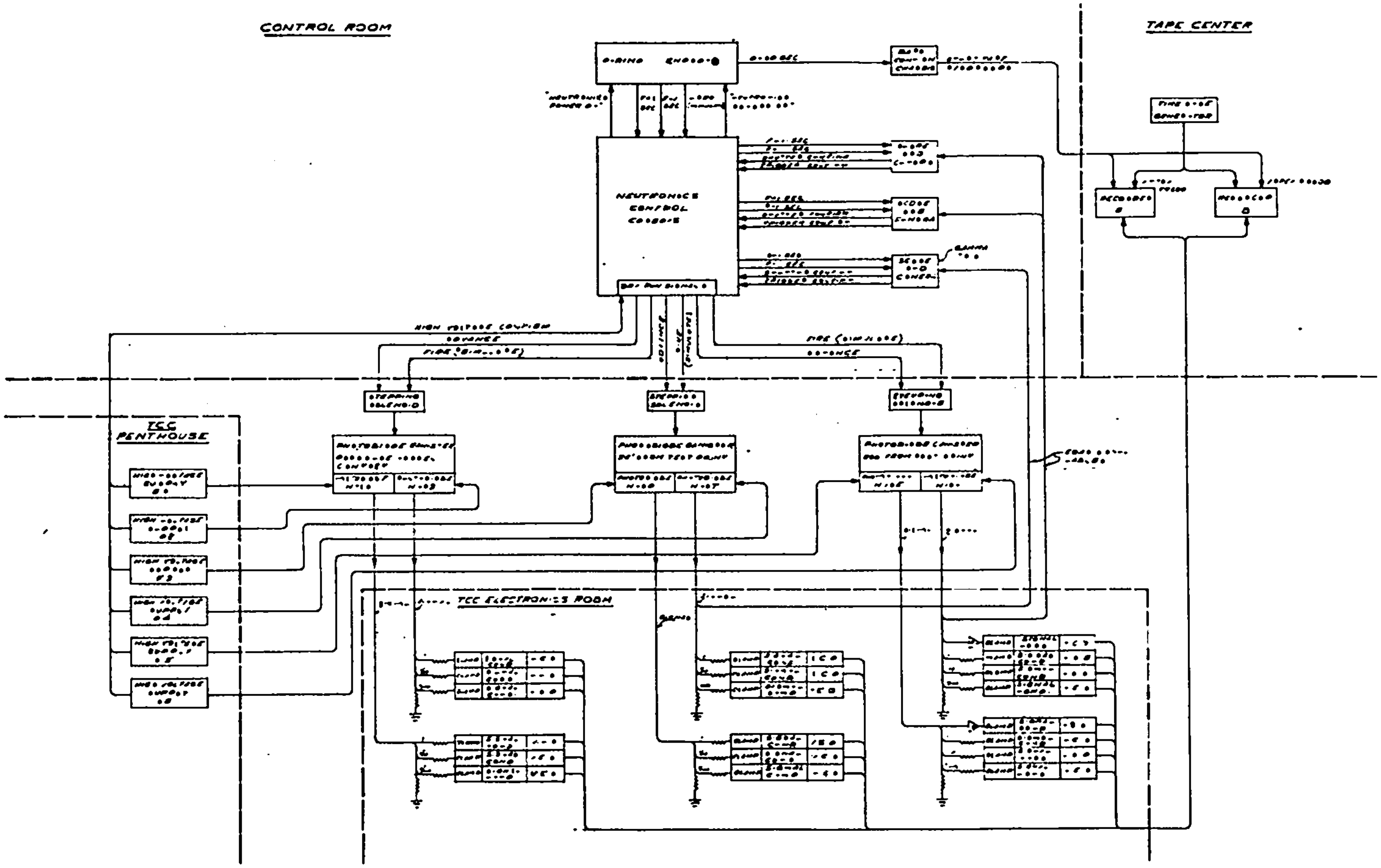

Figure 2-9. Uncollimated Gamma Detector Signal Flow Diagram

conditioners were located in the electronics room in the TCC basement. Tape recorders were located in the CP building. Normal voltage controlled oscillator units have a 108 kilocycle center frequency, but these were modified slightly so that 0 volts input resulted in a VCO output of 64.8 kilocycles. Tape recorders were run at 60 inches per second. Recording bandwidth was 20 kilocycles. A 100 kilocycle signal, which was an output of the frequency standard used to drive the time code generator, was imposed upon one track of each tape recorder.

The magnetic tape was played back for digitization using the 100 kilocycle signal as a data sample command for the digitizer/CDC 160A computer combination. The data were played back at one-eighth the recorded speed to enable the digitizer and CDC 160A to accept the high sampling rate.

Three Tektronix type 545 oscilloscopes and polaroid cameras were located in the control room to provide quick-look data (Figure 2-5). These worked well and gave good estimates of fission yield, peak rate, and time interval between the gamma trigger and the peak rate immediately after the test.

b. Gamma Trigger

A gamma trigger pulse was used to start core photography cameras and to trigger pin experiment, control room, and Compton detector oscilloscopes. This pulse was to be generated at 10^{15} fissions per second. Figure 2-10 shows a signal flow diagram of the gamma trigger system.

The signal was supplied by two NPM2B photomultiplier fluor detectors located at 24 feet from the reactor. Separate coaxial lines ran to a discriminator chassis in the TCC electronics room. Power to the photomultipliers was from separate 2 kilovolt supplies in the TCC penthouse.

The discriminator chassis was constructed using Philbrick type P65 and PP65 solid state operational amplifiers. The OR gate diodes were Fairchild FD100S. The silicon-controlled rectifiers were Solid State Products types 3B30S.

When a current from either of these detectors exceeded the trip level, the trigger pulse was generated. A premature trip from either discriminator circuit would produce a gamma discriminator trigger No-Go to the firing chassis. A small incandescent light bulb installed in each detector could be pulsed remotely to produce a trigger on dry runs.

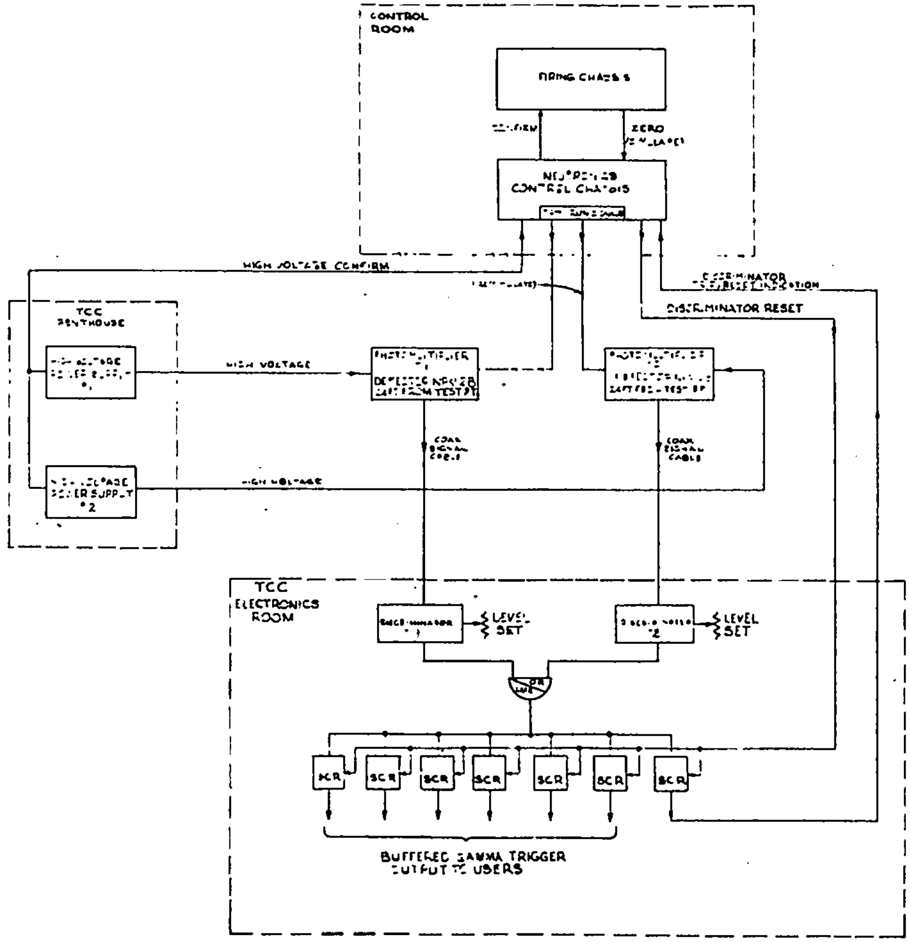

Figure 2-10. Gamma Trigger Signal Flow Diagram

UNCLASSIFIED
APPROVED FOR PUBLIC RELEASE
[redacted]

c. Other Detectors

A collimated gamma detector was located at 800 feet from the reactor (Figure 2-11). The field of view of this detector was restricted by two lead baffles to a 54 inch diameter circle centered on the reactor. This detector consisted of a 3 inch disc of MEL 150 plastic fluor and a FW114 photodiode. The detector has approximately 1/50 the sensitivity of the larger, uncollimated detectors. Its purpose was to see if gammas caused by neutron scattering contributed significantly to the shape of the pulse as seen by the uncollimated detectors. The collimated detector was expected to see only the peak. Data from this detector were recorded on two tape channels, essentially the same as the uncollimated detector data.

A fast neutron detector was also placed 800 feet from the TNT test point. This was a U^{238} fission chamber having a sensitivity of 1.5×10^{-28} coulombs per fission. Four decades of current were compressed onto a single channel through an Optical Electronics solid state log amplifier located in the TCC electronics room. Recording electronics were similar to that described for the other detectors. Figure 2-12 shows a signal flow diagram for the collimated and fast neutron detector channels.

d. Count Rate System

Three scalers and count rate meters were used in the control room for reactor multiplication monitoring and on those experimental plans that involved reactivity measurements. Amplifiers in the test cell were used to drive the 10,000 foot coaxial lines to the CP. These scalers were connected to the three output lines of a reactor safety monitor system while the reactor was on the pad.

The scalers were also used to count pulses from detectors used previously by N-2 at Pajarito Canyon. This equipment was used on an experimental plan whose objective was to compare the shutdown reactivity with that on the Kiva assembly.

The safety monitor was removed the day of the TNT test and the system was switched to monitor the output of two boron trifluoride detectors located at the test cell. The count rate system was monitored after boral vane withdrawal to insure that a rod had not stuck in the out position, and that the reactor was really subcritical for the test. This system would have been used, in the event the reactor did not completely come apart, to determine if any fissioning fragments remained. The count rate system was capable of detecting a reactor power level of 1 watt

Figure 2-11. Collimated Gamma Detector

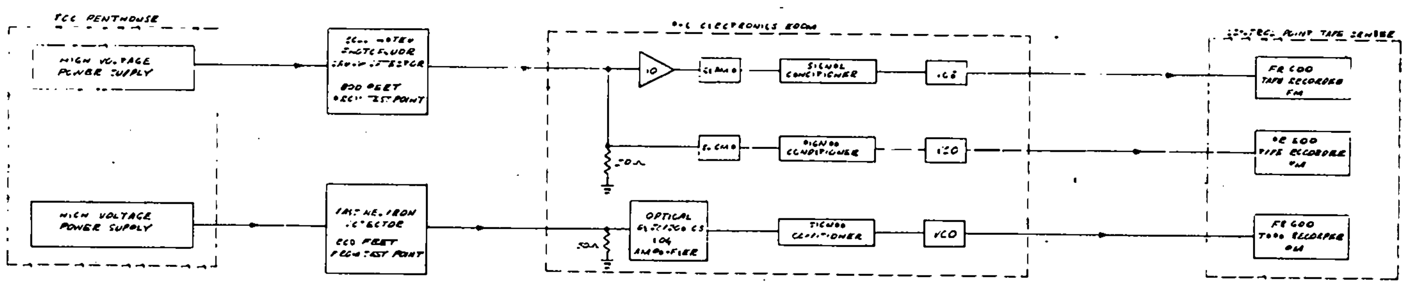

Figure 2-12. Signal Flow Diagram for Collimated and Fast Neutron Detectors

APPROVED FOR PUBLIC RELEASE

UNCLASSIFIED

at the TNT pad using the chambers at the test cell.

D. Instrumentation

1. Displacement and Pressure Measurements

Twenty pressure transducers and five displacement transducers were used to measure core pressures and displacements as well as blast pressures at various distances. The locations of the measurements follow:

a. Pressure Measurements Internal to the Pressure Vessel

Three active and three dummy variable reluctance (VR) transducers were located inside the pressure vessel. Four were at Station 10 in the core, and two were in the core inlet plenum.

b. Blast Pressure Measurements

Three active and two dummy transducers (VR) were located in the reactor midplane at a distance of 5 feet from the reactor centerline, and three active transducers (VR) were located in the midplane at a distance of 30 feet.

Six unbonded strain gauge pressure transducers were mounted at 100 feet from the reactor in the reactor midplane with an angular separation of 120°. Three units were Statham Instrument Co. Model PM6 transducers with a ± 0.5 psid range; the other three were Statham Model PM 732 pressure units scaled for ± 5 psid.

c. Displacement Measurements

Three active and two dummy displacement transducers were mounted on the pressure vessel to measure reflector to pressure vessel displacement.

All of the variable reluctance pressure and displacement transducers were manufactured by Physical Sciences Corporation. The pressure units were Model 1021 flush diaphragm transducers. The transducers inside the pressure vessel and those at 5 feet from the reactor center were modified to include a 20-foot-long rigid tube which carried the electrical leads and was evacuated and sealed to prevent ionized gas from shunting the electrical signals during the nuclear transient. The 20-foot evacuated leads were terminated in hermetically sealed connectors, which were joined to standard shielded cables in conduits buried in the earth. The connectors were placed a minimum of 4 feet below the surface of the ground.

Dummy transducers, modified to be insensitive to pressure, were included inside the pressure vessel and externally at 5 feet from the reactor centerline, to measure the effects of radiation on the pressure transducer sensing elements.

The variable reluctance transducers were all electrically connected to Physical Sciences Model 801-D AC carrier system demodulators operating at 20 kilocycles. The demodulators were all driven in synchronism by means of a 20 kilocycle square wave, crystal controlled generator. Since all the electronics circuits were transistorized, they were shielded by means of a tunnel dug horizontally from one wall of the bunker. The tunnel was covered by a minimum of 3 feet of earth. The demodulators, square wave generator, and automatic calibration circuits were all battery powered. The signals from the demodulators were conducted by underground shielded cable to TCC and connected to the standard data system there. Internal LASL memoranda describe the circuits, transducer specifications, and general considerations in transducer selection. A complete demodulator, oscillator, and transducer system was checked for response to transient nuclear radiation using the Sandia Corporation's Godiva reactor. The system exhibited about a 10% transient drop in sensitivity at approximately 20 times the gamma dose rates expected during the TNT transient.

Simultaneous failure of all variable reluctance pressure and displacement channels occurred just prior to the time of peak power in the Kiwi-TNT excursion. This was indicated by erratic full scale random oscillations of the output signal. All failures occurred at the same time and in the same manner even though the transducers themselves were in radiation fields differing by three to four orders of magnitude. This indicated that the cause of failure was due to the demodulator system.

An overheating problem in the shielded tunnel just prior to the excursion required the removal of some of the shielding to permit air circulation. It is believed that the removal of this shielding from the tunnel caused a higher than originally planned for radiation level which probably resulted in the instrumentation failure noted.

The unbonded strain gauge pressure transducers at 100 feet used DC excitation, and did not require any signal conditioning in the bunker. The cables from these transducers went directly to the TCC data system. The 100-foot transducers faced directly toward the reactor and had standard 0.25 inch flare fittings with no tubing attached.

Five of the six transducers produced useful signals in spite of transient nuclear and thermal radiation effects. All of the low range signals gave full scale deflection when the pressure pulse arrived.

2. Reactor Temperature Measurements

A total of ten thermocouples were used to measure reactor temperatures. The three different types and their uses are described below:

a. Two tungsten vs. tungsten, 26% rhenium (W/W26Re) thermocouples of standard construction with a relatively long response time were mounted at 00C-S26 and 210E4G-S26. Their purpose was to measure reactor temperature in the event of a low power fizzle.

b. Six fast response W/W26Re thermocouples were located in the core. Their locations and performance are indicated in Figure 4-8. Their purpose was to measure the neutron density a few decades before the power peak. They were not intended to measure the complete transient if its magnitude followed predictions.

The thermocouples contained an 80% niobium- 20% uranium-235 alloy tip approximately 0.3 inch long x 0.050 inch in diameter. One end of the tip had two 0.0005 inch diameter wires approximately 0.125 inch long, one of tungsten, the other of tungsten-26% rhenium attached to the alloy tip forming a thermocouple junction. The other end of the wires were attached to 0.010 inch diameter thermocouple wires contained in a stainless steel sheathed, magnesium oxide insulated cable. The tip and cable were supported by means of a stainless steel case approximately 0.007 inch thick attached to the end of the cable. Calculations of heat loss due to thermal radiation from the tip during a 1 millisecond period transient established that the error caused by thermal radiation is completely negligible up to 4000°F.

Because of the uranium loading the tip heated much faster than the case which surrounded the tip. The heating during the nuclear transient caused melting of the tip, and probably shunting of the thermocouple leads due to decrease of the resistivity of the magnesium-oxide cable insulation, and possibly shunting by ionizing nuclear radiations.

c. Two dummy thermocouples were built similar to the thermocouples in section b above, except that both of the thermocouple wires were tungsten. They were located at 00C-S26, and

210E4G-S26. No signal output was observed from these thermocouples until after the active thermocouples had started to fail.

The thermocouples described in sections b and c were fabricated by Physical Sciences Corporation according to their drawing #50551.

3. Pin Instrumentation

Early displacements of the reactor core and reflector cylinder were measured through a relatively small distance by a pin technique. Ten locations were instrumented with a group of seven pins at each location. Each pin within a group, when struck by the moving surface being monitored, produced an electrical pulse having a unique combination of polarity, decay time, and overshoot for purposes of identification. These pulses along with timing pulses were recorded by oscilloscope-streak camera combinations for primary acquisition at TCC (see Figure 2-13), and back-up recording was on magnetic tape at the CP. Twenty-one coaxial wire assemblies were inserted in selected propellant passages in the core as an experiment to determine the times of closure of these core passages. Signals produced by the collapse of these wires were similar in form to the pin signals and were recorded in the same way as the pin signals. A complete description of the pins, wires, circuits, and results may be found in LA-3388-MS, "Pin Techniques for Displacement Measurements in Kiwi-TNT."

4. Fireball Temperature Estimation

The radiation from the fireball was measured by two detectors located on the CP roof. The ratio of the detector signals was used to determine the temperature.

The detectors consisted of lead sulphide cells mounted behind an IR and a UV filter. The signal flow diagram is shown in Figure 2-14. The sensors were 10 x 10 millimeter Infratron lead sulfide cells purchased from Infrared Industries, Inc. The IR filter was an interference filter with a band pass at 10,400 Å and the UV filter was glass with a bandpass at 3,000 Å. A potential of 157 volts was supplied from two dry cell batteries. The signals from each detector were measured by a John Fluke Voltmeter during calibration and recorded on magnetic tape during the excursion.

The system was calibrated at two points by taking simultaneous readings on each detector, first viewing a sun gun with a Sylvania DWY lamp and then a carbon rod arc lamp with current supplied by a welding machine. There was no problem with the sun gun which appeared to generate constant radiation.

[redacted]

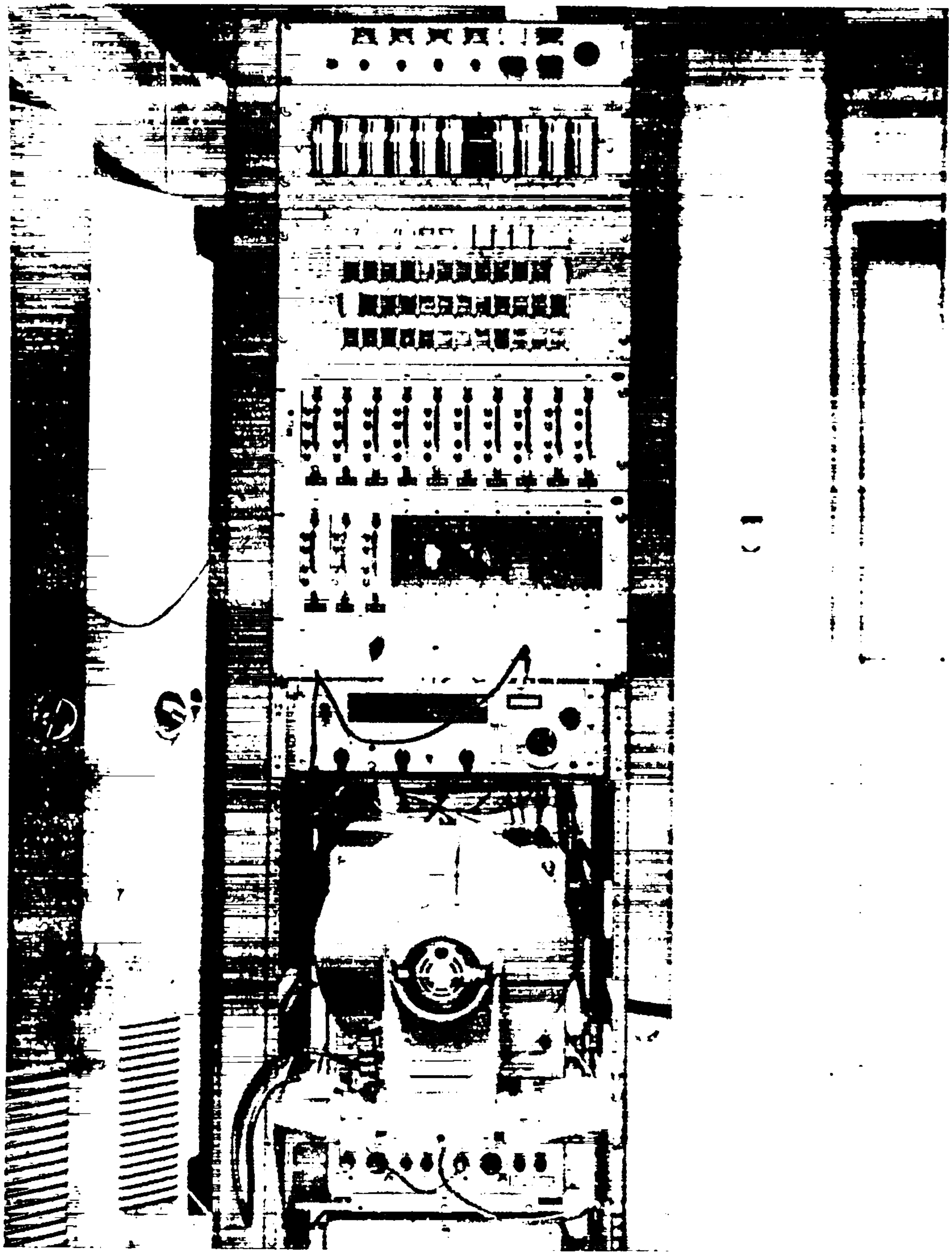

Figure 2-13. Control Panel, Oscilloscope-Streak Camera Combinations

[redacted]

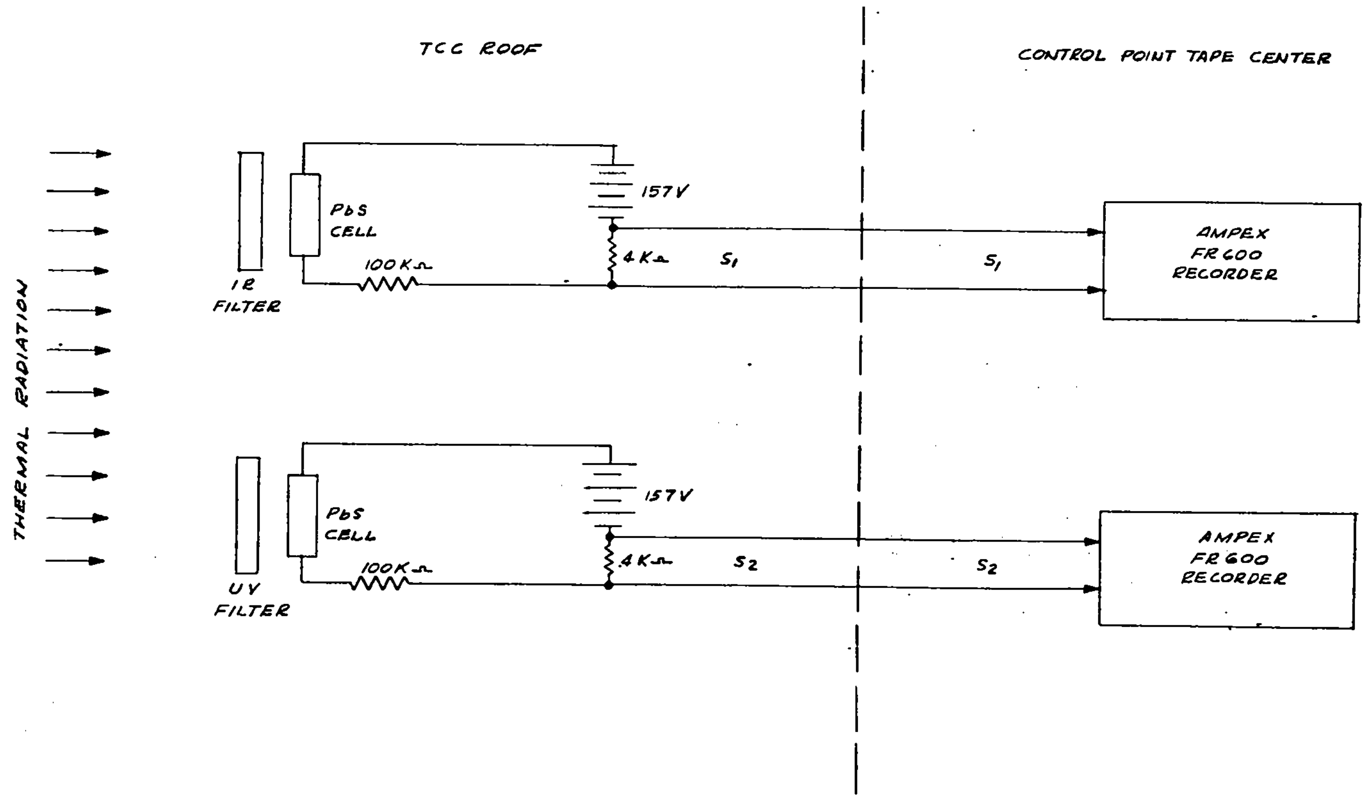

Figure 2-14. Signal Flow Diagram Fireball Temperature Estimate

The arc radiation used for calibration was in a direction at right angles to the plane of the two carbon rods. Difficulties were encountered because the output radiation from the arc varied. When the radiation stabilized momentarily, the detector output signal, in millivolts, and the arc potential and current were recorded. The signals measured from the two detectors were then adjusted to compensate for the difference in electrical power input into the arc at that moment. The ratio (S_1/S_2) for the two sources is shown in Figure 2-15.

This system of temperature measurement is based upon the following assumptions:

a. The fireball, sun gun, and carbon arc radiate thermal energy as a blackbody in the two bands used.

b. The signal level for each lead sulphide cell is proportional to the incident radiation in each band.

c. The ratio (S_1/S_2) of signals is a linear function of the absolute temperature of the source.

d. The thermal radiation from the carbon arc is directly proportional to the electrical power input.

e. The power factor of the carbon arc is unity.

f. The temperature of the carbon arc is 4,300°K. This is approximately the average of 4,200°C boiling point of carbon and a value of 4,200°K given in handbooks for the temperature of a carbon arc.

g. The temperature of the carbon arc is constant, even though the input power varies somewhat.

h. The temperature of the sun gun is 3,400°K, as rated by the manufacturer.

5. Data Processing

TNT data processing differed drastically from Kiwi data reduction since all TNT channels were wideband frequency multiplexed and continuous recorded rather than PAM time multiplexed. The requirements were for a sampling rate of 100 kilocycles in the neutronics channels and 10 kilocycles for all other wideband channels (pressure, temperature, and displacement), instead of the usual 40 samples per second. In order to process these data, some hardware changes had to be made in the analog to digital converter and some new programs written.

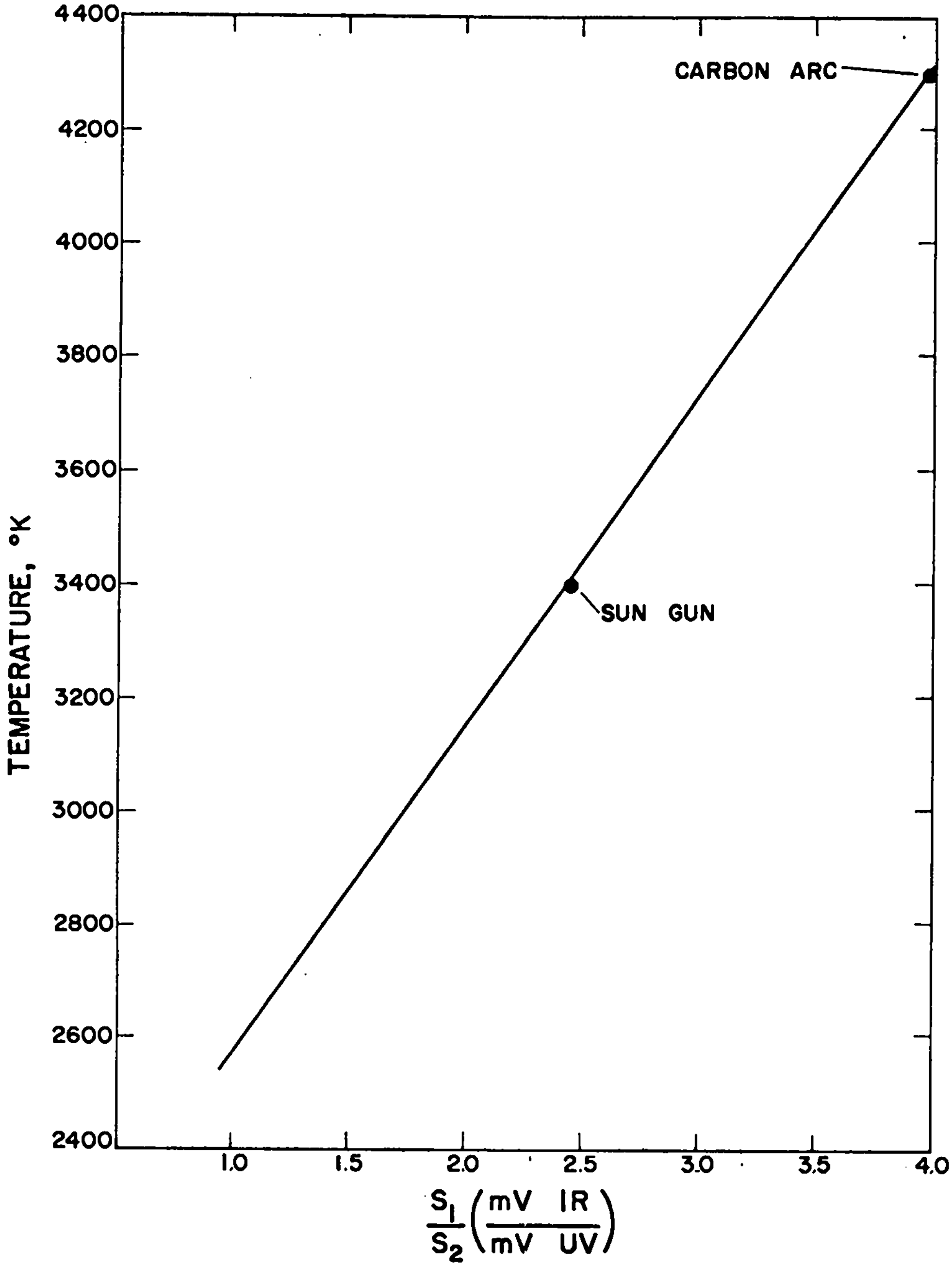

Figure 2-15. Temperature Calibration Curve, Lead Sulfide Detectors

The required digitizer modification consisted of the following:

a. Adaption of the sampling circuitry to enable it to use the 100 kilocycle tape speed compensation signal recorded on tape as a sample command. One track on each magnetic tape recorded had a 100 kilocycle signal from the timing system recorded by an Ampex direct record module. The 100 kilocycle signal was an output of the frequency standard used to drive the time code generator. As a result, this signal was phase and frequency coherent with all timing signals used in the TNT test. When the magnetic tape was played back for digitization, the 100 kilocycle signal was used as a data sample command in the Astrodata Digitizer/CDC 160 Computer combination.

The neutronics data were played back from magnetic tape recorders at one-eighth the recorded speed through Ampex FM reproduce units. This enabled the digitizer to sample the data signal at an equivalent 100 kilocycle sampling rate since the sampling command was the 100 kilocycle signal slowed down by a factor of one-eighth.

The balance of the wideband data (pressure, temperature, and displacement) were played back and digitized at the recorded speed. The 100 kilocycle signal was divided by ten by the digitizer and used as a sample command, thus yielding a 10 kilocycle sampling rate.

b. Changes to the time code translator to enable it to operate upon a time code signal played back at one-eighth the recorded speed. The time base provided for the digital data was derived by translating the magnetic tape playback 1 kilocycle modulated carrier time code in the digitizer. The digitizer time code translator detects axis crossings of the 1 kilocycle carrier and accumulates the axis crossings in a counter which is reset at the beginning of each second. The 1 kilocycle carrier thus acts as a millisecond time base. The 1 kilocycle carrier signal used in the modulated carrier time code is derived internally from the time code generator logic and hence is phase and frequency coherent with the 100 kilocycle sampling signal as well as the actual test time.

New programming requirements for TNT consisted of the following:

a. Modification to the high speed acquisition code to accommodate the 12.5 kilocycle data rate (12.5 kilocycles obtained from using the 100 kilocycle sampling signal with 8:1 tape slow down).

b. A new formatting code which translated and formatted digital data acquired in high density form to a low density format. The digital data were recorded on one of the CDC 160A computer tape units in high density form and later reformatted in low density form for entry into the IBM 704 which then operated upon the data, voltage calibration, and transducer calibration to produce plot tapes.

c. An IBM 704 code to convert the new formatted data to finished data plots. The code, which was especially prepared for TNT, performed a test of the consistency of the time code with the data sampling rate. This code used the full scale and zero scale calibration steps to establish the channel range. The data were then scaled within the range. For channels with nonlinear transducer calibration, a transducer calibration table was used which is accurate to 0.1% of the standard table over the channel range. The output of this code was a tape, formatted for one of the standard plotting codes.

Since time was only given to 1 millisecond accuracy once every 50 data points, the time put on the plots had to be generated internally. This generated time was compared to input time whenever it was available, and a summary of encountered errors was printed.

The time delays of the data channels and processing equipment were measured for typical neutronics, rods, and temperature channels. The following values were obtained:

Channel	Typical Channel Time Delay, msec
10 kc Sampling Rate	
Time	1.70
Rods Position	2.68*
Pressures	0.30 to 1.11**
Temperatures	
52 kc Carrier	0.99
70 kc Carrier	0.59
Displacements	0.59
100 kc Sampling Rate	
Time	1.42
Neutronics	0.14
Gamma Pulse	
Direct	0.016
Neutronics/FM	0.14

*Improved measurements in progress
**Dependent upon data channel utilized

[redacted]

6. <u>Photo Coverage</u>

The exposed hot end of the core was photographed from the north camera bunker through a large mirror mounted on the poison vane support structure (Figure 2-8). The visible graphite support blocks were painted white, and the core end was illuminated by 200 flash bulbs which were fired from a gamma pulse triggered at 10^{15} fissions per second. Two Dynafax cameras (Figure 2-16) with a 3 x 4 foot field of view were operated at 10,000 and 23,680 frames per second, respectively, to record initial lateral core motion.

High speed photo coverage of the excursion was provided by four Fastax cameras. A 4000 frames per second camera and a 2500 frames per second camera were located in each bunker and covered roughly a 100 x 40 foot field. There were also three 96 frames per second Mitchell cameras and a 400 frames per second Milliken camera located in the bunkers to provide general coverage (Figure 2-17).

Cloud photography and larger field of view pictures were obtained from cameras in the west tower, the east tower (Figure 2-18), the CP roof, the Reactor Maintenance and Disassembly (R-MAD) building roof, and a portable upwind station. The last three of these were manned stations. General orientation of photo stations can be seen from Figure 2-19.

The high speed photography gave some information on core disintegration and growth of the fireball. The first evidence of the motion is at the top of the core. The hot vapors first erupt out of the top of the core and then can be seen bursting out near the bottom of the pressure vessel.

Excellent color film was obtained of the cloud formation and its travel to 25,000 feet at an average azimuth of 300°. Its instantaneous height, azimuth, and velocity were plotted. Some of these results are discussed in Chapter 4. The film shows a stem of rising dust and debris during the initial stage connecting the upper portion of the cloud to the test pad. This stem is gradually dissipated (see Chapter 4, Figures 4-19 through 4-22). Effects of wind velocity and shear are also clearly visible and have been measured.

E. <u>Operations</u>

1. <u>Shutdown Reactivity Test</u>

The first safety test of the TNT device was conducted December 3, 1964. The primary objective of this test was to ensure that the reactor assembly was subcritical with all rods out and with the

[redacted]

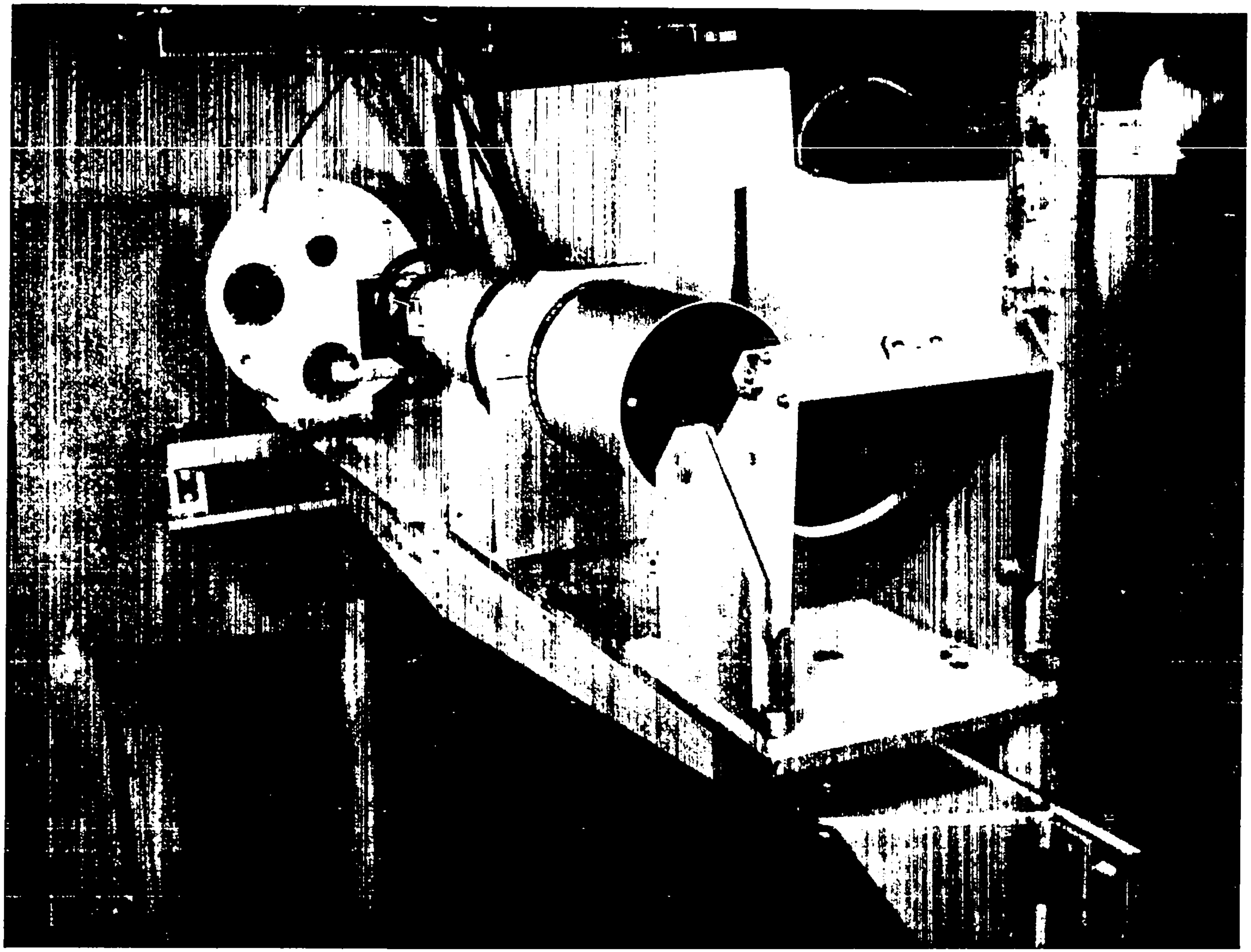

Figure 2-16. Core Dynafax Cameras in North Bunker

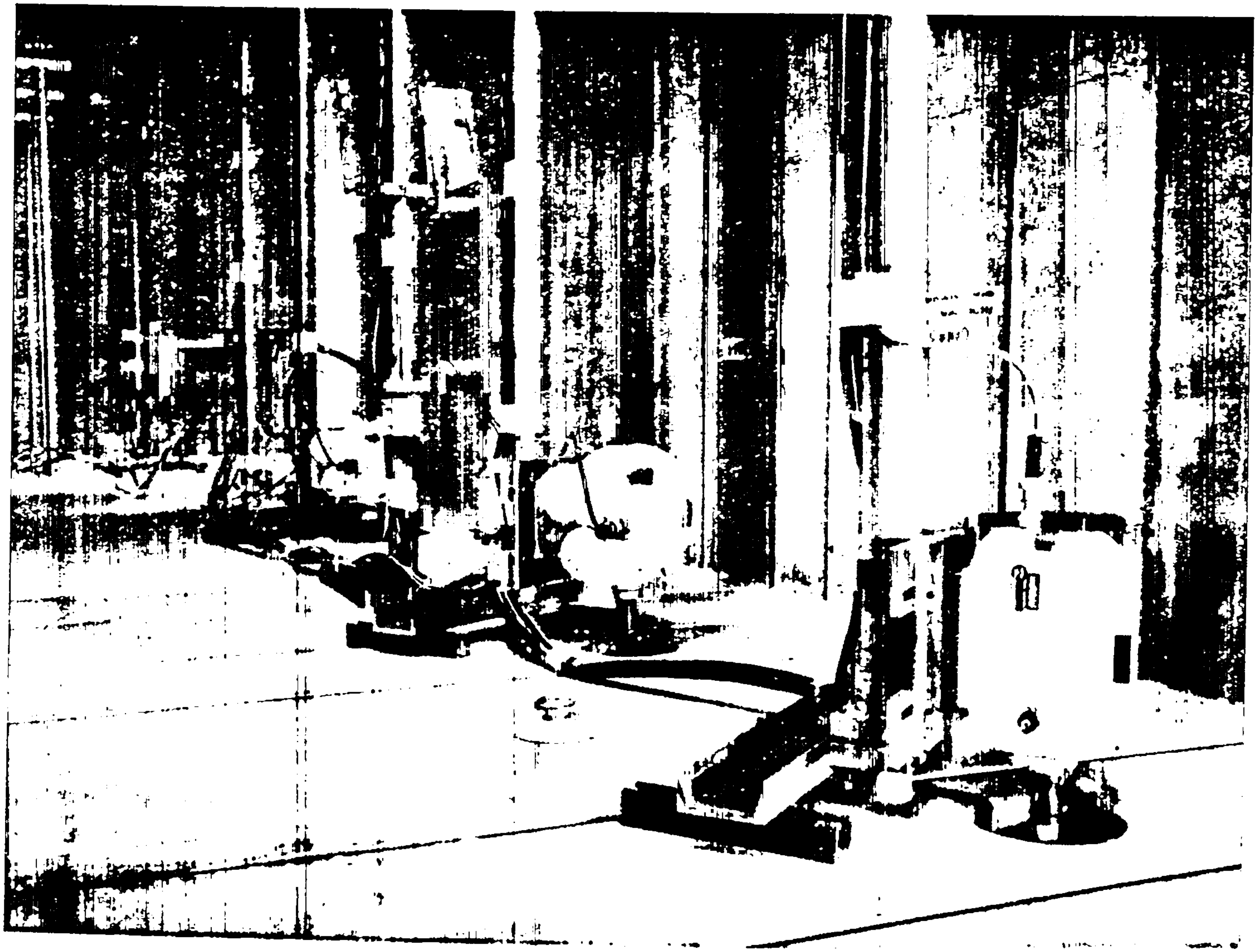

Figure 2-17. Mitchell and Milliken Cameras in West Bunker

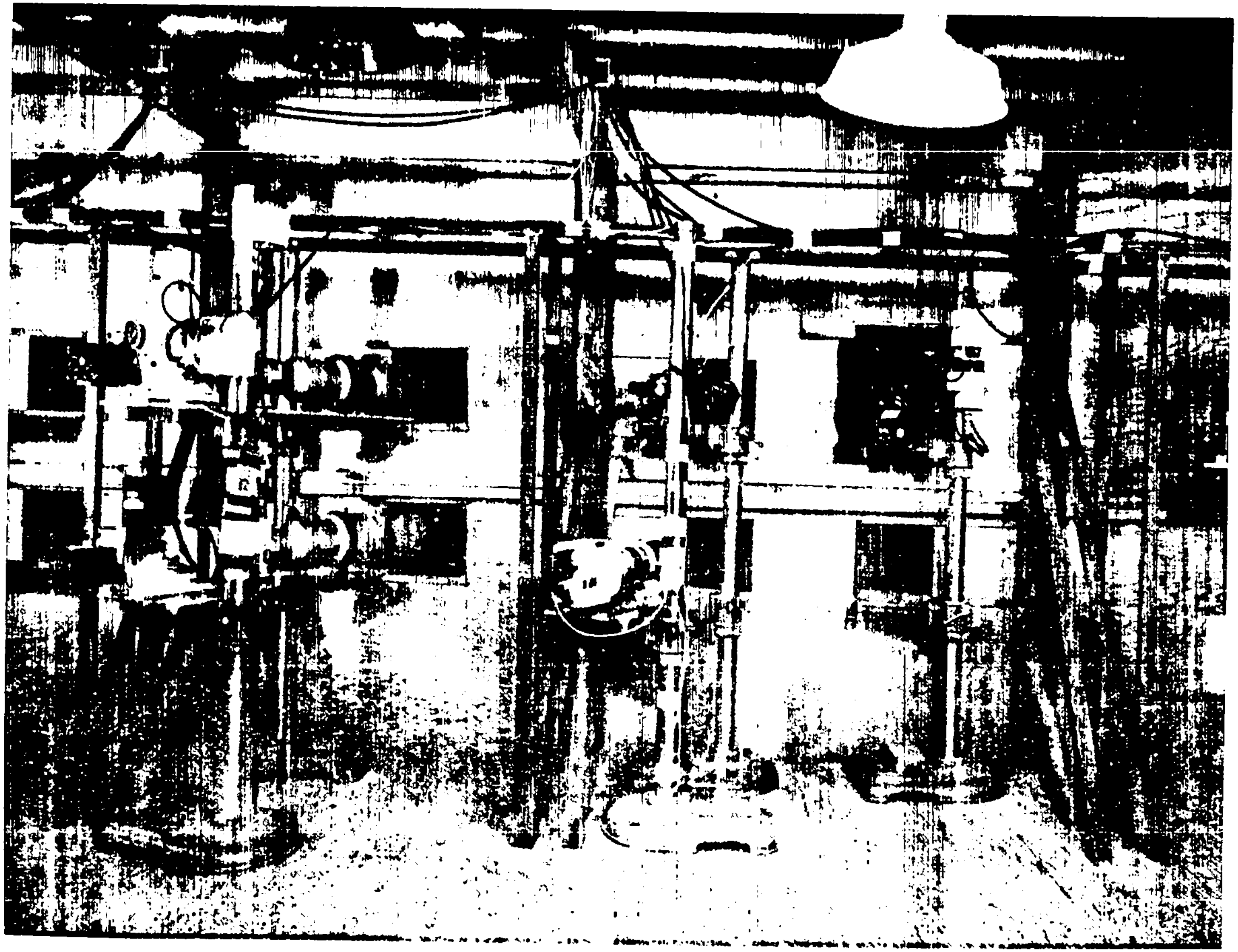

Figure 2-18. East Tower Cloud Cameras

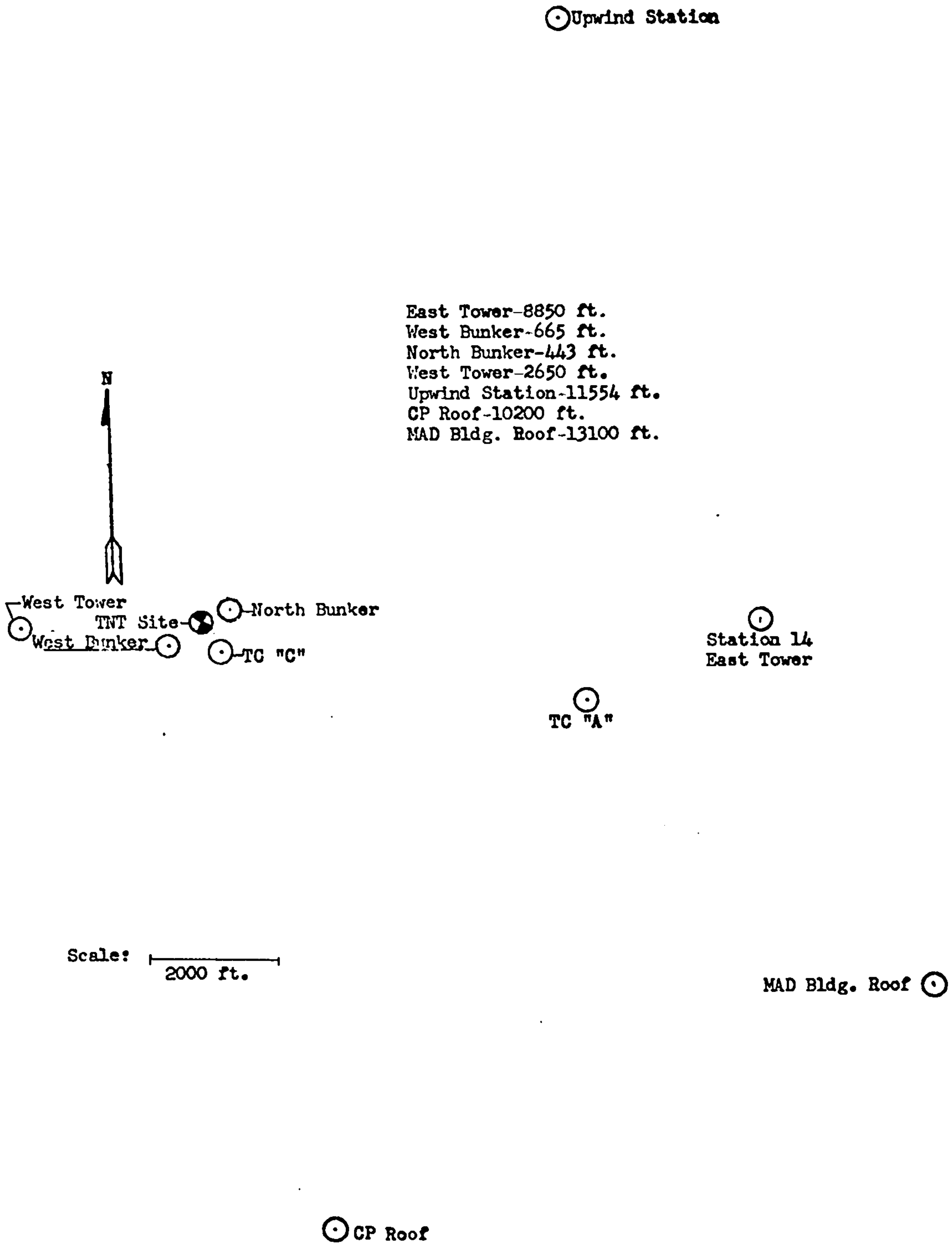

Figure 2-19. TNT Photo Stations

cadmium strips and boral vanes in place. The secondary objective was to see that each rod would follow a command from the CP and to measure simultaneity of rod motion. With the 40 cadmium strips in place, both boral vanes inserted, and the control rods out (180°), the shutdown reactivity was measured to be 5$. The checkout of the rods showed a 20 millisecond spread in reaching the 90° position. Work was started to reduce this value to below 10 milliseconds.

2. <u>Criticality Test</u>

On December 9, 1964, an operational check of the poison vanes was conducted. The objectives of this test were to check the operation of the vanes from the CP and to measure the reactor shutdown with the poison vanes out and the cadmium strips and control rods inserted. A lesser objective was a calibration of the poison vane position indication. In this configuration the reactor shutdown was approximately 5$. The time spread for the control rods reaching 90° was measured at less than 10 milliseconds on this test. This improvement was made by adjusting the electric delay circuits on each rod.

3. <u>Dry Runs</u>

The first TNT dry run took place on December 22, 1964. A number of circuit problems were incurred making it impossible to perform a complete dry run; however, these were corrected, and a complete dry run was performed December 23, 1964. Essentially all systems were operated, and some inconsistencies were discovered.

A formal dry run was conducted December 29, 1964, and involved all systems. Results were better than those obtained on previous dry runs. Most systems operated in a satisfactory manner. On January 6, 1965, the cadmium strips were removed and the shutdown reactivity was quite large. With the boral vanes withdrawn, and all control rods in, shutdown reactivity was measured at 0.60$.

A successful dry run was conducted on January 7 in preparation for a TNT test date of January 8, 1965; however, weather caused postponement of the test. Run status was held over the weekend of January 9 in the event weather was favorable and sampling aircraft were available. Another dry run was performed on January 10.

4. <u>Hot Run</u>

The nuclear excursion of the TNT device occurred at 10:57:45 a.m. PST, January 12, 1965. The excursion was within predicted limits, yielding 3.1×10^{20} total fissions. The minimum period was measured at 0.60 milliseconds with a peak fission rate of 1.1×10^{23}, and the full width at half-maximum was 2.4 milliseconds. The rod simultaneity to 90° was 6.5 milliseconds.

Chapter 3

REACTOR DESCRIPTION

A. Introduction

The Kiwi-TNT was a nuclear transient reactor having the same basic configuration and nuclear characteristics as the Kiwi-B-4E-301. The primary function of this reactor was to generate a nuclear transient of an appropriate order-of-magnitude for evaluation and study. No propellant was used.

To generate the desired amount of excess reactivity, the reactor core was adjusted or shimmed to a reactivity level closer to the delayed critical point than has been normal practice with the Kiwi nuclear propulsion reactors. Safe working conditions were ensured by providing a clear annular space between the core and the reflector cylinder. Poison strips or blades were inserted in this space to partially or completely surround the core as required during the work and check-out phases.

B. Design Considerations

To design a reactor for a destructive experiment such as the TNT excursion required a different philosophy than that normally used in nuclear reactor design. Flow, pressure, and temperature considerations were essentially eliminated. It was necessary to provide for a very rapid control drum movement, adjustable-after-assembly core poisoning, and installation of rather unique instrumentation and test evaluation devices; while retaining the basic geometry and nuclear characteristics of the Kiwi-B-4 reactor. It was desirable where possible to simplify fabrication of needed components, to substitute less expensive for costly materials, to use propulsion reactor reject parts such as fuel elements and support blocks, and to use obsolete on-hand components.

Figure 3-1 is a perspective of the Kiwi-TNT reactor and test cart. Figure 3-2 is a section view of the reactor assembly.

A detailed description of the Kiwi-B-4E-301 reactor is given elsewhere.[28] Only a few of the basic dimensions will be given here along with design changes and modifications pertinent to the Kiwi-TNT reactor.

C. Core

1. Core Dimensions

The basic core configuration and perimeter geometry remains unchanged. The reactor core was 35 inches in diameter and 53-1/2 inches long. The fueled region was 33-1/2 inches in diameter and 52 inches long. The core contained 1542 fueled elements and 259 unfueled elements.

2. Fuel Elements

The fuel consisted of pyrocoated uranium carbide beads admixed in a graphite matrix.

The fuel elements were hexagonal in cross section, 52 inches long, and approximately 3/4 inch across the flats. The element contained 19 cylindrical coolant channels or holes on a triangular array.

The fuel elements extruded particularly for the TNT reactor were uncoated. Those elements used that were rejects from propulsion reactor production lots (about 800) were coated with niobium carbide in the 19 coolant holes and for approximately 1 inch axially on the exterior surfaces of the hot end.

Twelve different types of elements were used to assemble the TNT core. By means of different uranium loadings or densities the radial power distribution in the reactor core was flattened as is normally done in the Kiwi nuclear propulsion reactors. Table 3-1 lists the types and number of fuel elements in the Kiwi-TNT core.

3. Clusters

The fuel elements were assembled into clusters for support and convenience of handling. There were 169 regular clusters made up of 6 fuel elements surrounding a central or support unfueled element. A graphite block supported the hot end of the assembly, and an aluminum cluster plate held the cold end of the assembly. Tips on the hot ends of the elements were located in recesses in the support blocks to position the elements at the hot end. An aluminum

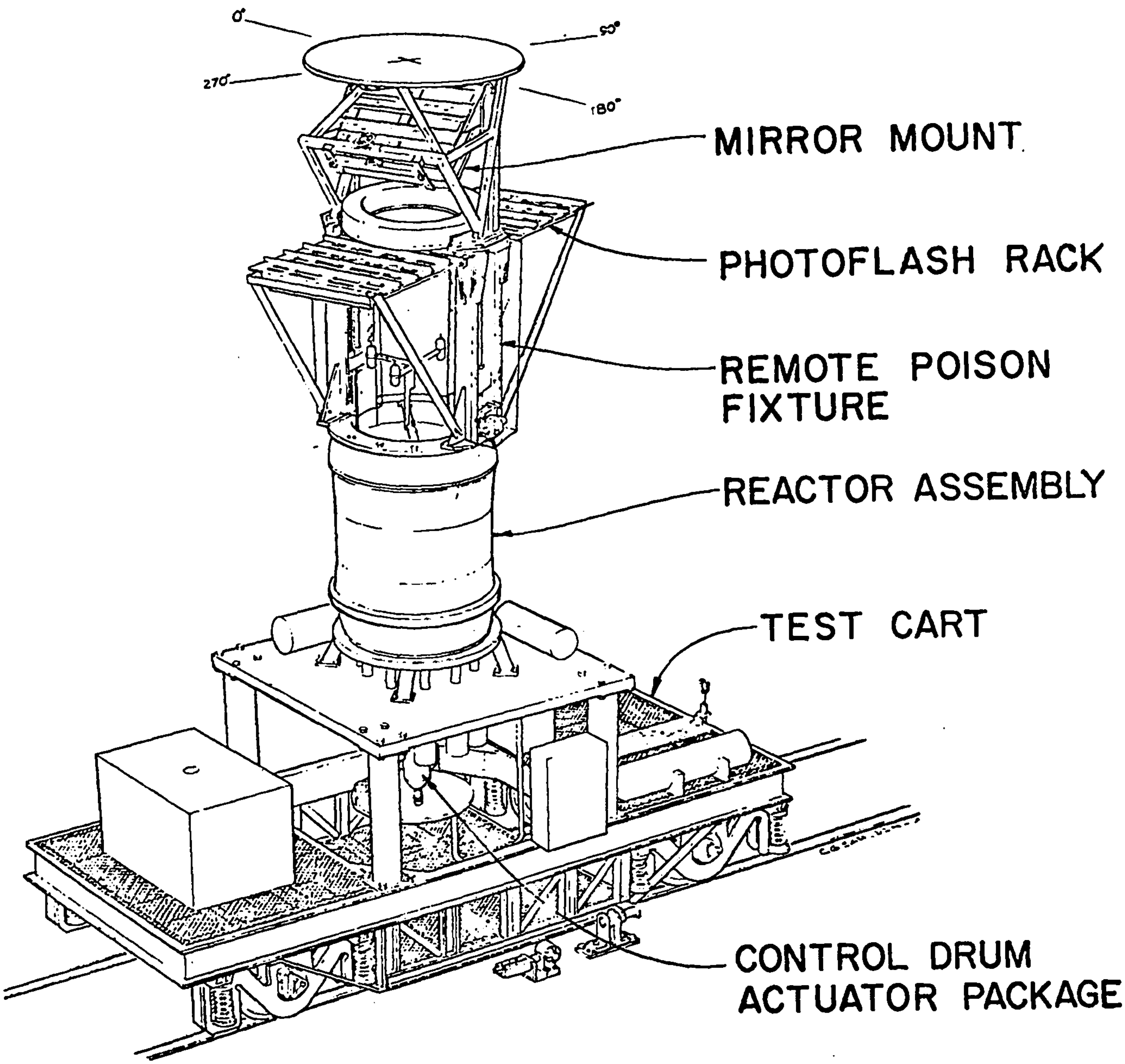

Figure 3-1. Kiwi-TNT/Perspective

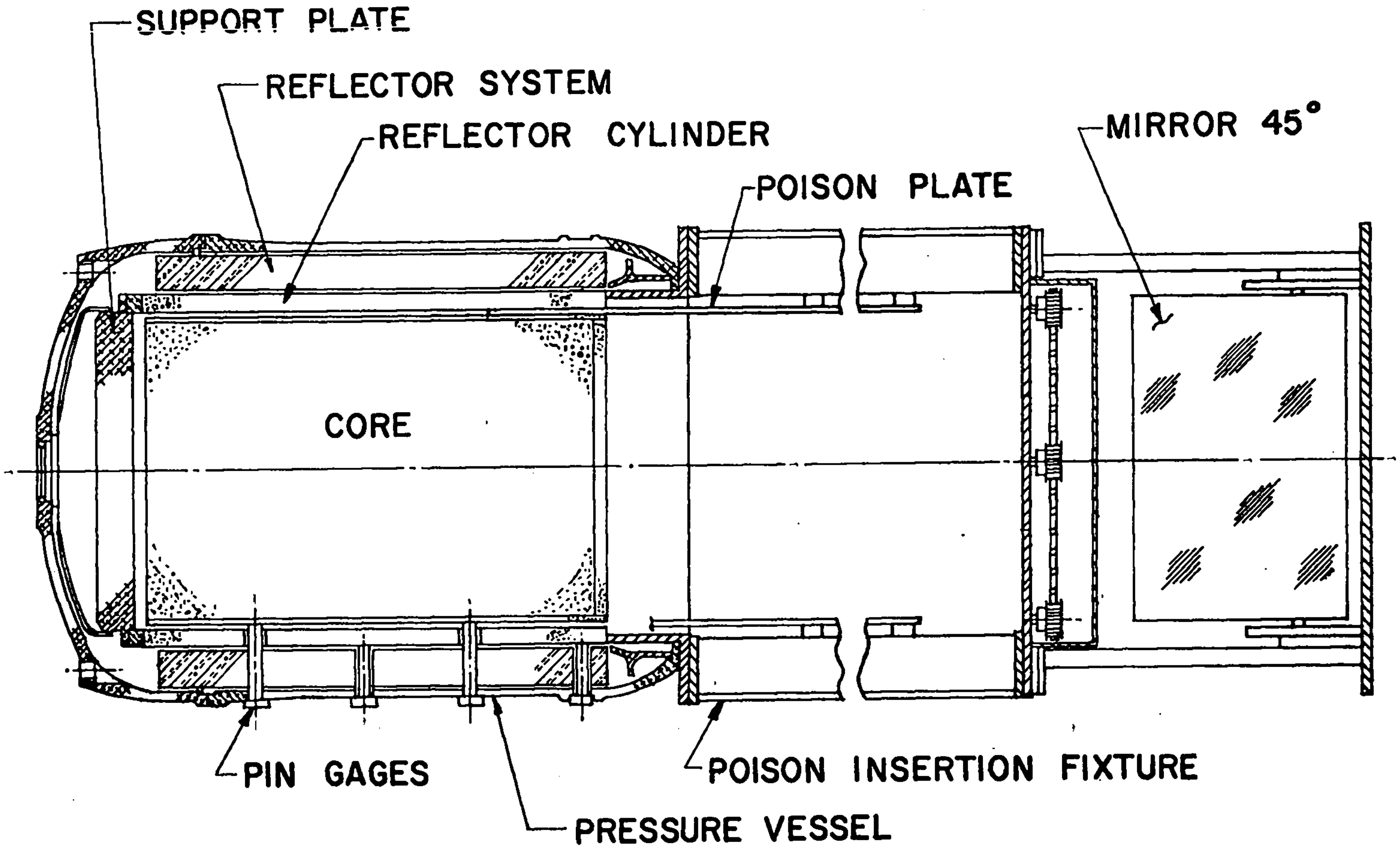

Figure 3-2. TNT Cross Section

APPROVED FOR PUBLIC RELEASE
UNCLASSIFIED

TABLE 3-1

Types of Fuel Elements Used in Kiwi-TNT

Type	No. of Holes	U/Element (Average)	Nb Coating	No. Used
45	19	135.3 gm	Yes	295
44	19	135.9	No	779
40	19	115.0	Yes	30
39	19	117.1	Yes	60
34	19	99.1	Yes	36
30	19	87.2	Yes	78
26	19	75.5	Yes	54
22	19	63.3	Yes	54
20	19	47.6	Yes	18
156	16	35.7	Yes	42
17	19	49.7	Yes	60
15	19	43.3	Yes	36
Total				1542

plug in each fuel element positioned the cold end from the cluster plate by means of projecting bushings.

There were 30 perimeter clusters of 5 irregular shapes that transformed the hexagonal form of the core to a twelve-sided configuration with recessed corners. Each of the perimeter clusters had 3 support elements. The clusters were supported through the central or support elements by means of stainless steel tie rods. These served as tension members between the support blocks and the support plate. Pyrographite tubes were positioned inside the support element hole. These were in turn lined with an 0.005-inch-thick stainless steel tube.

The unfueled central or support elements are normally made of unloaded graphite. To adjust reactivity of the core they may be replaced by elements made of graphite containing tantalum loadings. The Kiwi-TNT core contained 54 of these.

For post-test radiochemistry examination, 13 of these central or support elements were replaced by stainless steel elements. These center elements and 78 other fuel elements spaced throughout the core were periodically marked for identification and axial position. The support blocks were all uncoated cold-flow reactor blocks. The support cones were made of aluminum rather than molybdenum. Only the central hole in each fuel element had an orifice jet and these were flow reject jets of any size. The cluster plates were unplated aluminum since no core-inlet poisoning was required.

4. Perimeter Filler Slats

The perimeter slats were located at the periphery of the core. The normal function of these slats is to transform the geometry from the modified twelve-sided polygon of the loaded core to a cylinder, to provide an initial support for the pyrographite insulating tile, and to remove the radial heat leakage from the core by coolant passages. This last function was not a requirement for the Kiwi-TNT.

A complete set of perimeter slats previously used in zero-power assemblies were modified by removing the retaining lugs. Coolant passage liner tubes were left in these components, although they were not a requirement. The metal wrapper normally placed over the slats to prevent radial propellant leakage was omitted from the assembly.

[redacted]

5. Core Axial Support

The 259 fuel clusters were attached to an aluminum support plate as the clusters were "stacked" or assembled to form the reactor core. The support plate was 40 inches in diameter and 4-1/2 inches thick. It was perforated axially with approximately 1900 holes, located in a triangular array of about 3/4 inch centers. The perforations gave a void fraction of about 42%.

A flange on the outer edge of the plate was held in position against the reflector cylinder by 15 spring and retainer stud assemblies which were screwed into the pressure vessel dome.

Support rods were all 17-7 PH stainless steel made obsolete by a change of material.

6. Core Lateral Support

The lateral core support requirement for the Kiwi-TNT reactor consisted of providing for retention of the core clusters and perimeter slats in a closed cylindrical configuration during the assembly, movement, and checkout phases of the TNT experiment. This did not require the sophisticated lateral support system used for the Kiwi-B-4E reactors.

After the core was "stacked" or assembled onto the support plate and the perimeter slats placed in position, the core was "closed" or radially squeezed by a series of inflatable bands. While in this closed position it was banded by fiberglass reinforced filament tape at five different axial stations. The inflatable bands were then removed.

The reflector cylinder assembly of the Kiwi-B-4E was replaced by a simplified graphite cylinder that did not incorporate the lateral support load rings, seal, springs, and plungers. This cleared the annular space between the core slat periphery and the reflector cylinder of obstructions, and provided an accessible area for the insertion of poison strips or blades during and after reactor assembly.

The reflector cylinder was lowered into position over the stacked core. Centering of the core within the reflector cylinder was provided at the cold end by the support plate and the aluminum spacer ring. The core was positioned within the cylinder at the hot end by means of six graphite plungers threaded through the reflector cylinder for adjustment. The plungers were located so as not to interfere with movement of the boral blades of the remote poison fixture.

[redacted]

7. Core Component Weights

Following is a tabulation of the core and reflector cylinder assembly weights as assembled at NRDS:

Cluster Assemblies	Avg. Wt., kg	No.	Matl.	Total Wt., kg
Fuel Elements		1542	C	818.08
			Nb	54.27
			U-235	181.36
Support Element, Unloaded	0.610	192	C	117.12
Support Element, Ta Loaded	0.607	54	C	32.78
	0.076		Ta	4.10
Support Element, Stainless Steel	3.300	13	304SS	42.90
Support Block, Regular	0.086	169	C	14.53
Support Block, Irregular	0.271	30	C	8.13
Support Rods	0.095	246	17-7 PH SS	23.37
Support Cones	0.001	246	Al	0.26
Pyro Sleeves, etc.	0.097	246	C	23.81
Stainless Liner Tubes	0.024	246	304SS	5.90
Sleeve Positioner Spring	0.001	246	302SS	0.18
Cluster Plate, Regular	0.012	169	Al	1.96
Cluster Plate, Irregular	0.037	30	Al	1.11
Bushing, Cluster Plate	0.007	259	Al	1.81
Bushing, Orifice Jet	0.0002	1542	Al	0.29
Orifice Jet	0.0002	1542	Al	0.24
Preload Spring	0.050	259	302SS	12.95
Holder, Support Rod	0.026	259	303SS	6.63
Nut, Support Rod Holder	0.015	259	Fe	3.89
Filler Elements			C	20.53
Perimeter Slats		48	C	98.76
Coolant Tubes	0.011	432	Invar	4.95
Reflector Cylinder		1	C	368.29
Support Plate	122.00	1	Al	122.00
Spacer Ring	20.42	1	Al	20.42
Core-Cylinder Assembly Total Weight, kg				1990.62

In addition the in-core instrumentation consisting of four pressure probes at Station 10, 21 pin shorting gauges. and 10 thermocouples contributed approximately 0.83 kg of primarily stainless steel to the core weights.

As a verification, the total calculated weight of all assembled clusters was 1376.20 kg. The actual total weight of the cluster

[redacted]

assemblies as recorded during the NRDS assembly sequence was 1375.36 kg. Figure 3-3 shows the fuel loading arrangement.

D. Reflector System

1. General Description

The principal side reflector of the Kiwi-B reactors was of beryllium metal, 4-1/2 inches thick radially and located within the pressure vessel outside of the graphite reflector cylinder. The control rods were located within the beryllium reflector, and functioned by rotating a strip of poison toward or away from the core. There were no axial reflectors.

The reflector system was assembled from 12 sector assemblies. Each sector assembly was composed of two axial halves, held together by tie tubes. Coolant holes were drilled the length of the sectors. Other holes contained beryllium filler rods, which could be replaced by aluminum rods if necessary to shim the reactivity. Each sector assembly was supported at the pressure vessel dome end by two standoffs which located the assembly and also took the axial load. At the nozzle end two standoffs were guided by the pressure vessel cruciform bracket, and were constrained by a nickel hold ring. This design positioned the twelve sector assemblies into a cylindrical configuration to form the reflector system.

Each sector assembly contained one control rod, mounted centrally in the sector. The control rods were of beryllium with a 120° sector poisoned by B^{10} boron-aluminum plates. Control was achieved by rotating the rods in unison from the maximum poison position with the plates facing the core, to the minimum poison position with the plates facing outward. Spiral springs held the rods in maximum poison position against stops until the rod actuators were installed.

Each control rod was assembled from 4 axial segments and two bearing shafts, all held together by means of four tensioned tie rods. The control rod was located and supported within the sector assembly by two radial ball bearings. The bearing at the dome end of the assembly provided axial support and positioning for the control rod, while the bearing at the other end provided radial positioning only.

Figure 3-4 shows the sector assembly components.

[redacted]

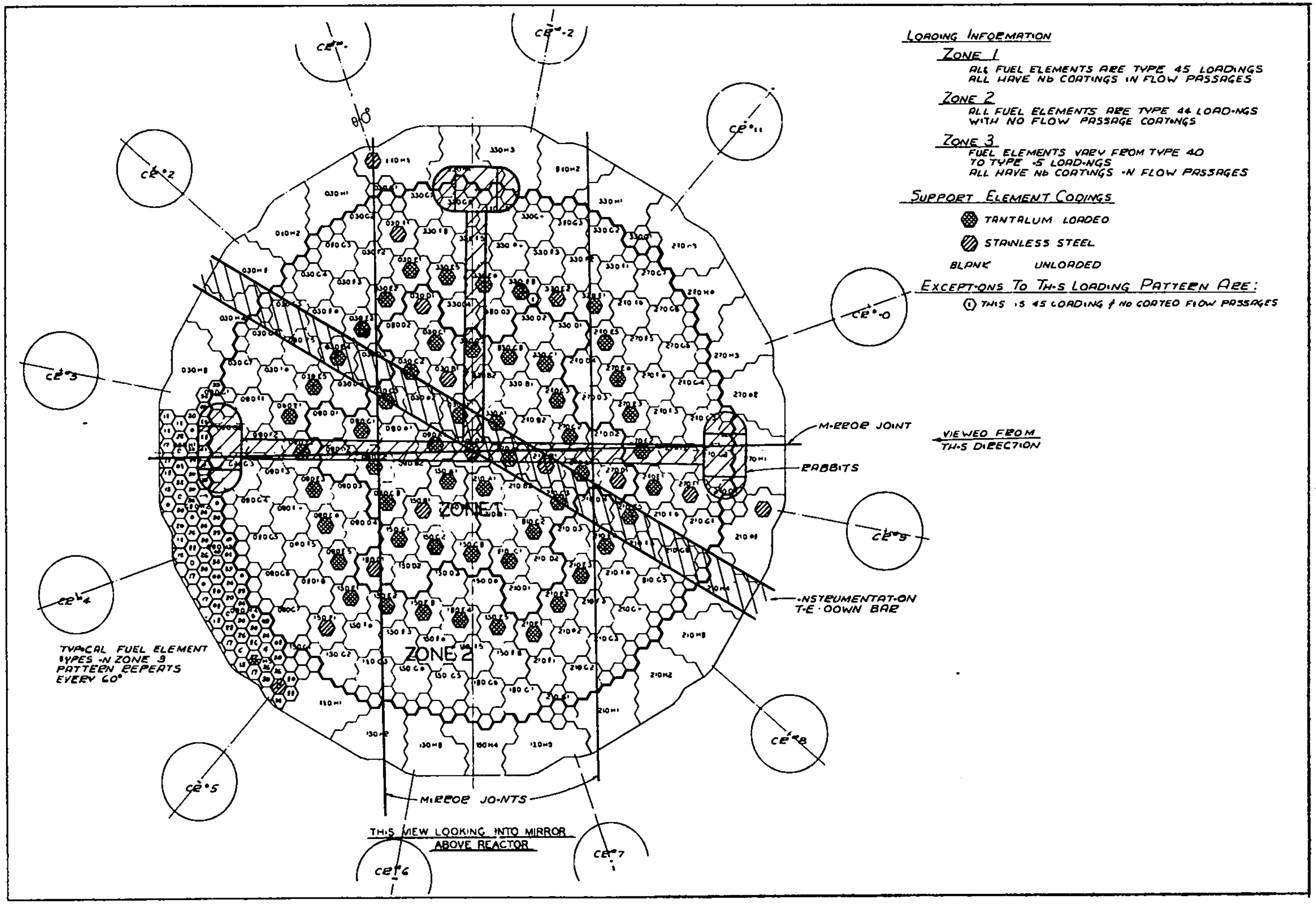

Figure 3-3. Kiwi-TNT Core Loading Arrangement

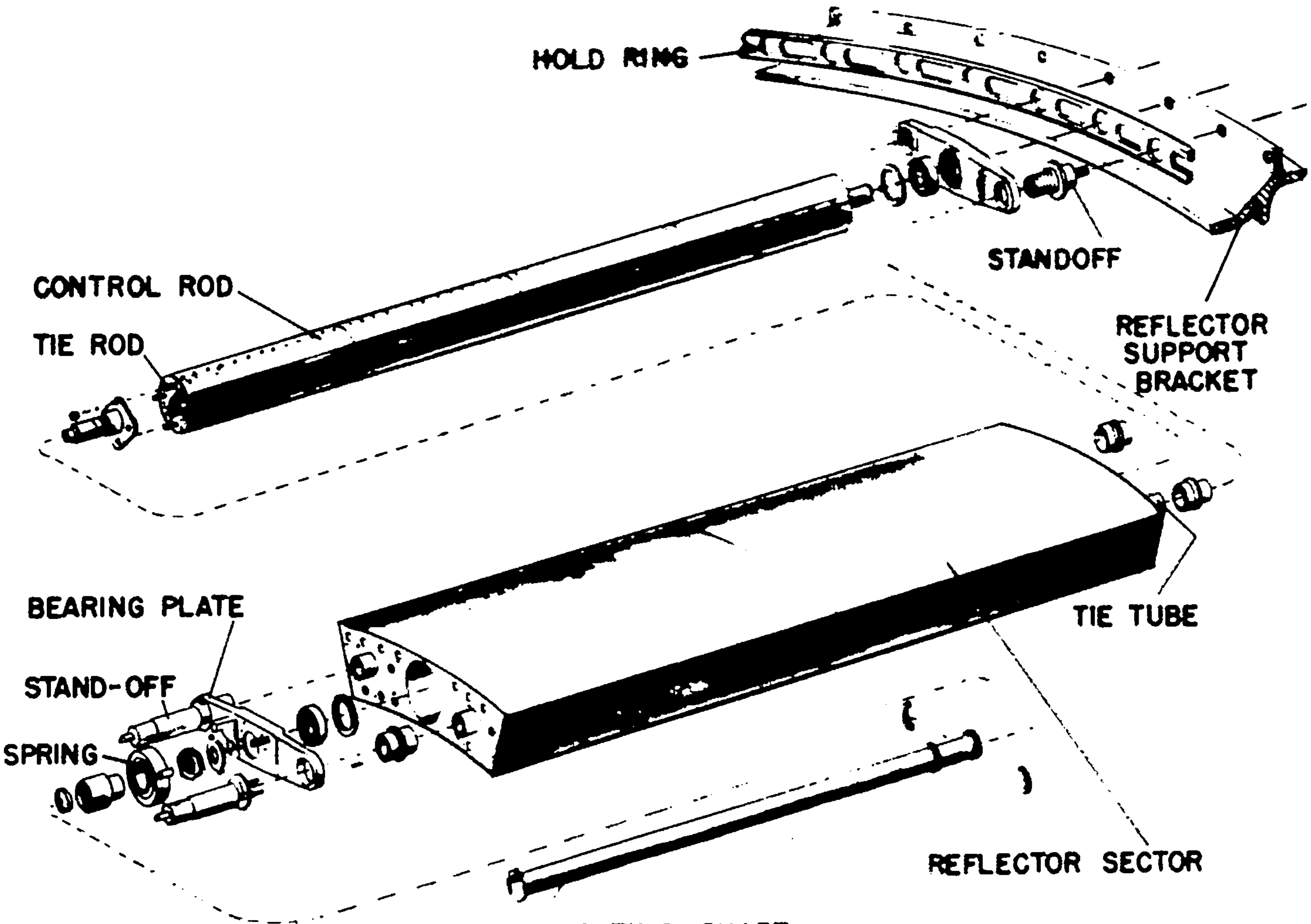

Figure 3-4. Sector Assembly Reflector System

UNCLASSIFIED
APPROVED FOR PUBLIC RELEASE

2. TNT Modifications

a. General

To provide for pin-gauge instrumentation, eight penetrations 1 inch in diameter were made through the reflector system. These were located between adjacent sectors at $\theta = 15^\circ$ and 285° at Stations 13, 26, 39 and 51.

Control drums were assembled without the normal annular flow impedance rings. The tensioning tie rods were tightened to a high stress level to provide additional friction loading between the flange and segment interfaces. Control rod bearings were carefully selected and lubricated to obtain a loose-but-smooth internal fit-up.

Drive shaft assemblies procured for a discontinued Kiwi-B-5 reactor were used. The floating shaft length was adjusted to suit the reactor test cart requirement. Minor assembly components were modified to permit the use of these drive shafts with the Kiwi-B-4E assembly hardware.

The sector assembly tie tubes were tightened to a higher stress level. The dome-end standoffs used had a heavier cross section than the Kiwi-B-4E design.

At final assembly of the reflector system, fiberglass reinforced filament tape was used to band the system around the perimeter to help retain it in a closed configuration. Clamp bands between adjacent sectors were not used.

b. Control Rod Actuation

The hydraulic control rod actuators used for the Kiwi-TNT were the normal Kiwi-B type with incorporated velocity-increasing modifications. The normal Kiwi-B actuators were required to rotate at a maximum limited velocity of 45°/sec in the "out" direction and 400°/sec in the "scram" direction. For the Kiwi-TNT reactor the actuators were required to rotate in the "out" direction at a velocity of approximately 4000°/sec, or at nearly a factor of 100 times the normal rate. In addition the actuators and control rods were required to reach the 90° position simultaneously within 0.010 seconds (10 milliseconds).

Changes made in the actuators and the hydraulic systems were:

(1) The area of the hydraulic ports into and out of the actuator was increased by 50%.

[redacted]

(2) The diameter of the hydraulic lines from manifold to control valves to actuators was increased.

(3) Close-coupled hydraulic manifolds with accumulators were used.

(4) Control valves with a capacity of 30 gpm were used instead of the normal 3-1/2 gpm capacity valves.

(5) Hydraulic oil pressure was increased from 700 psi to 1350 psi.

(6) Delay circuitry was used in the firing control chassis to obtain the necessary simultaneity.

Detailed information concerning these modifications and the development testing may be found in an internal N-4 document, titled "Kiwi-TNT Control Rod Actuator Changes and Test Results." Figures 3-5, 3-6, and 3-7 show the hydraulic actuator, the control rod arrangement, and the actuation "package" during reactor assembly.

E. Pressure Vessel

1. The aluminum pressure vessel was made in two sections, joined by a clamp ring over clamp ring segments. The dome end had an instrumentation pass-thru opening in the center. It also provided axial support and positioning for the core and the reflector system.

2. At the nozzle end the cruciform bracket was bolted to the pressure vessel. It served as a handling fixture for the reflector system during the reactor assembly sequence.

No nozzle outer impedance rings, flow separation screen, or seals were used on the Kiwi-TNT reactor. All unused holes were plugged. An external cover plate with drain was used on site prior to the test.

F. Remote Poison Fixture

The remote poison fixture replaced the nozzle of the reactor. It served the following functions:

1. Positioned and held down the reflector cylinder and core at the exit end.

2. Housed the mechanism for insertion and removal of two opposed poison blades in the annular space between the core and reflector cylinder.

[redacted]

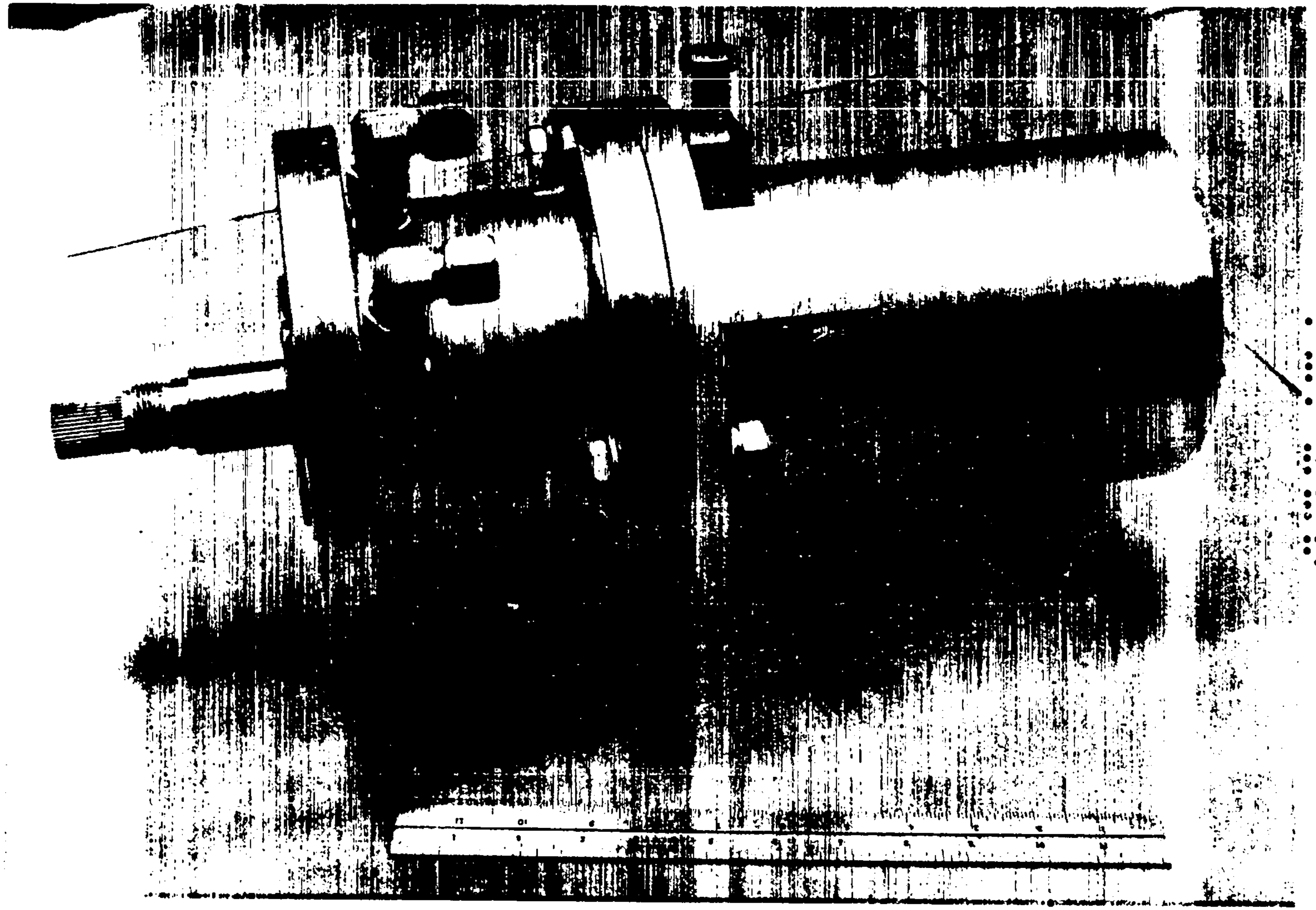

Figure 3-5. Hydraulic Control Rod Actuator

APPROVED FOR PUBLIC RELEASE

UNCLASSIFIED

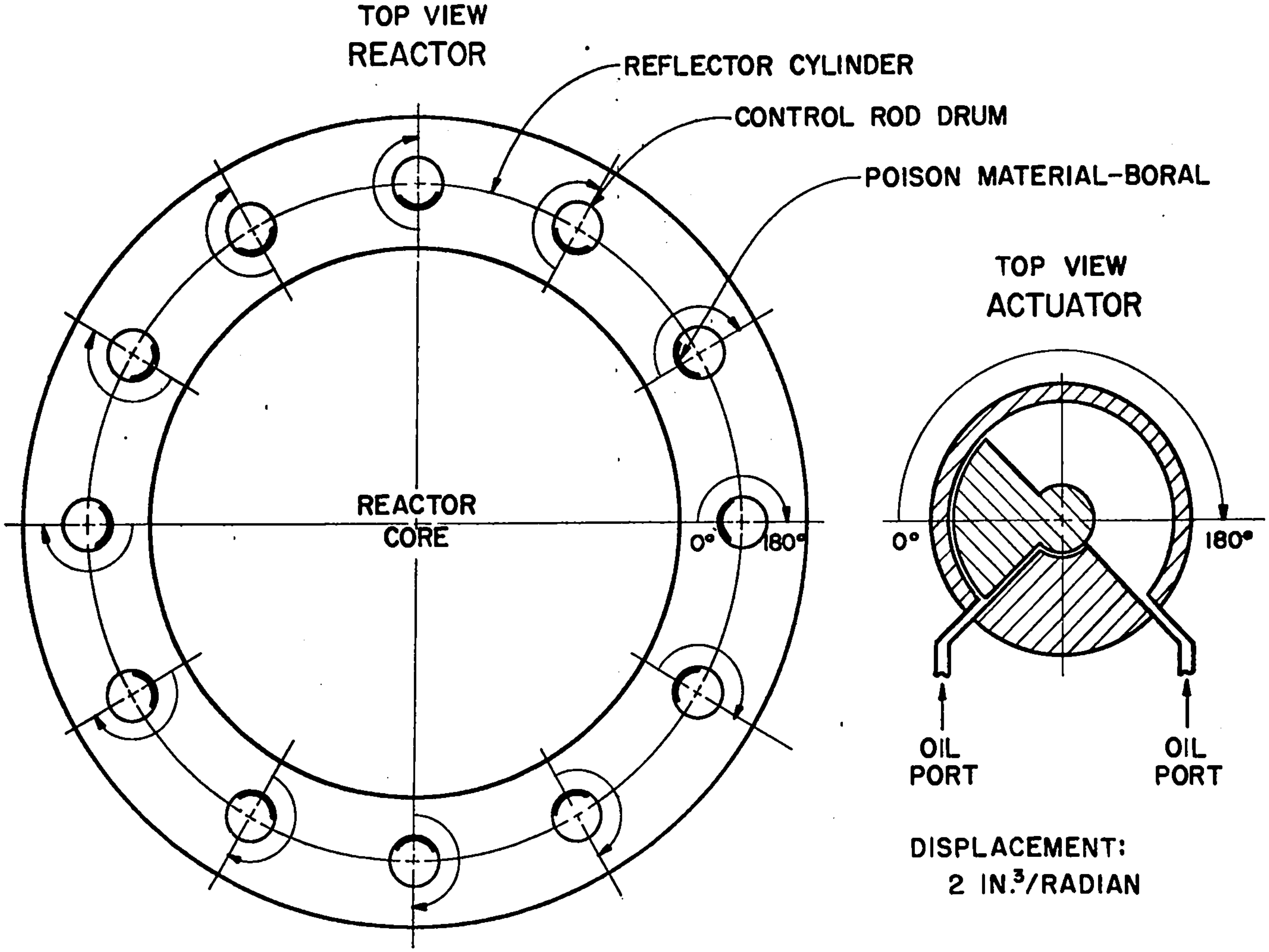

Figure 3-6. Twelve Control Rod Drum Layout Schematic

[redacted]

SIFIED

UNCLASSIFIED

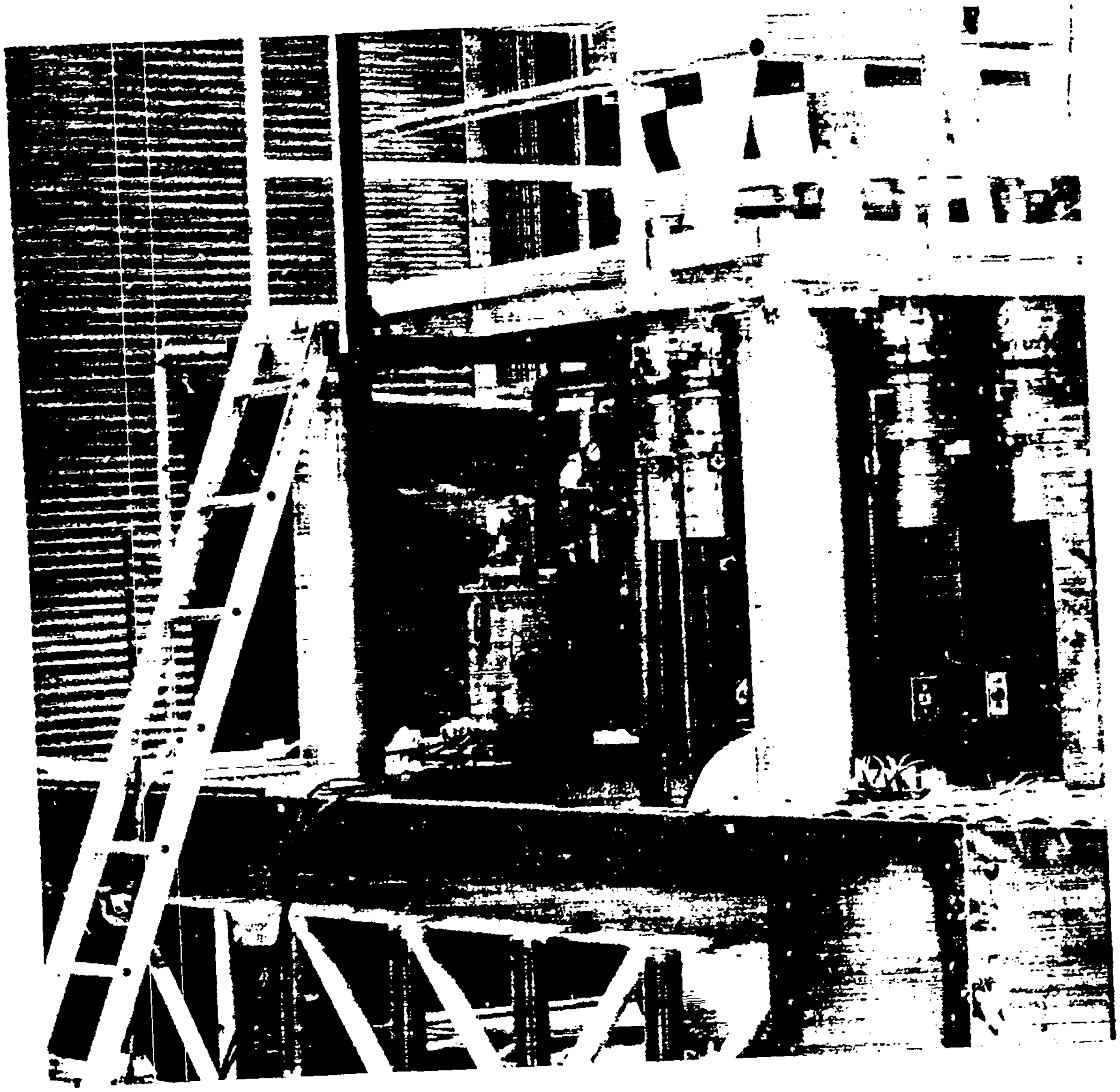

Figure 3-7. Actuators on Reactor

UNCLASSIFIED

[redacted]

[redacted]

3. Provided a means for tie down and clamping or supporting of instrumentation originating at or routed through the core exit.

4. Structurally supported a mount for an adjustable mirror aligned to obtain photographic coverage of the core exit end.

The poison blades and insertion mechanism consisted to two 3/16-inch-thick commercial boral plates curved to fit the annular space. Each blade or vane was mounted on a holding fixture arranged to operate vertically along two guide rods by means of a driven ball lead screw. When fully inserted the blades covered or curtained two complete 60° sectors for the entire fueled length of the core. When fully withdrawn the blades did not curtain any part of the core or reflector system in the radial direction. The driving motor for the mechanism operated both blades in unison. It was remotely operated from the control room.

Figure 3-8 shows the assembly arrangement of the poison fixture.

G. Reactivity Measurements on TNT

The reactor was assembled at the Los Alamos Critical Assemblies Laboratory for measurements to calibrate the control rods and determine the shutdown margin provided by the boral safety vanes in combination with control rods.

Chronologically, the measuring proceeded by assembling the TNT core with 135 Ta support elements and obtaining delayed critical with all control rods at 95.9°. The control rod worth was then determined by incremental measurements of one rod over the entire range from 0° to 180°. The reactor was re-shimmed with only 60 Ta supports in the core and the new D.C. was found at 50.4°.

Additional rod worth measurements showed the control rod span to have increased by 13.6%, so the previous rod calibration data was adjusted by this amount. The resulting rod worth curves are shown in Figure 3-9.

Reactivity values of the two boral safety vanes were measured, and the results for several configurations are given in the first column of Table 3-2. TNT was 1.3% subcritical with twelve control rods "IN" and the safety vanes "OUT". Upon re-assembly at the NRDS MAD Building, only 54 Ta supports were used in an attempt to gain 0.25$ and hit the design point of 1.00$ shutdown. Multiplication measurements performed at the MAD Building indicated that TNT would be 1.1$ subcritical (rods "IN", vanes "OUT"). Comparison with the Kiva data is given in Figure 3-10.

[redacted]

APPROVED FOR PUBLIC RELEASE

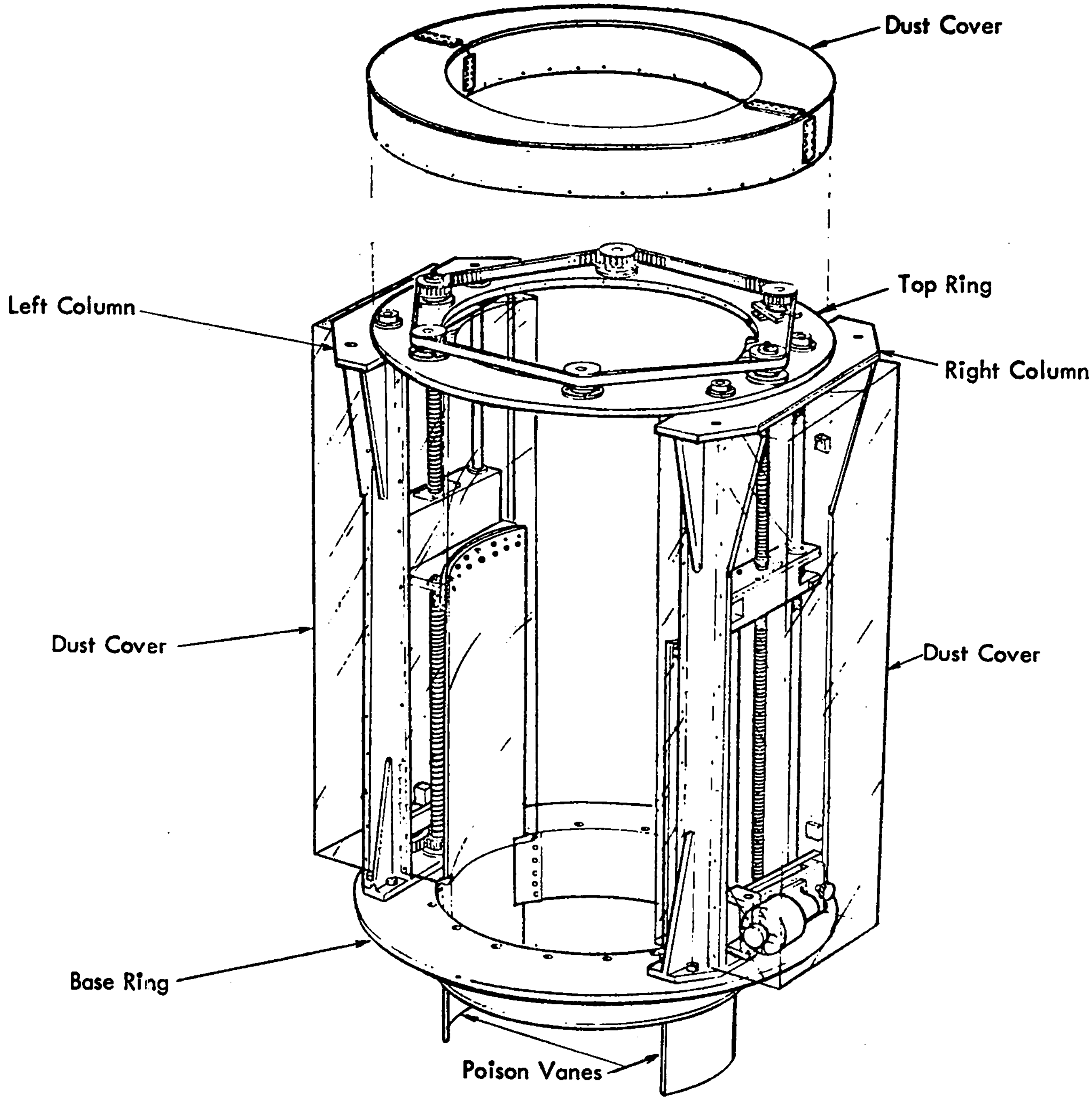

Figure 3-8. Kiwi-TNT Remote Poison Fixture

[redacted]

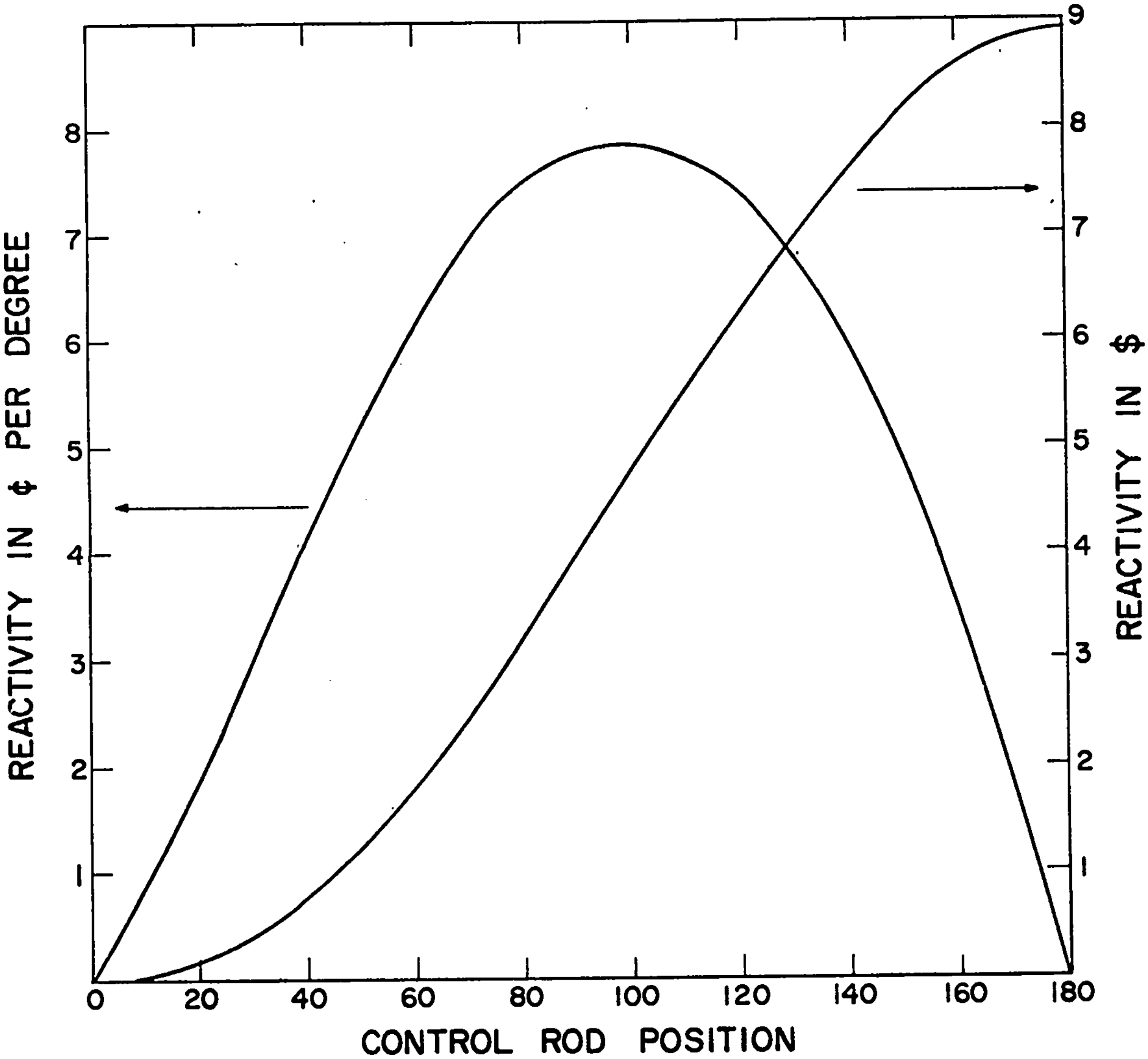

Figure 3-9. Kiwi-TNT Differential and Integral
Control Rod Effectiveness Ganged Rods

[redacted]

TABLE 3-2

Kiwi-TNT Reactivity

Configuration	Reactivity, $	
	Kiva	NRDS test point
Number of Ta Supports	60	54
1. 2 boral vanes in 12 control rods at 0°	-6.9	-6.2
2. 1 boral vane in 12 control rods at 0°	-3.7	-3.0
3. Both boral vanes out 12 control rods at 0°	-1.3	-0.6
4. 2 boral vanes in 12 control rods at 180°	-2.0	-1.3
5. Control rods at 50.4°	Delayed Crit.	+0.7
6. Control rods at 180°	+7.6	+8.3

[redacted]

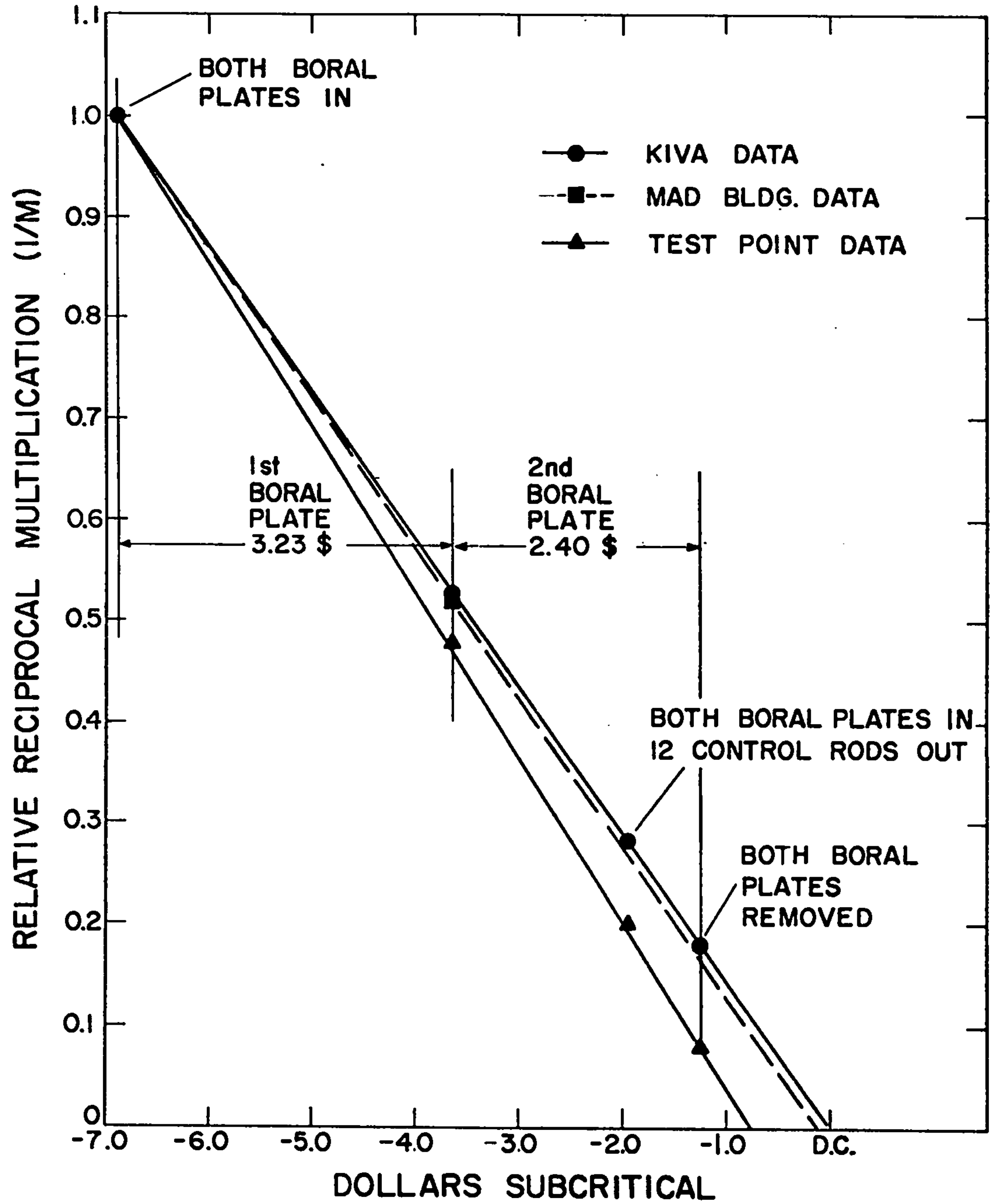

Figure 3-10. Reactivity of TNT for Various Poisoned Configurations

[redacted]

After the reactor had been taken to the Test Point and the remaining equipment installed on the exterior of the pressure vessel (test samples, instrumentation, etc.), a final reactivity measurement was made to determine the starting point of the power excursion. Data were taken for a number of shutdown cases, and are compared in Figure 3-10 with data from the Kiva check-out. At this time, TNT was found to be 0.6$ subcritical. The corresponding increase in reactivity was attributed to added reflection from the equipment installed on and above the pressure vessel.

The final point of significance is that for control rods all the way out during the test, TNT was 7.3$ above prompt critical.

Chapter 4

RESULTS OF THE KIWI-TNT EXPERIMENT

A. General

An extensive measurements program was undertaken for the test which included conventional instrumentation as well as techniques developed especially for this test.

Measurements were made of the following quantities:

1. Reactivity time history
2. Fission rate time history
3. Total fissions
4. Core temperatures
5. Core pressures
6. Core and reflector motion
7. External pressures
8. Radiation effects
9. Cloud formation and composition
10. Fragmentation and Particle Study
11. Geographic distribution of debris

In addition to these measurements, high speed framing cameras recorded details of the excursion. Figure 4-1 is a color photograph taken about 5.4 seconds following initiation of the excursion.

Figure 4-1. Appearance of Kiwi-TNT Excursion at +5.4 Seconds

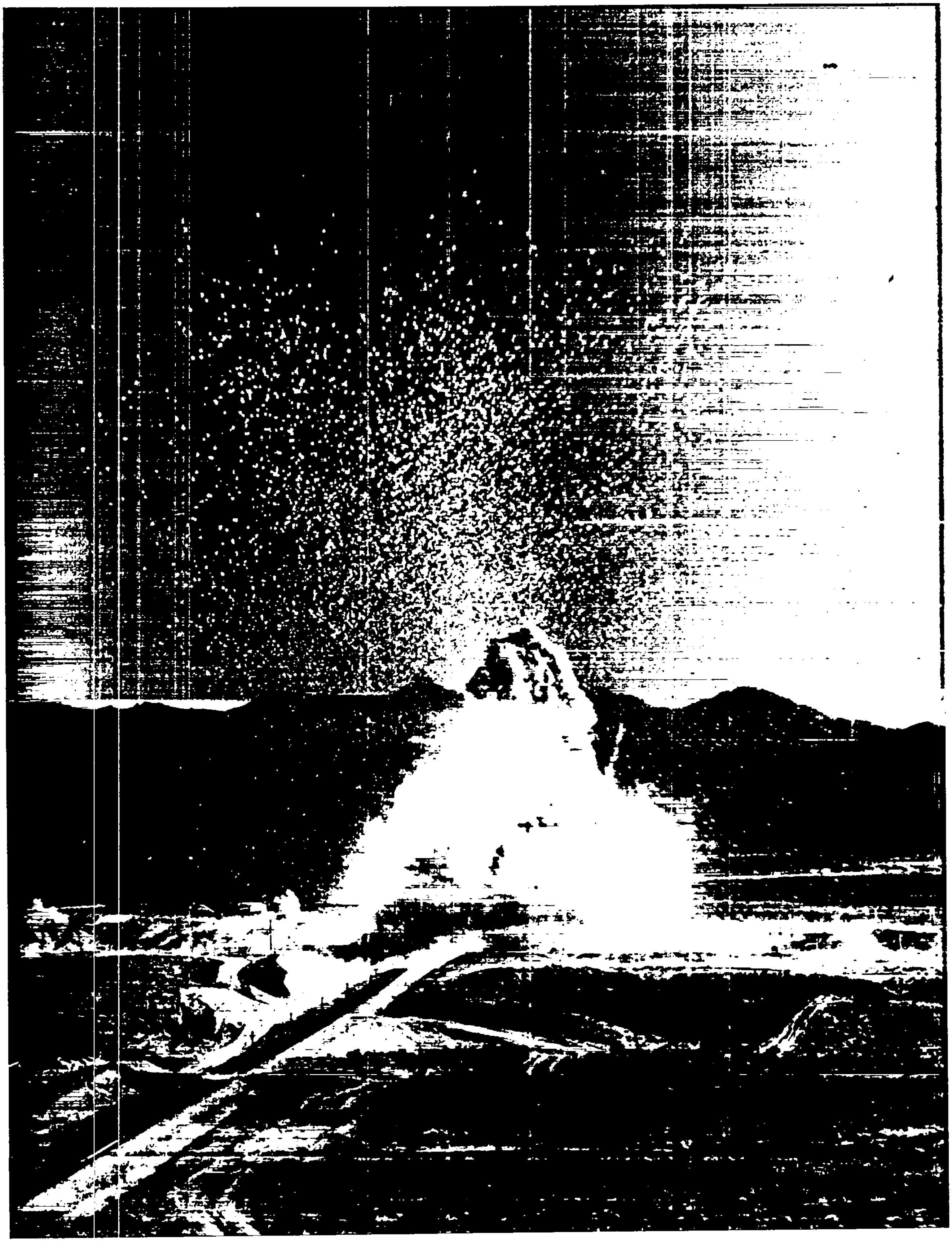

APPROVED FOR PUBLIC RELEASE

The results reported here were abstracted and summarized from the referenced reports. For details of the measurement techniques and interpretation, the reader should refer to these reports.

B. Detailed Results

1. Reactivity Time History

At the initiation of the excursion the reactor was about 0.60$ subcritical. The twelve control drums were rotated outward at a rate which varied from an initial rate of 1500°/sec to a maximum rate which exceeded 4000°/sec. Table 4-1 lists the time history for position and corresponding reactivity insertion, zero time being taken as the second during which the excursion took place. Table 4-2 lists the times of other phases of the excursion. The photographically derived events shown in the table appear to be timed to within 0.4 msec. This allows for subjective errors in picture interpretation and for the time resolution of the Fastax film. All times are related to the peak of the excursion given by the collimated gamma detector.

In addition to other measurements, the excursion was photographically recorded by high speed cameras. This system, described in Chapter 2, utilized four Fastax cameras for overall views of the reactor and two Dynafax cameras for photography of the upper core end. An eight picture Fastax sequence taken at 3830 frames/sec is shown in Figure 4-2. Each photo in this sequence was scanned with a microdensitometer using a Wratten No. 96 filter to determine the time of maximum air fluorescence corresponding to peak power which occurred between frames four and five. This event and the time base recorded on this film were used to correlate these data with the fission rate time history. The three encapsulated flux monitors placed 1 ft above the core top were obscured by the rising vapors between frames five and six in this sequence. These monitors can be seen in the first four frames of this sequence, in the top elevation of the core shown in Fig. 3-3 and in Fig. 4-3. This event was used to establish time correlation of the Dynafax films with the Fastax film. Unknown time delays in the electrical timing and time correlation signals to these films precluded their being used for the intended purpose. Also both Dynafax films contained a multitude of marks rather than a single time correlation mark; thus, the need to correlate these data in the above manner.

Two six-frame Dynafax sequences taken at 23,680 frames/sec are shown in Fig. 4-3. The streak of light on the left of the pictures in Fig. 4-3a is a sun reflection from the aluminum structure. The dim illumination of the surface of the core is due to the light from the two banks of photo-flash bulbs which were fired by the 10^{15}

TABLE 4-1

Control Rod Performance

Avg. Rod Position, Degree	Avg. Time for Rod Angle, msec	Simultaneity Range, msec	Avg. Rod Velocity, °/sec	Reactivity, $	Reactivity Insertion Rate, $/sec
10	97.4	11.0	1550	-0.65	12.7
20	102.5	8.8	2500	-0.53	40.6
30	106.2	8.6	2990	-0.26	89.0
40	109.4	8.8	3230	+0.07	134.0
50	112.5	7.1	3360	+0.54	172.0
60	115.3	9.0	3470	+1.13	213.0
70	118.2	9.3	3580	+1.76	247.0
80	121.0	9.0	3690	+2.50	274.0
90	123.6	9.2	3790	+3.28	294.0
100	126.2	8.9	3880	+4.05	303.0
110	128.8	9.2	3970	+4.83	295.0
120	131.3	9.1	4050	+5.54	298.0
130	133.9	9.3	4140	+6.25	280.0
140	136.2	9.4	4220	+4.40	250.0
150	138.5	9.8	4260	+7.45	209.0
160	141.0	10.0	4030	+7.88	139.0
170	144.0	8.0	2680	+8.13	48.0
180	151.24	-	-	+8.30	-

TABLE 4-2

Time History of Excursion

Event	Relative Time, msec	Time from Start of Rods, msec
F-0	41.45	
Rod Motion Starts (Av Time)	88.74	0
Rods at Delayed Critical (38°-Av Time)	110.74	22.00
Rods at Prompt Critical (58°-Av Time)	117.24	28.50
Gamma Trigger (10^{15} Fissions/Sec)	143.30	54.56
Rods at 180° (Av Time)	151.24	62.50
First Visible Internal Nuclear Heating	152.64	63.90
Core Motion Starts (Center)	152.96	64.22
Cooled Vapor Starts to Obscure Core End	153.14	64.40
Maximum Alpha (1680 sec^{-1})	146.2 - 153.2	57.46 - 64.46
Pressure Vessel Rupture	155.32	66.58
Excursion Peak	155.45*	66.71
Flux Monitor Capsule Obscured by Rising Vapors	155.85**	67.11
Vapors at Mirror Bottom	157.93	69.19
Mirror Half Obscured by Rising Vapors	159.59	70.85
Initial Vapor Jet Velocity (at Core Top)	1250 ft/sec	

* Fastax timing correlated to neutronic measurement timing through maximum air fluorescence at this event.

** Dynafax and Fastax films time correlated by this event.

Figure 4-2. Fastax Sequence, West Bunker, at 3830 frames/sec (Sequence 154.54 to 156.36 msec, Peak Power 155.45)

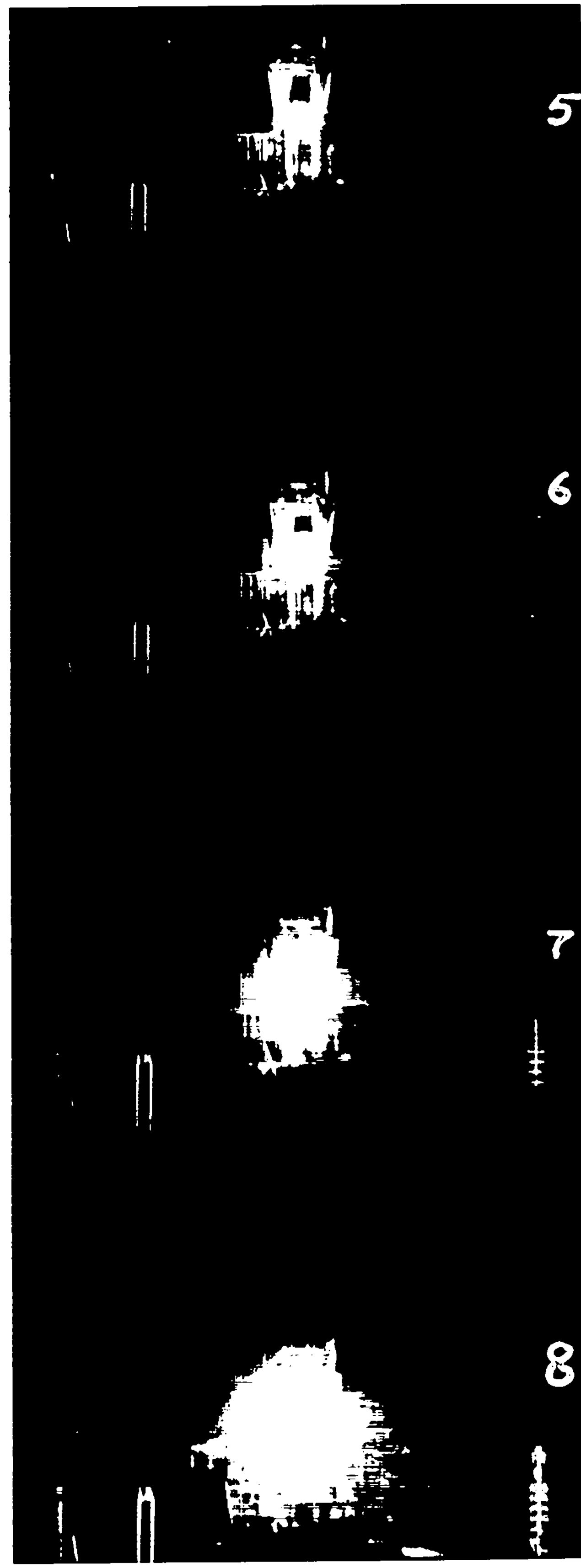

APPROVED FOR PUBLIC RELEASE

APPROVED FOR PUBLIC RELEASE

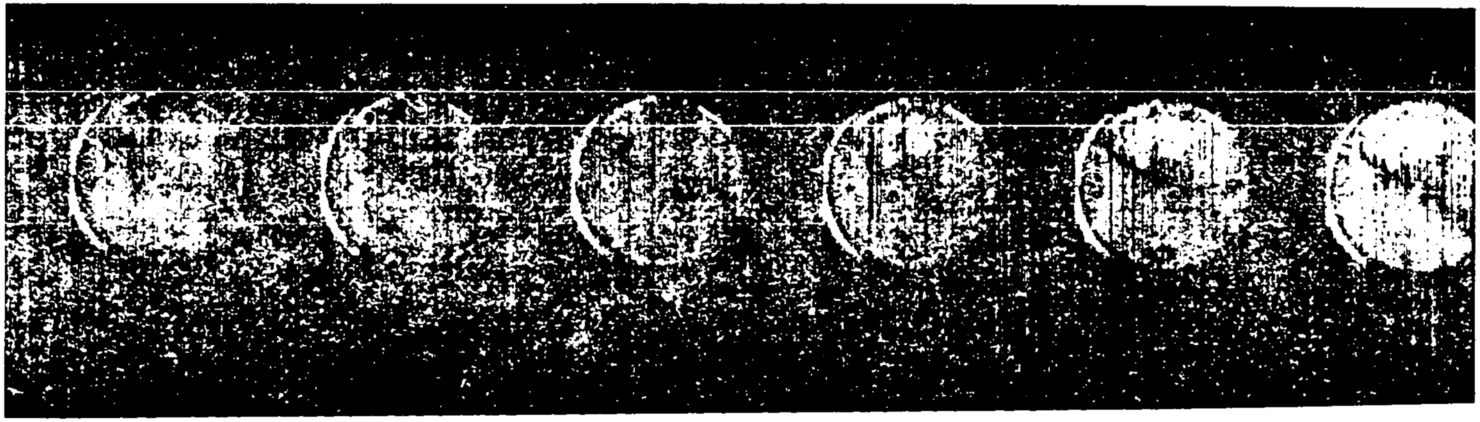

Figure 4-3a. Pictures 1 to 6.

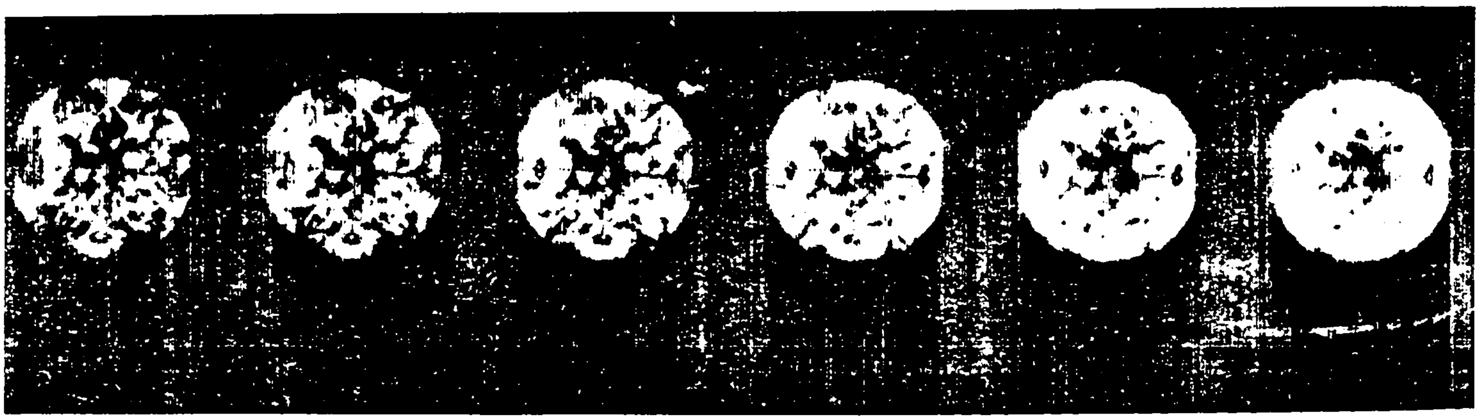

Figure 4-3b. Pictures 1 to 6.

Figure 4-3. Alternate Dynafax Camera Views of the Top of the Reactor

APPROVED FOR PUBLIC RELEASE
UNCLASSIFIED

[redacted]

fissions/sec trigger. The thin black lines are joints in the mirror. The encapsulated flux monitors can be seen at the 90, 180, and 270° positions. The diagonal bar supporting internal instrumentation can also be seen. Only alternate pictures, or every second frame actually taken, are shown in these sequences. In the upper portion of picture number 1 in Fig. 4-3a one sees the first visual indication of self illumination due to fission heating. This appears as pin points of light emerging from the interior of the reactor through coolant channel passages. The highest number of fissions per gram of uranium is known to occur at the fuel-reflector interface. This probably accounts for the more intense illumination at the core edge. The other frames in this sequence show increasing self illumination around the edge as well as in the upper sector of the core. Picture number 6, Fig. 4-3b, was exposed at peak power and shows flux monitors at the 180° position to be nearly obscured by the rising vapors. Other frames in this sequence are prior to peak power and show the rising torus of vapor increasing in brightness with time.

2. Fission Rate Time History

The time history of the energy generation was of prime importance in the understanding of the energy release mechanism. The fission rate was inferred from a measurement of prompt gamma ray emission using a system of photocells and fluors. The system, described in Chapter 2, consisted of six uncollimated detectors and one fast neutron detector. These detectors were calibrated during previous reactor tests in the Kiwi-B4E-301 test series to obtain the ratio of gamma flux at the detector to neutron fissions in the core. Two were placed on the pressure shell to record early history, two were positioned at 24 feet from the reactor to detect intermediate gamma levels, and four were positioned at 800 ft to cover the peak rate of the event. The ranges of sensitivities of the detectors were selected so as to include approximately seven decades covering power levels between 10^{16} fissions/sec and 10^{23} fissions/sec. Individual detectors recorded over a range of one and two decades. Measurement of alpha, or the reciprocal period, was obtained by taking the logarithmic derivative of these records.

A semilog composite plot of these detectors is shown as a part of Fig. 4-4. The shape of the peak in this curve was obtained from the collimated detector trace also shown in the figure. The peak rate was 1.1 x 10^{23} fissions/sec. This value is believed to be within better than 50 percent of the true value, the error in measurement arising from uncertainties in detector calibration and variation in the core flux distribution during the test from that which existed during the calibration runs.

[redacted]

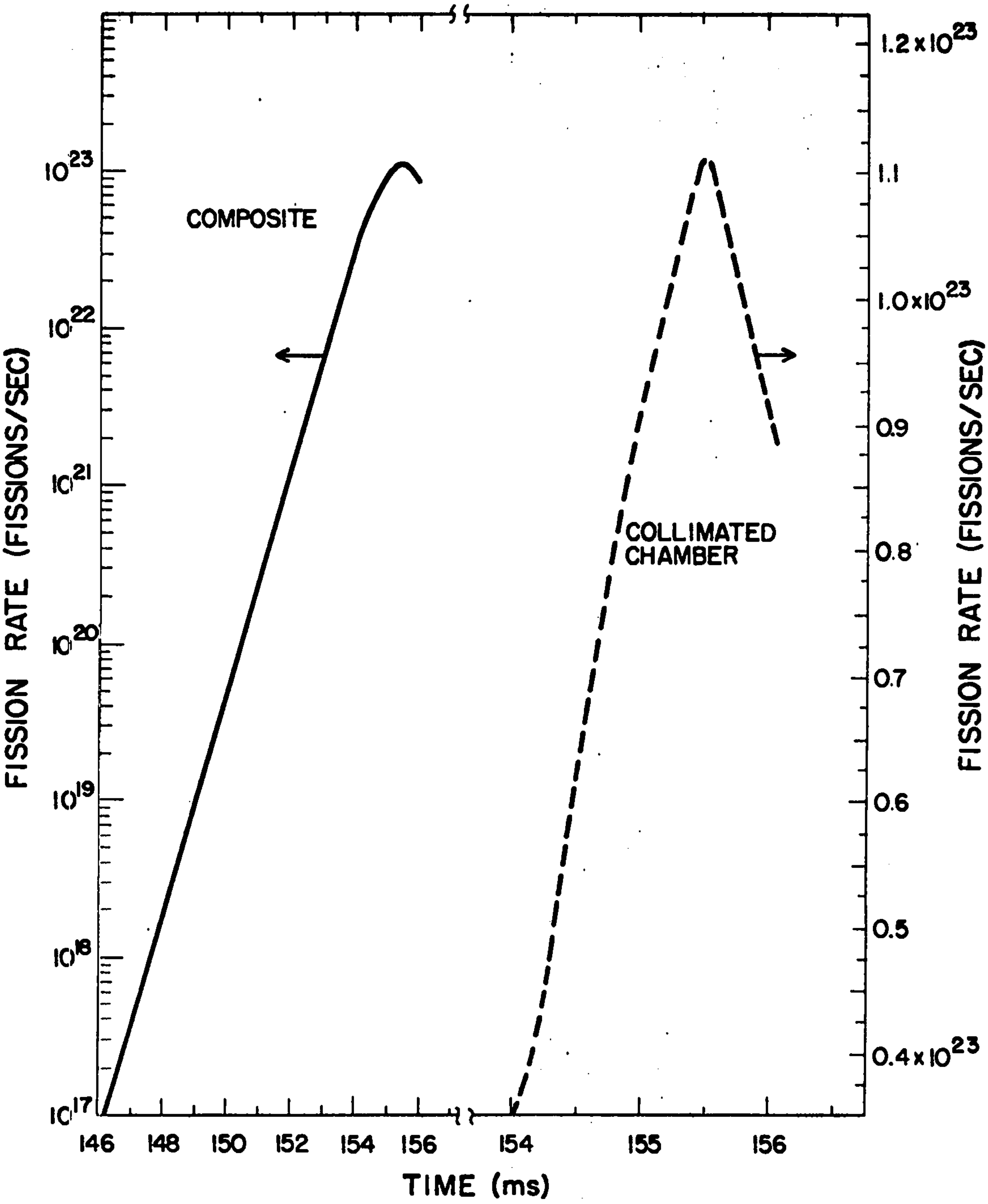

Figure 4-4. Fission Rate Time History

Figure 4-5 shows the results of the logarithmic derivation. The alpha was sensibly constant over approximately 6 decades with a value of 1680 ± 50 gen/sec.

3. Total Fissions

The primary measurements of the total energy release and the fission distribution were obtained by radiochemistry.[5] Total fission data were obtained by three different methods. The first was based on analysis of the stainless steel center elements giving a value of 3.12×10^{20} fissions. The second method was based on an analysis of the identifiable pieces of inlet end fuel still remaining on the test cart. This determination gave 3.08×10^{20} fissions. The third method made use of one external neutron flux monitor which was recovered after the test. A value of 3.5×10^{20} fissions was obtained from it. This latter determination was expected to be about 10% high due to external modifications in Kiwi-TNT as compared with Kiwi-B-4E on which the flux monitors had been calibrated.

Radial and axial fission distributions were determined[5] by analysis of 13 solid stainless steel elements which were substituted for graphite center elements at four different radii along three radial lines and one along the core axis. All of these elements were recovered following the excursion. The axial fission distribution was derived from results of radiochemical analysis of samples cut at five axial locations from the center element. The radial fission distribution was determined from samples cut near the midplane. The results are shown in Figures 4-6 and 4-7.

The results of the analysis of fuel samples[5] collected on the ground after the test are shown in Table 4-3.

4. Core Temperatures

a. Thermocouple Measurements

Six of the seven W/W-Re thermocouples gave traces as shown in Figure 4-8. The identification in this figure includes channel number and location in the core, e.g., T.105.YA is the channel number, 210E4G-S26 indicates the location as being element G of the fourth cluster in the E row in the 60° sector centered about the 210° azimuth (see Figure 3-3) and S26 or Station 26 gives the axial location as 26 inches above the core inlet end. These measurements were made in the event of a low yield excursion. Since the excursion was large, the traces level off or decrease in amplitude before their full temperature capability was reached. This is due to shunting effects in the magnesium oxide at high temperature and possible radiation induced ionization.

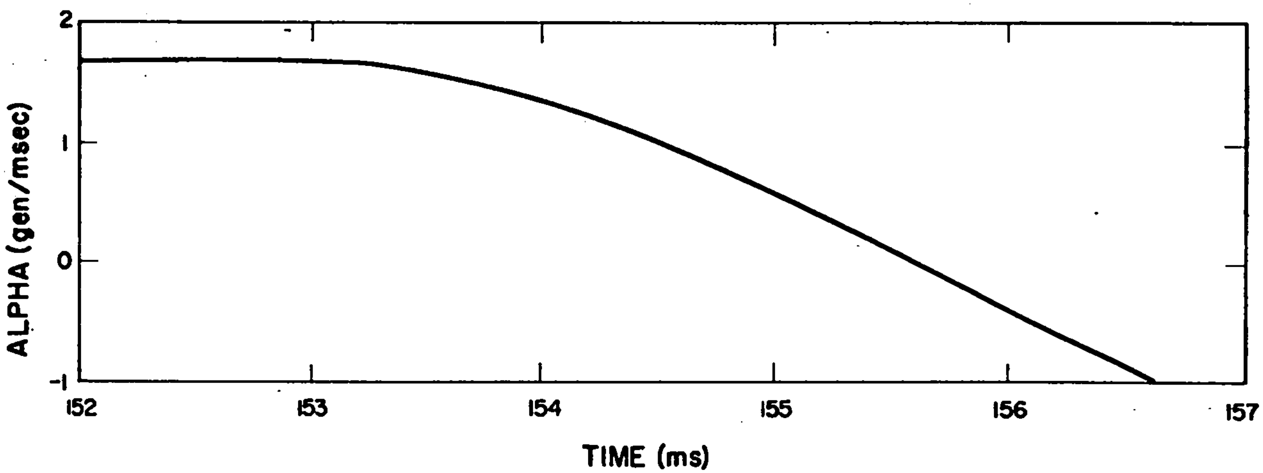

Figure 4-5. Period of Excursion

[redacted]

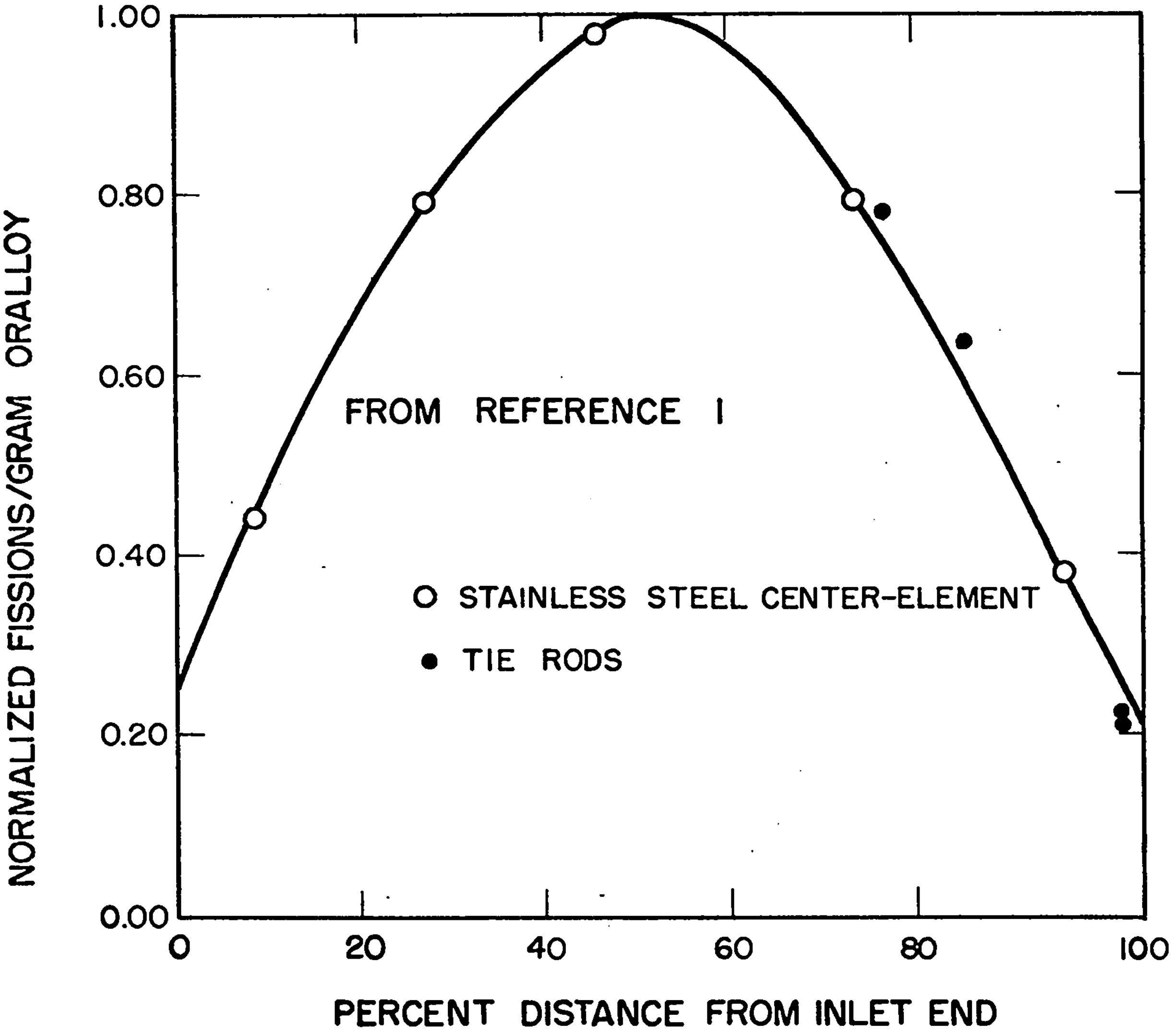

Figure 4-6. Axial Fission Distribution

[redacted]

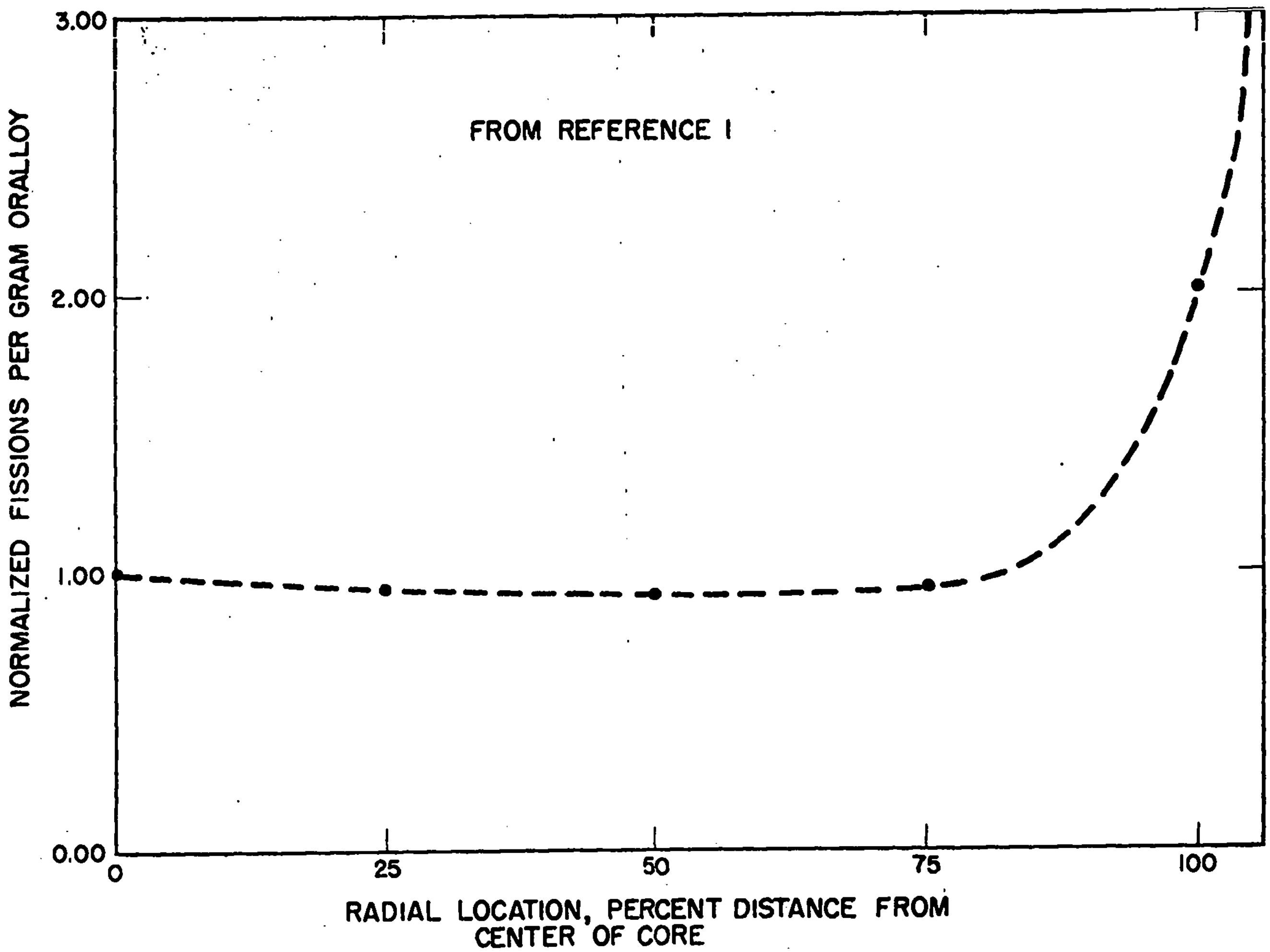

Figure 4-7. Radial Fission Distribution

TABLE 4-3

Results of Analyses of Fuel Samples Collected on the Ground after the TNT Test

Source of sample: On desert	In core: Inches from inlet	In core: Radius (in.)	Fissions/gm Oy: Mo^{99} (units of 10^{14})	Fissions/gm Oy: Nd^{147} (units of 10^{14})	Sr^{89}	Y^{91}	Zr^{95}	Ag^{111}	Cd^{115m}	Te^{132}	Cs^{136}	Cs^{137}	Ba^{140}	Ce^{144}
					Fractional retention referred to Mo^{99} or Nd^{147}									
Fuel recovered from support plate	2.5*	2.3	8.85	7.85	0.14	0.07	0.66	0.32	0.16	0.17	0.08	0.15	0.12	0.54
	2.5*	4.2	7.63	6.80	0.16	0.08	0.60	0.53	0.14	0.20	0.08	0.18	0.09	0.50
	2.5*	6.6	7.96	7.48	0.16	0.07	0.66	0.61	0.10	0.21	0.05	0.18	0.11	0.53
	2.5*	7.8	7.93	7.09	0.21	0.08	0.60	0.58	0.13	0.20	0.04	0.19	0.13	0.51
	4.0	9.9	8.20	8.08	0.26	0.20	0.96	0.70	0.09	0.20	0.19	0.25	0.26	0.89
	3.3	10.5	7.96	7.76	0.41	0.28	0.90	0.80	0.13	0.39	0.41	0.36	0.42	0.90
	3.1	11.2	7.70	7.48	0.40	0.37	0.94	0.77	0.12	0.42	0.59	0.37	0.51	0.96
	3.1	12.3	7.34	7.38	0.43	0.34	0.96	0.78	0.17	0.42	0.47	0.39	0.50	1.01
Fuel picked up 100' from cart	52	?	---	4.14	0.77	---	0.98	1.11	1.33	---	0.84	0.74	0.78	0.98
	47	?	---	7.79	0.31	---	0.76	1.15	0.96	---	0.32	0.24	0.41	0.76
Sampling trays 1000 ft	---	---	---	12.2	0.06	0.17	0.58	---	---	---	---	---	0.16	0.44
2000 ft from test site	---	---	---	12.4	0.03	0.14	0.53	---	---	---	---	---	0.11	0.38
				Average:	0.28	0.18	0.76	0.72	0.33	0.28	0.31	0.31	0.30	0.70

*Gas passages lined with niobium carbide.

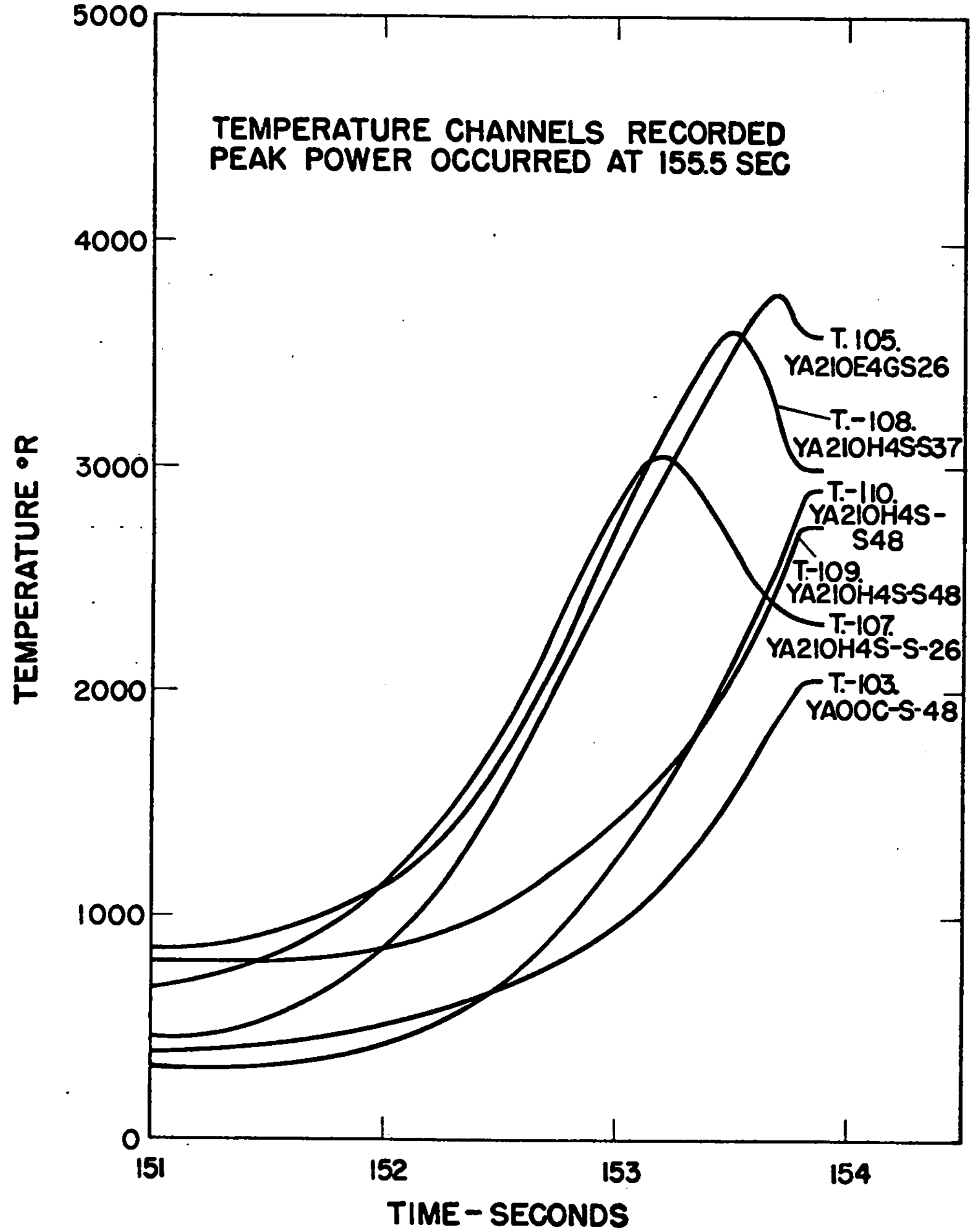

Figure 4-8. Thermocouple Measurements

The curves should be accurate to approximately 60% of the maximum reached. The initial scatter is due to improper zero suppression on the thermocouple channels. Two dummy thermocouples (210E4G-S26 and 00C-S26) utilizing tungsten-tungsten junctions gave no noise or radiation pickup indications during the time interval shown in Figure 4-8.

b. Brightness Temperature Measurement

Brightness temperatures (3750 to 6750 Å) shown in Fig. 4-9 were obtained by three calibrated cameras.[6] The Photo-Sonic camera results are considered more reliable and indicate a maximum brightness temperature of 3520°K at 10 msec. A calibrated grating spectrograph recorded the spectral brightness (4000 to 6900 Å) as a function of time[7] as shown in Fig. 4-10. The maximum brightness temperature observed was 3200°K at 25 msec. The observed spectrum was generally a continuum with a few broad absorption bands. An early absorption band at about 5900 Å could be due to the high pressure C_2 system but this cannot be conclusively confirmed. The early attenuation of green and blue wavelengths may be due to self absorption or CO absorption bands. At 30 msec several weak absorption features correspond closely to CO band systems. A possible source for the emission band starting at 40 msec is the 5586 Å C_2 system.

The difference between the two measurements of brightness temperatures arises from the difference in the analysis of the two sets of data. The brightest spots of a rather inhomogeneous luminous mass were used in the analysis of the camera data, whereas the spectrograph slit integrated the light emitted by a larger area. It should be pointed out that these measurements provide information on surface temperature only; therefore, a lower limit to the maximum internal temperature.

5. <u>Core Pressures</u>

None of the three measurements made of internal core pressures yielded meaningful results. Apparently these transducers, Physical Sciences Corporation, type PT1021, did not function properly in the radiation environment of the test. The fault is thought to be due to radiation effects upon the transistorized AC demodulators in the bunker rather than in the transducers themselves (see Chapter 2, D-1).

6. <u>Core and Reflector Motion</u>

Core and reflector motion was successfully measured at four axial locations on the outer surfaces of these components using a "shorting" pin technique developed for this test.[8] The displacement vs. time history is shown in Figure 4-11.

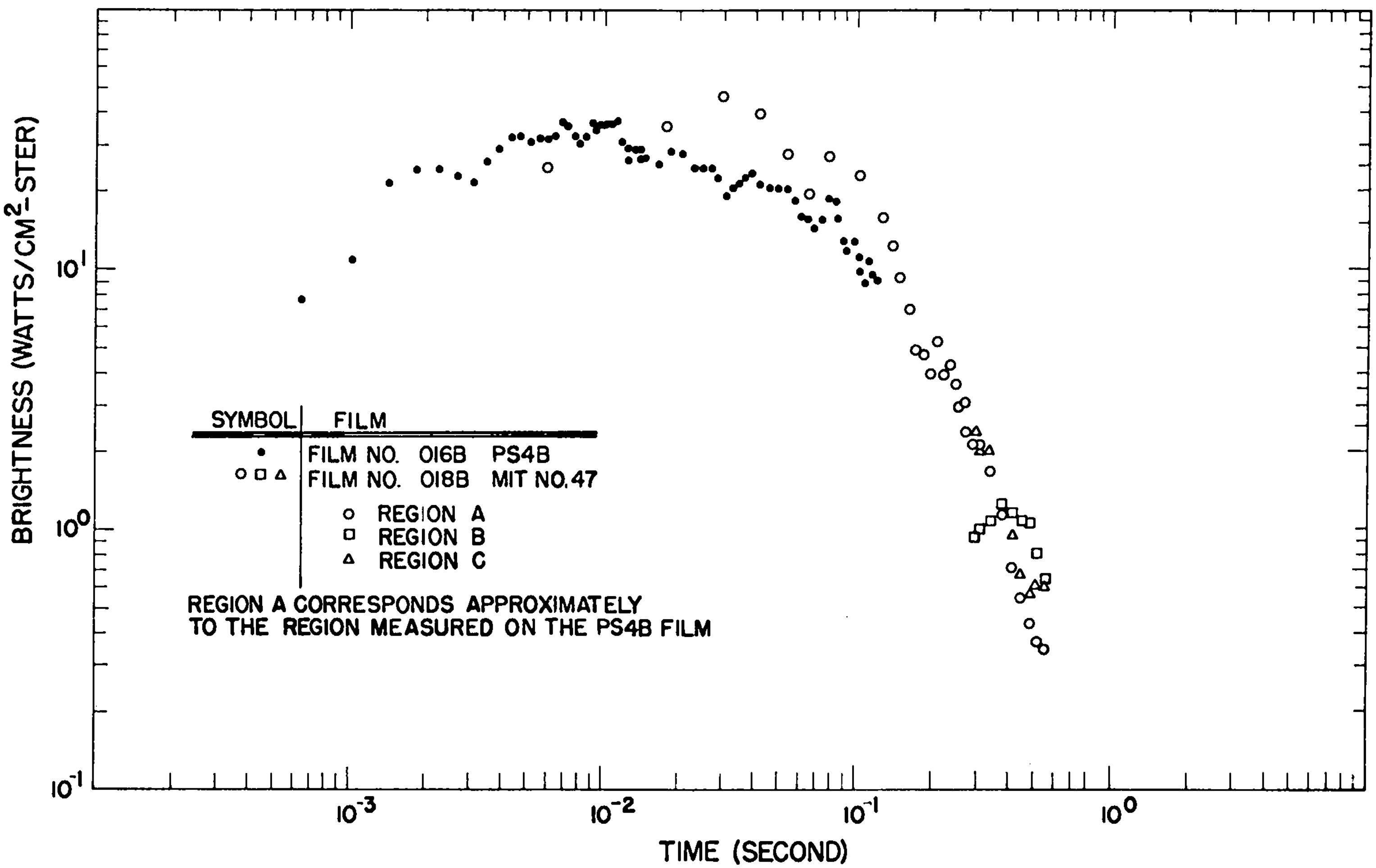

Figure 4-9. Brightness Temperature Measurement

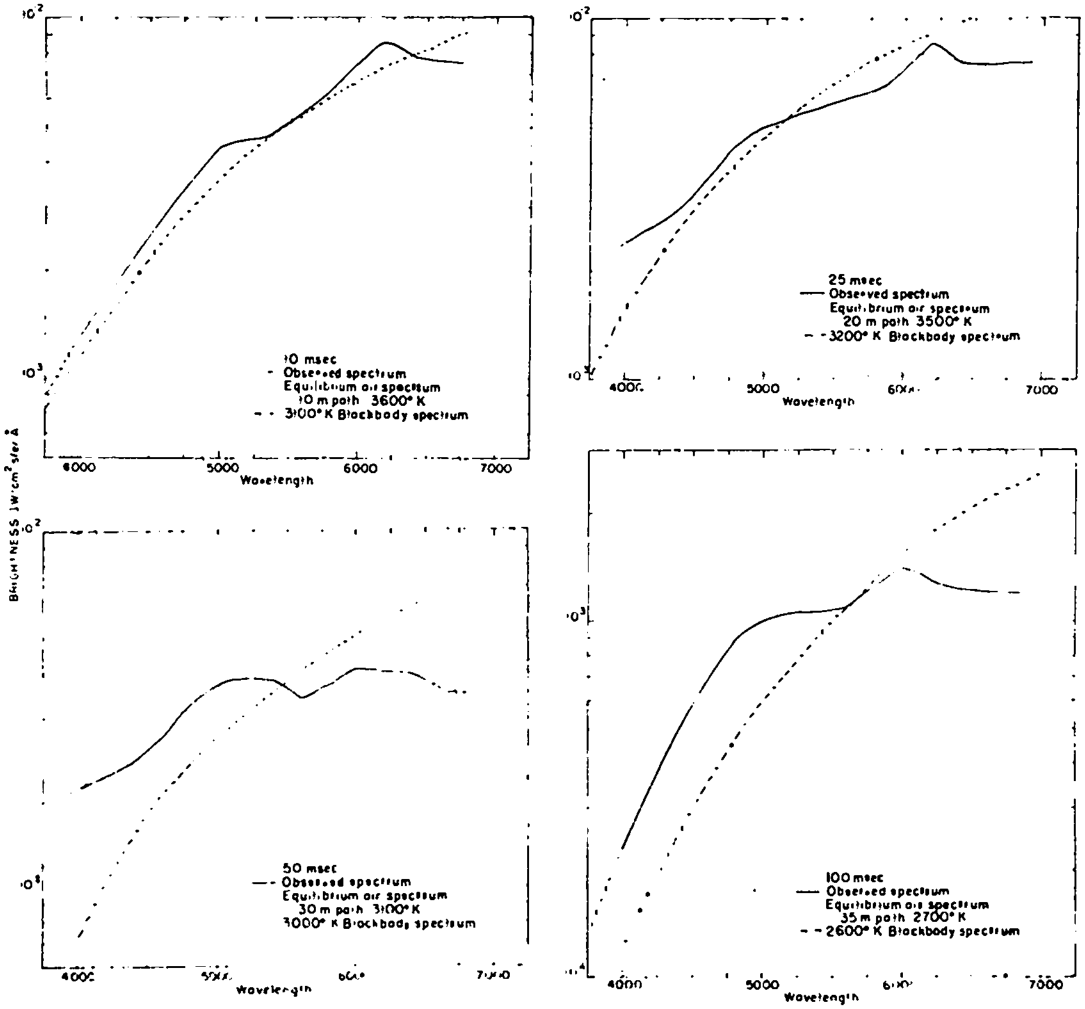

Figure 4-10. Spectral Measurements, Brightness vs. Wavelength

UNCLASSIFIED
APPROVED FOR PUBLIC RELEASE

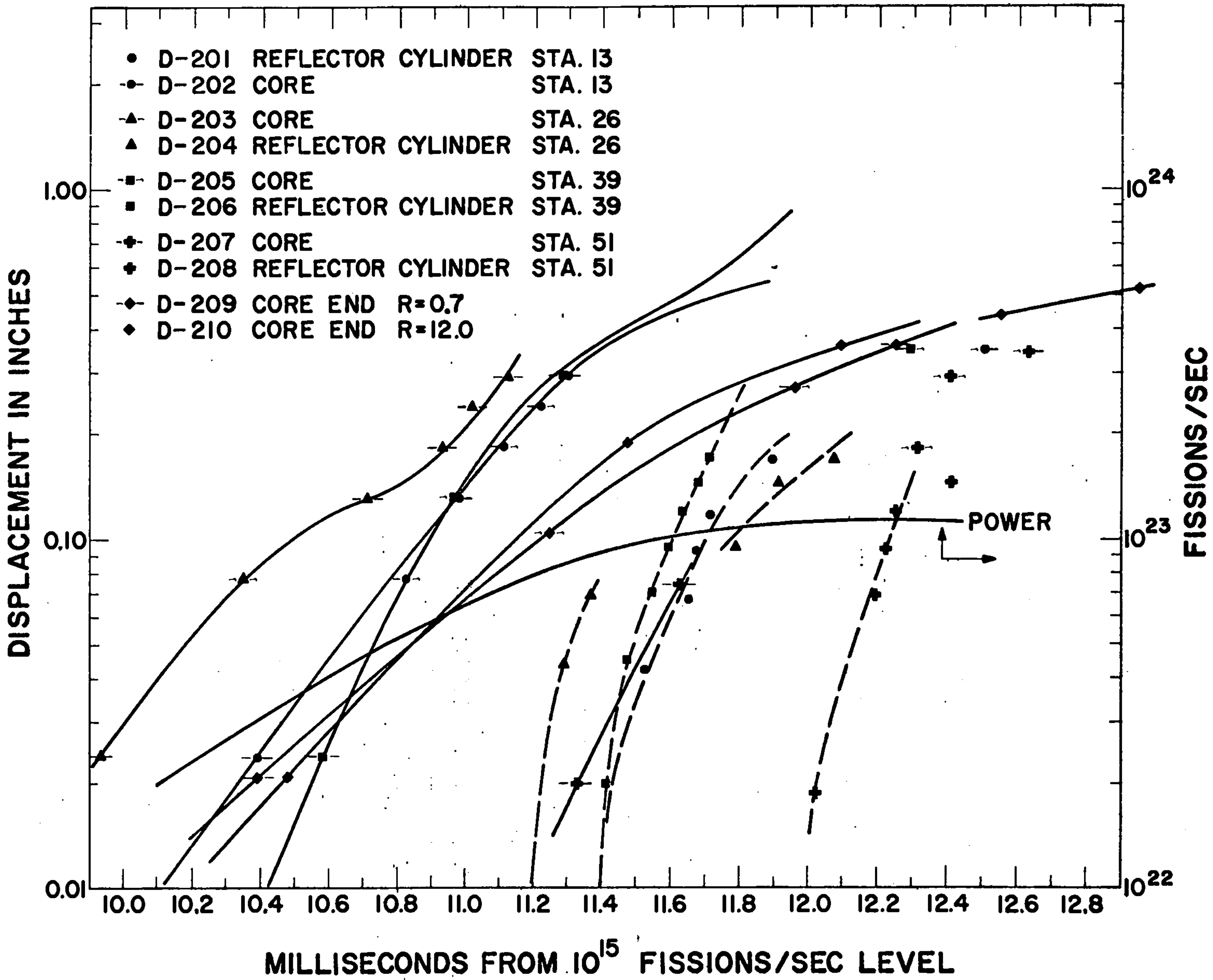

Figure 4-11. Displacement vs. Time History

Core displacement measurements using a linear variable reluctance transducer did not give meaningful data.

7. External Pressure

Dual range variable reluctance pressure transducers placed at two radial (5 ft, 30 ft) positions from the Kiwi-TNT location gave erratic indications starting at the time of peak power and did not yield data. Two sets of unbonded strain gauge pressure transducers were located at 100 feet. One set scaled for ± 0.50 psid full range went full scale at approximately 69 msec after peak power. Two of three pressure transducers set for ± 5 psid indicated approximately 3-5 psi at 69 msec after peak power. All pressure transducers at 100 feet exhibited sensitivity to transient gamma and thermal radiation effects and were quite noisy at the time of the pressure pulse. The pressure pulses decayed with approximately a 10 msec time constant.

8. Radiation Effects

Documentation of the radiation effects was accomplished by integral neutron and gamma dosimetry,[9] gamma dose rate determinations,[10] and air sampling instrumentation.[11]

Integral neutron and gamma dose rates[9] were determined by a large number of neutron threshold detectors and gamma-sensitive glass detectors. The actual integral doses as a function of distance from the test point are shown in Figure 4-12. The integral neutron flux distribution is shown in Figure 4-13.

Isodose radiation contours resulting from the dispersal of debris near the test point are shown in Figure 4-14. The data are normalized to one hour past test time. Similar downrange values are shown in Figure 4-15.

The radiation levels produced by the effluent cloud were measured[12] by a variety of equipment including air samplers, resin-coated trays, and dosimetry systems. These were located at 10° intervals between 180 and 270° on 4000, 8000, 16000, and 32000 feet as well as at approximately 12, 25, and 50 miles. The actual dosages on the cloud centerline at the time of cloud passage are shown in Figure 4-16. Measurements on the activity deposited per unit area are shown in Figure 4-17.

The calculated thyroid dose due to inhalation of iodine isotopes present in the effluent cloud is shown in Figure 4-18.

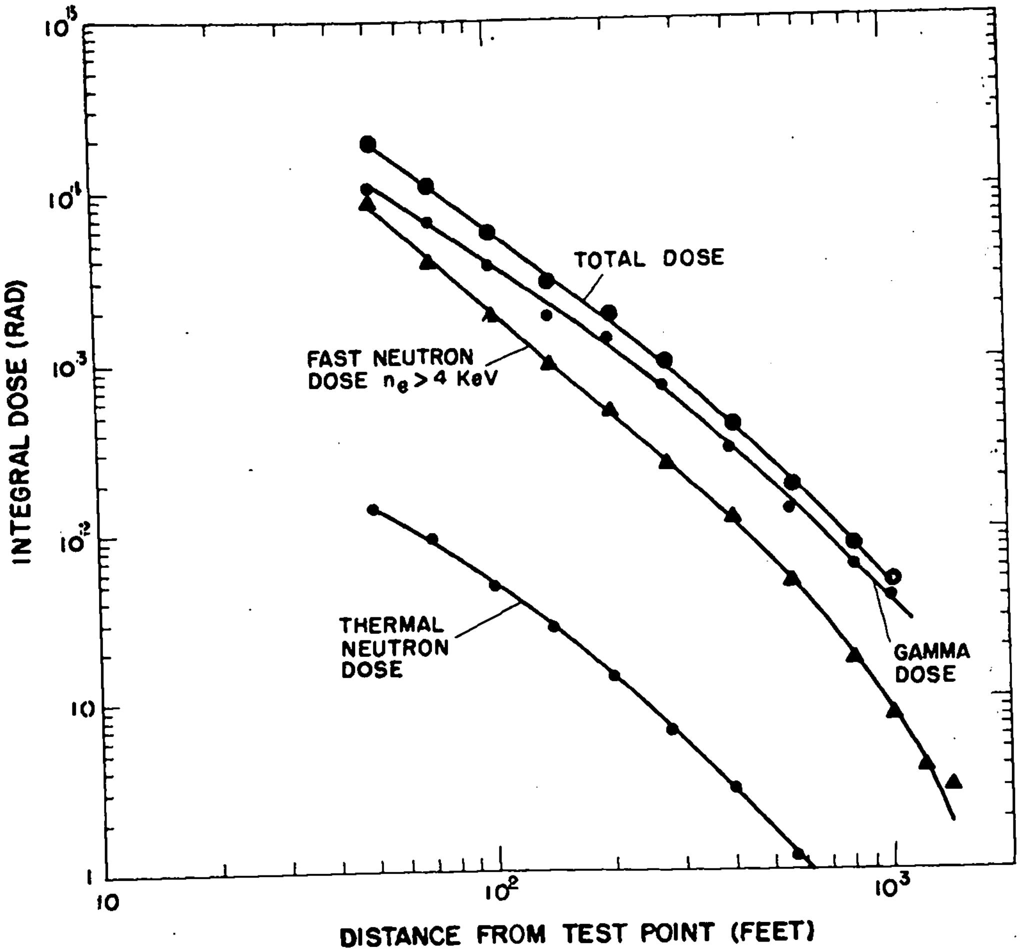

Figure 4-12. Integral Doses as a Function of Distance

[redacted]

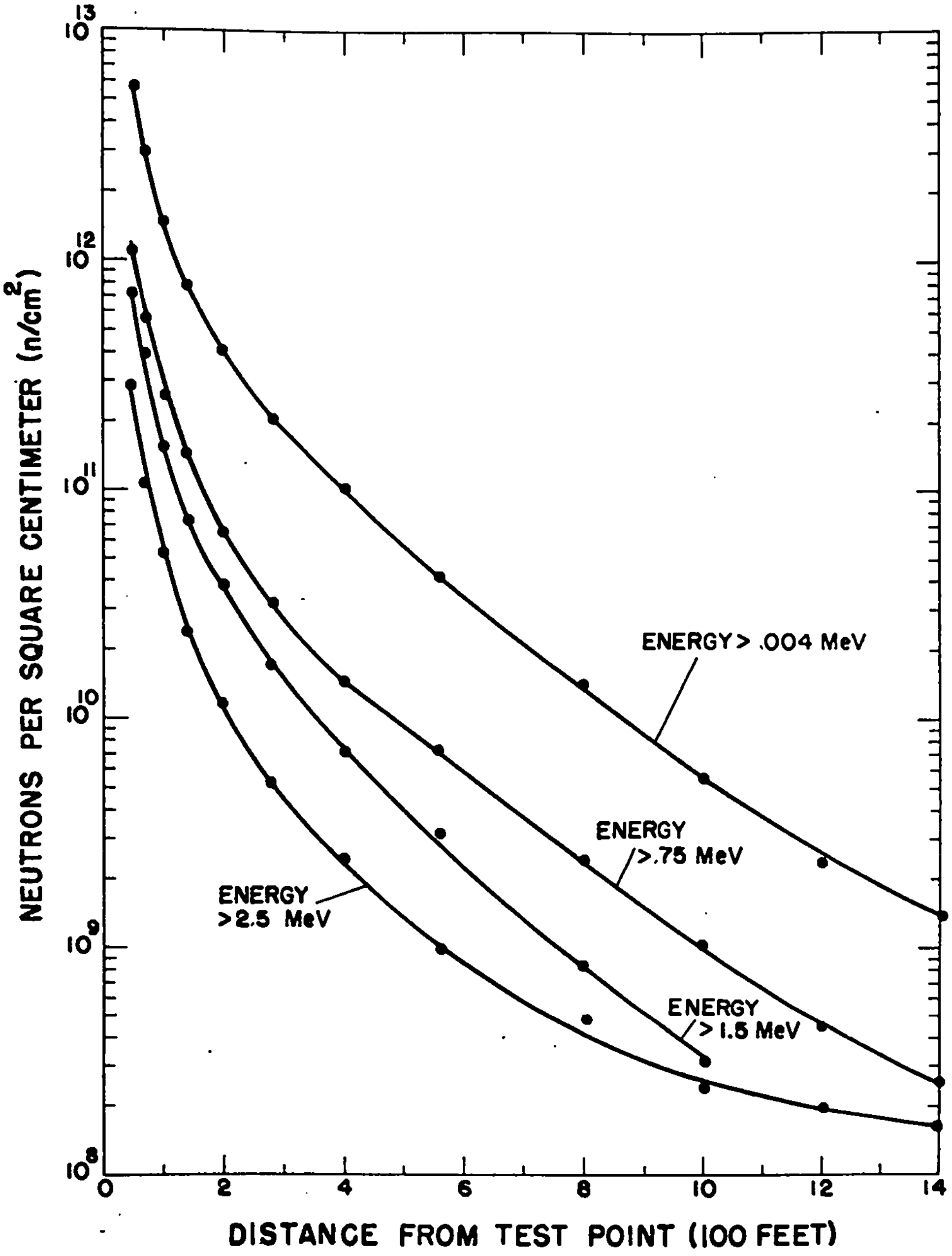

Figure 4-13. Integral Neutron Flux Distribution as Function of Distance

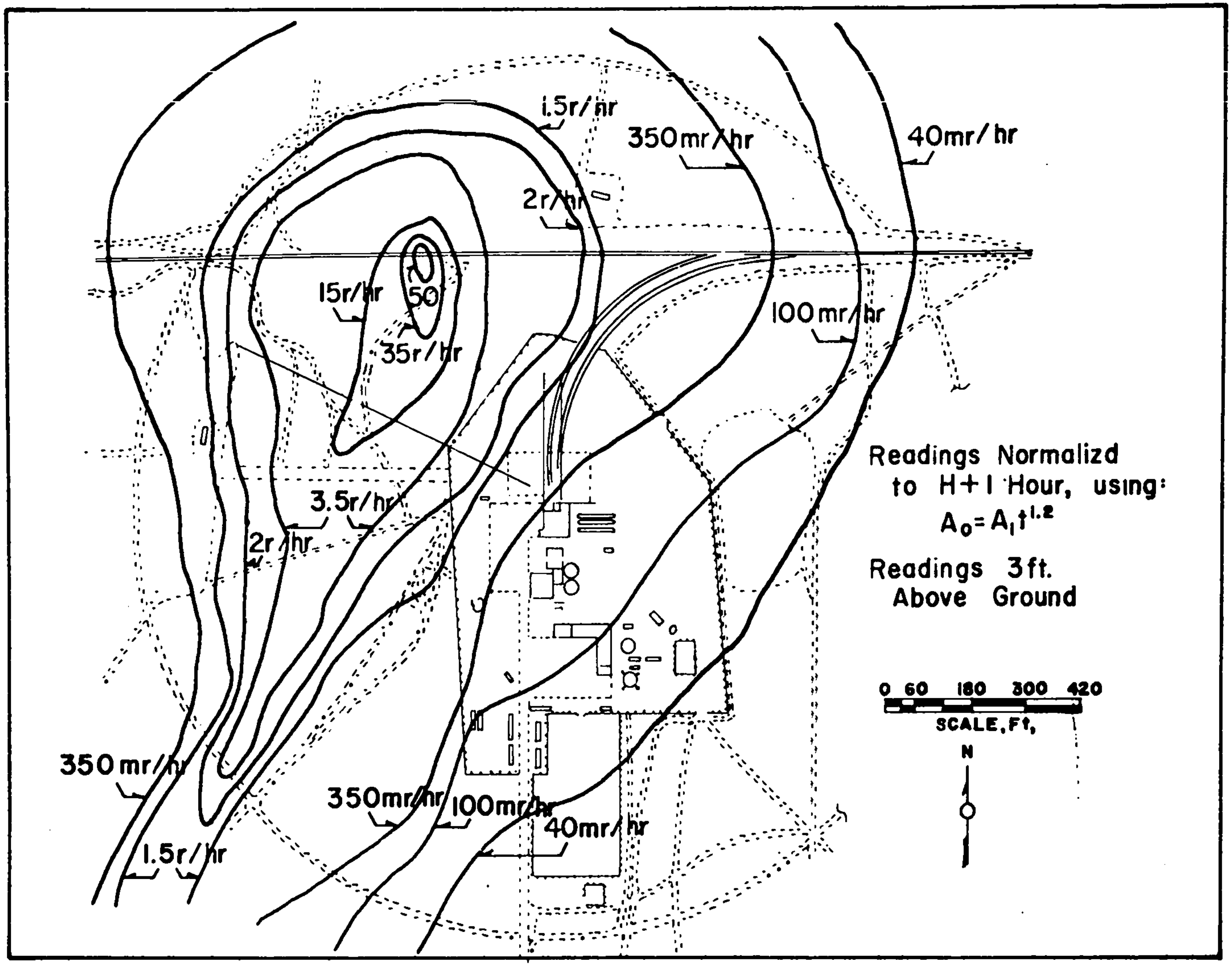

Figure 4-14. Isodose Radiation Contours Near Test Point

[redacted]

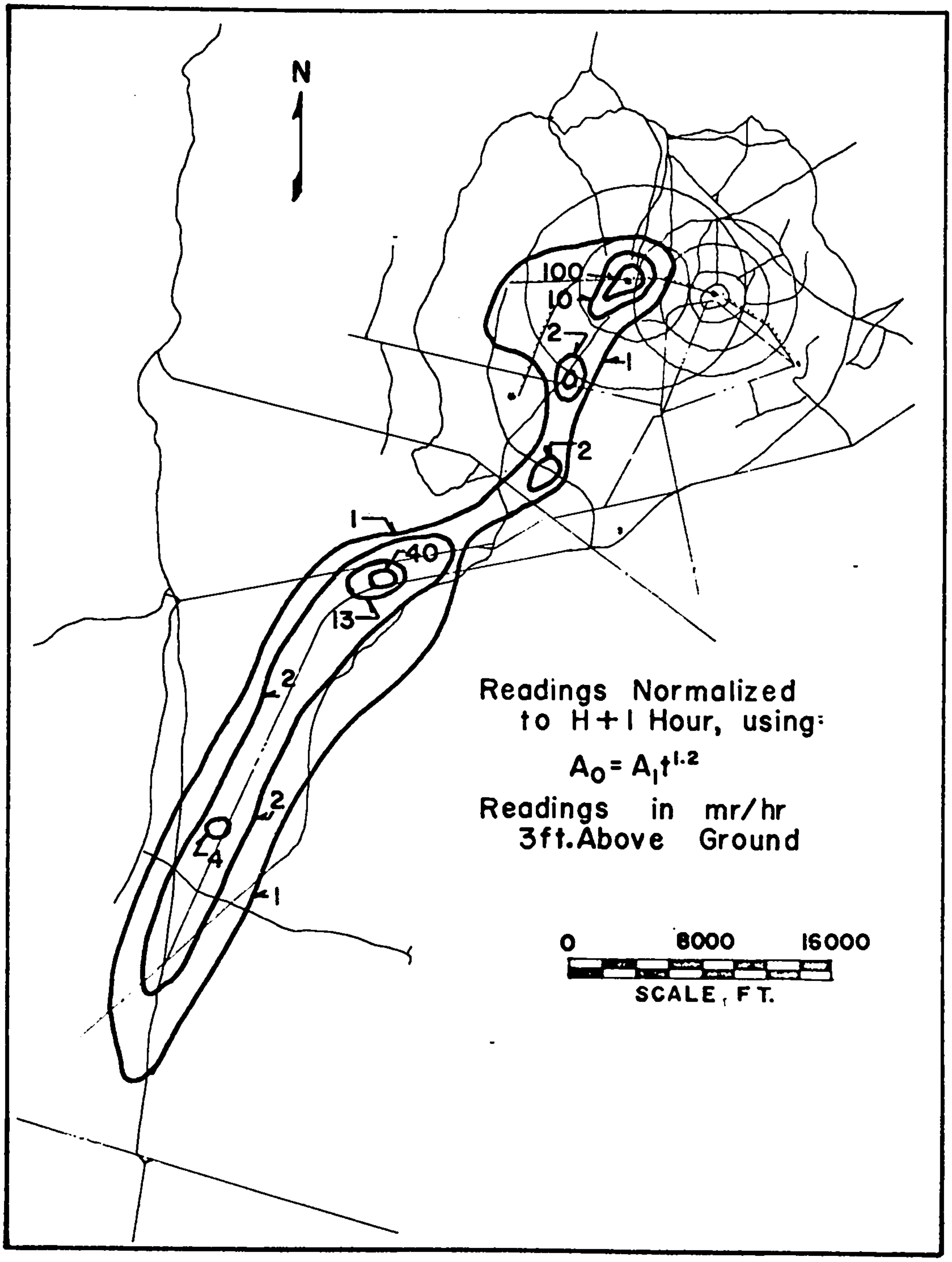

Figure 4-15. Downwind Isodose Contours

[redacted]

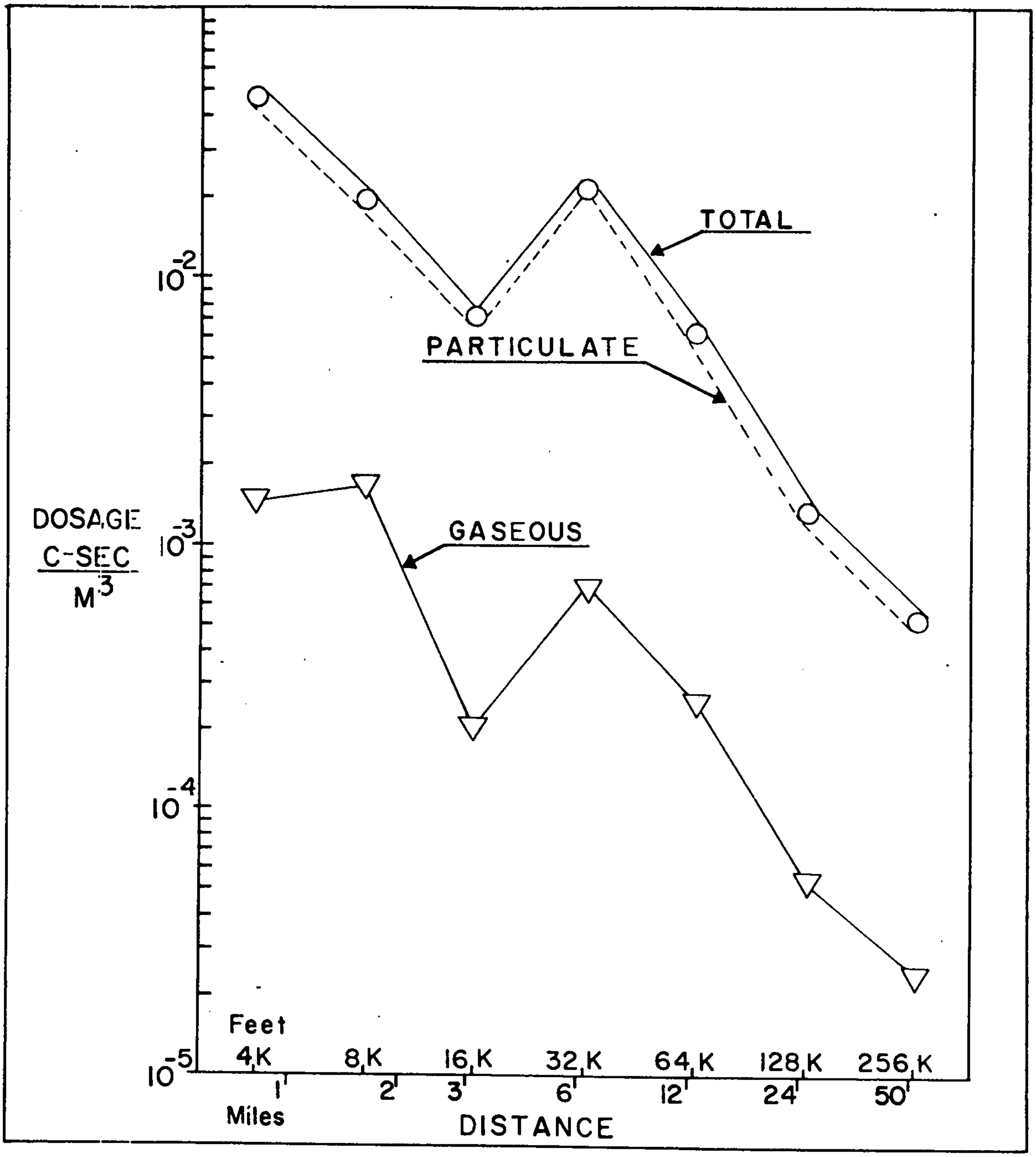

Figure 4-16. Cloud Passage Dose as a Function of Distance Downwind

[redacted]

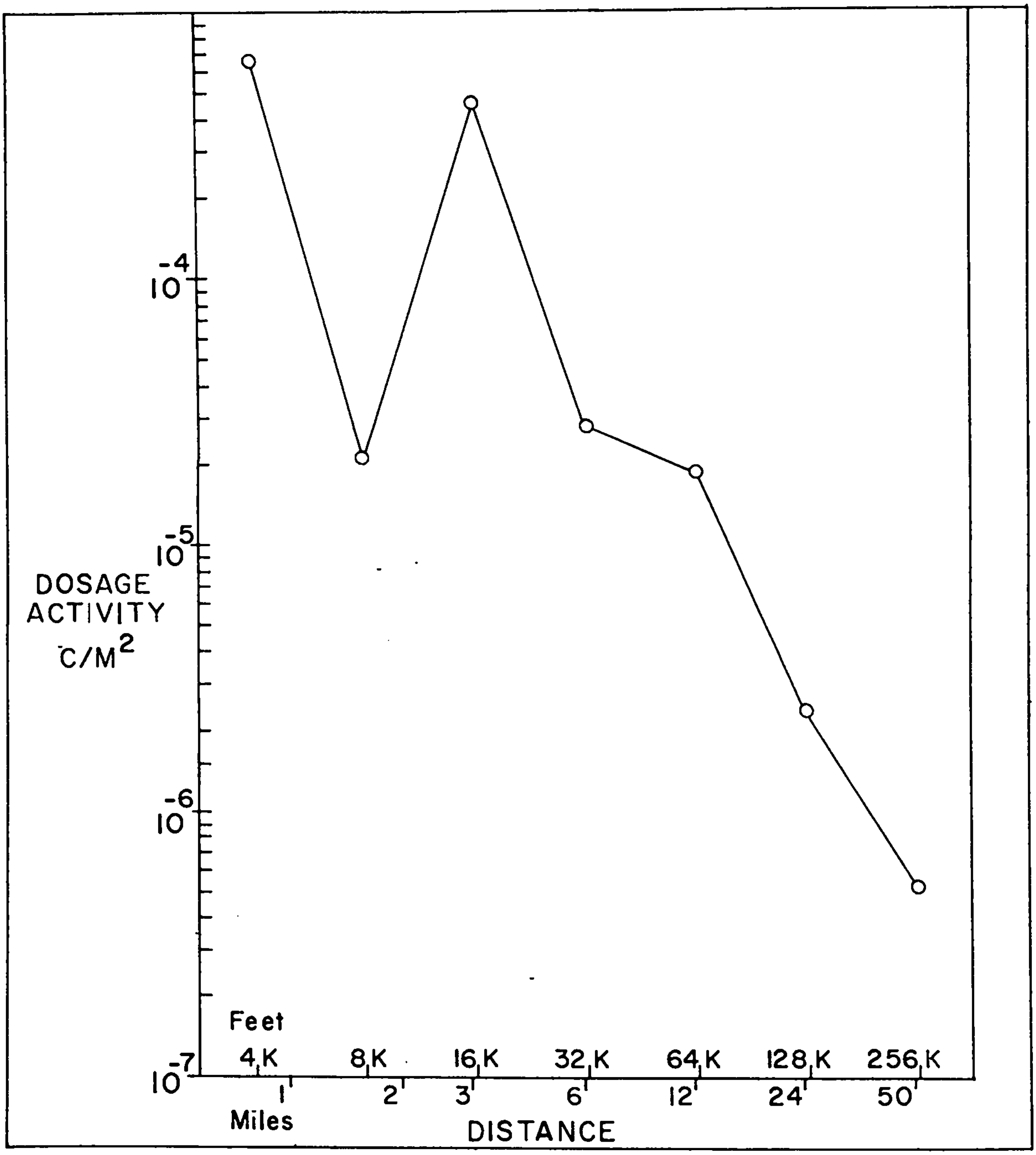

Figure 4-17. Ground Activity as Function of Distance Downwind

[redacted]

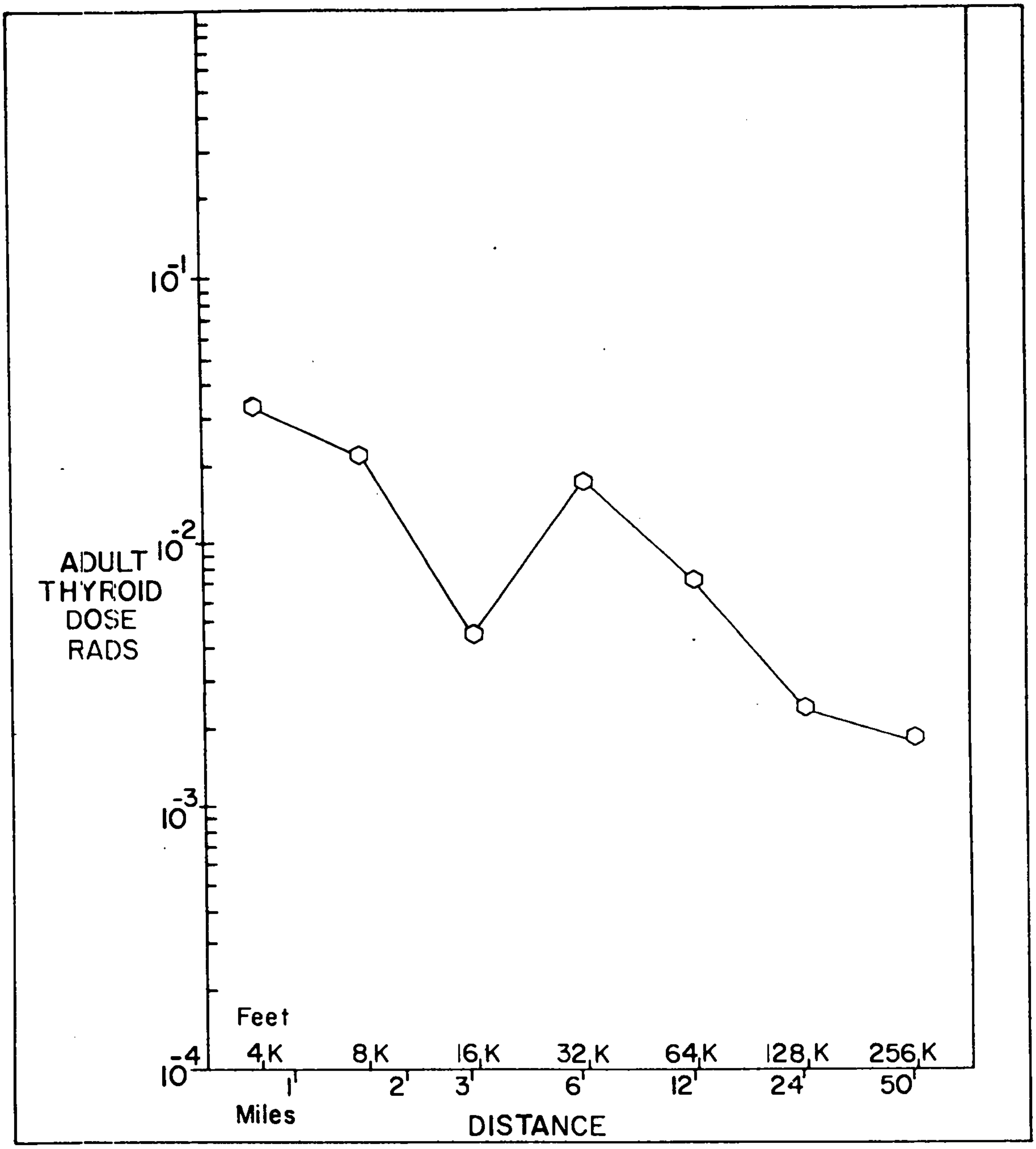

Figure 4-18. Calculated Dose from Iodine Inhalation as a Function of Distance Downwind

9. Cloud Formation and Composition

The rapid insertion of 10^4 MW-sec of thermal energy into the fuel fragmented and partially vaporized the core. After one second the hot vapor and pulverized material was about 150 feet in diameter.

After three minutes the resulting cloud had stabilized at an average height of 2500 feet with a vertical and horizontal diameter of about 2000 feet. Typical views of the excursion at 0.05, 0.5, 1.5, and 5 minutes after initiation are shown in Figures 4-19 through 4-22. Cloud heights at 0.5, 1.5, and 5 minutes are about 650, 1450, and 2600 feet, respectively.

The cloud was elongated vertically with a stem extending toward the ground and was driven downwind at 15 to 25 miles per hour. A wind shear at 6000 feet caused the cloud to separate into two parts which merged again about 12 miles downwind. Figure 4-23 gives the wind conditions which existed during the test and the general direction of the cloud motion.

Two B-47-C aircraft began collecting samples from the cloud at a distance of about one mile from the test site and continued sampling until the cloud had moved about eight miles farther downwind. The first cloud penetration occurred about seven minutes after the test and the last 25 minutes after zero time. Each plane in ten passes collected the fission products from about 10^{14} fissions in each of two wing tip sampling units.

Table 4-4 shows the results of a fission product analysis[9] of a sample collected in the cloud. Within a factor of about 1.5, all fission products were released to the cloud to the same extent. It is estimated from two independent methods that about two-thirds of the refractory materials such as Nd^{147} and Mo^{99} generated in the core were released into the cloud and a larger fraction of some of the more volatile materials. Such a large release is presumably due to the explosive vaporization of the pyrocarbon coated UC_2 fuel beads.

The maximum energy per cubic centimeter of fuel material was sufficient to vaporize only a small fraction of the graphite matrix surrounding the fuel beads. In the region of maximum fission density about one-third of the graphite matrix might have been vaporized while in the minimum energy density region this would be a factor of five lower. Any fine particles of graphite presumably were burned in the air or quickly fell to the ground since no significant amount was detectable in the cloud. An appreciable amount of niobium oxide was present in the cloud from vaporization of the niobium carbide cladding material used on fuel components.

Figure 4-19. Cloud Formation at About 0.05 Minute After Excursion

[redacted]

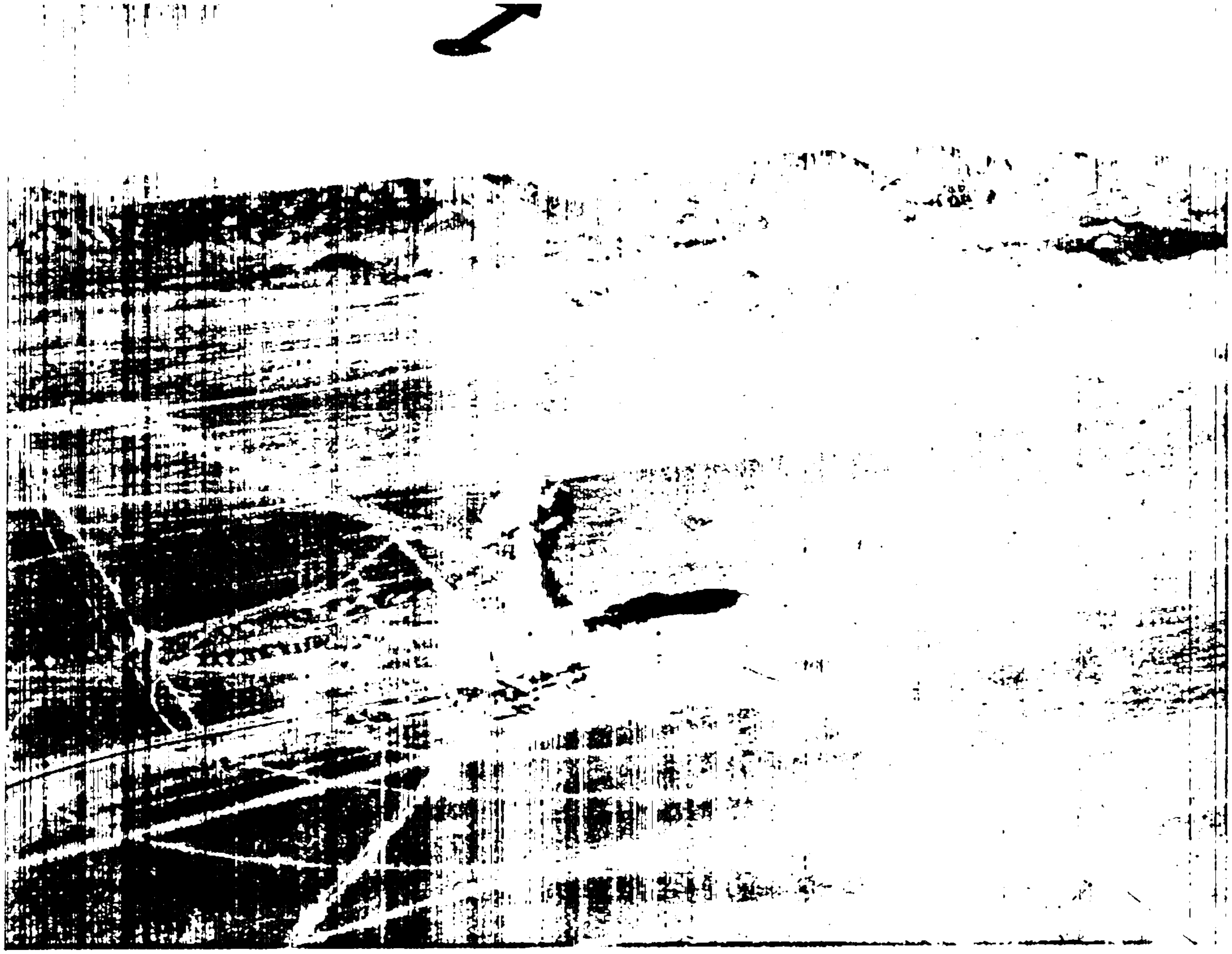

Figure 4-20. Cloud Formation at About 0.5 Minute After Excursion

[redacted]

APPROVED FOR PUBLIC RELEASE

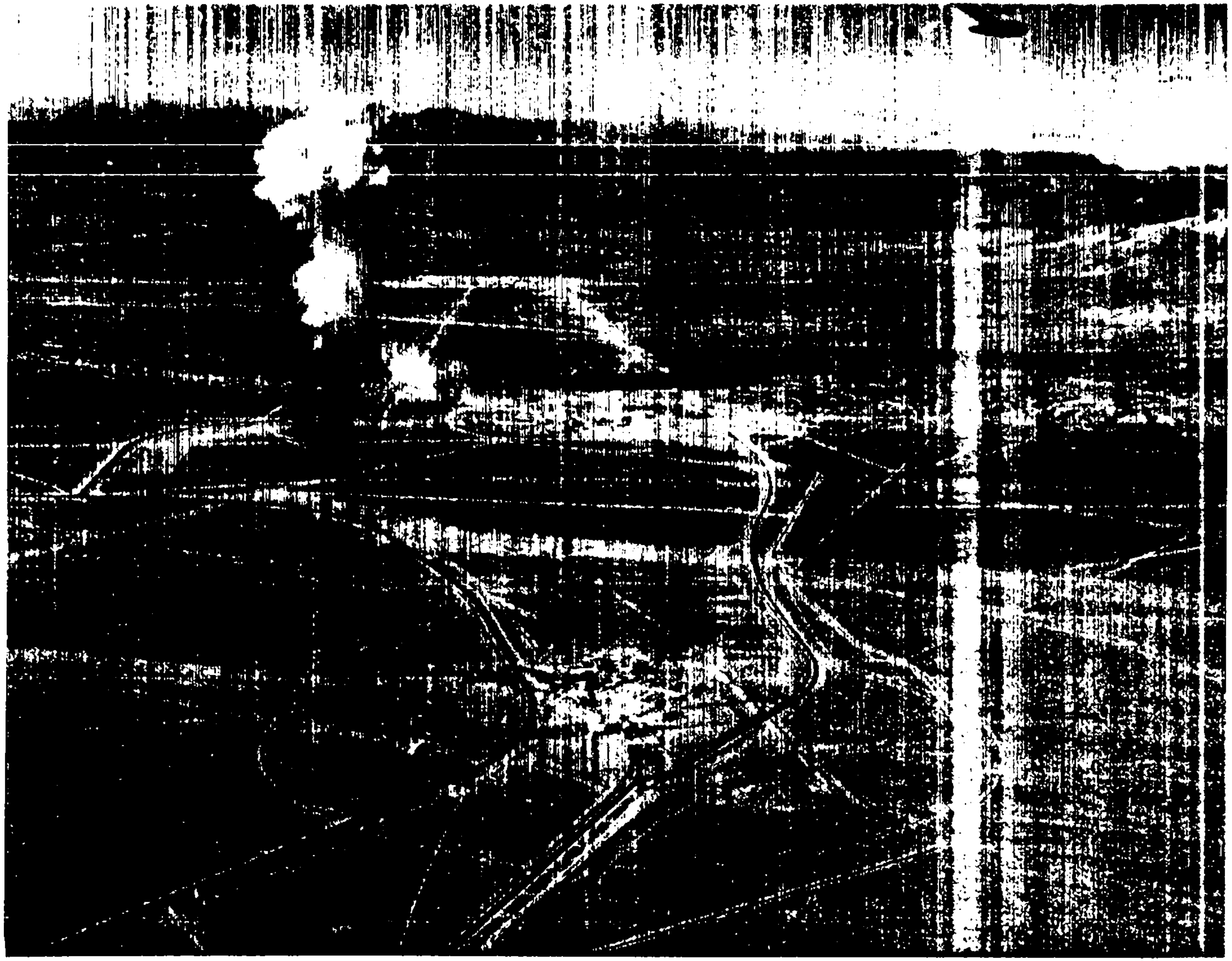

Figure 4-21. Cloud Formation at About 1.5 Minutes After Excursion

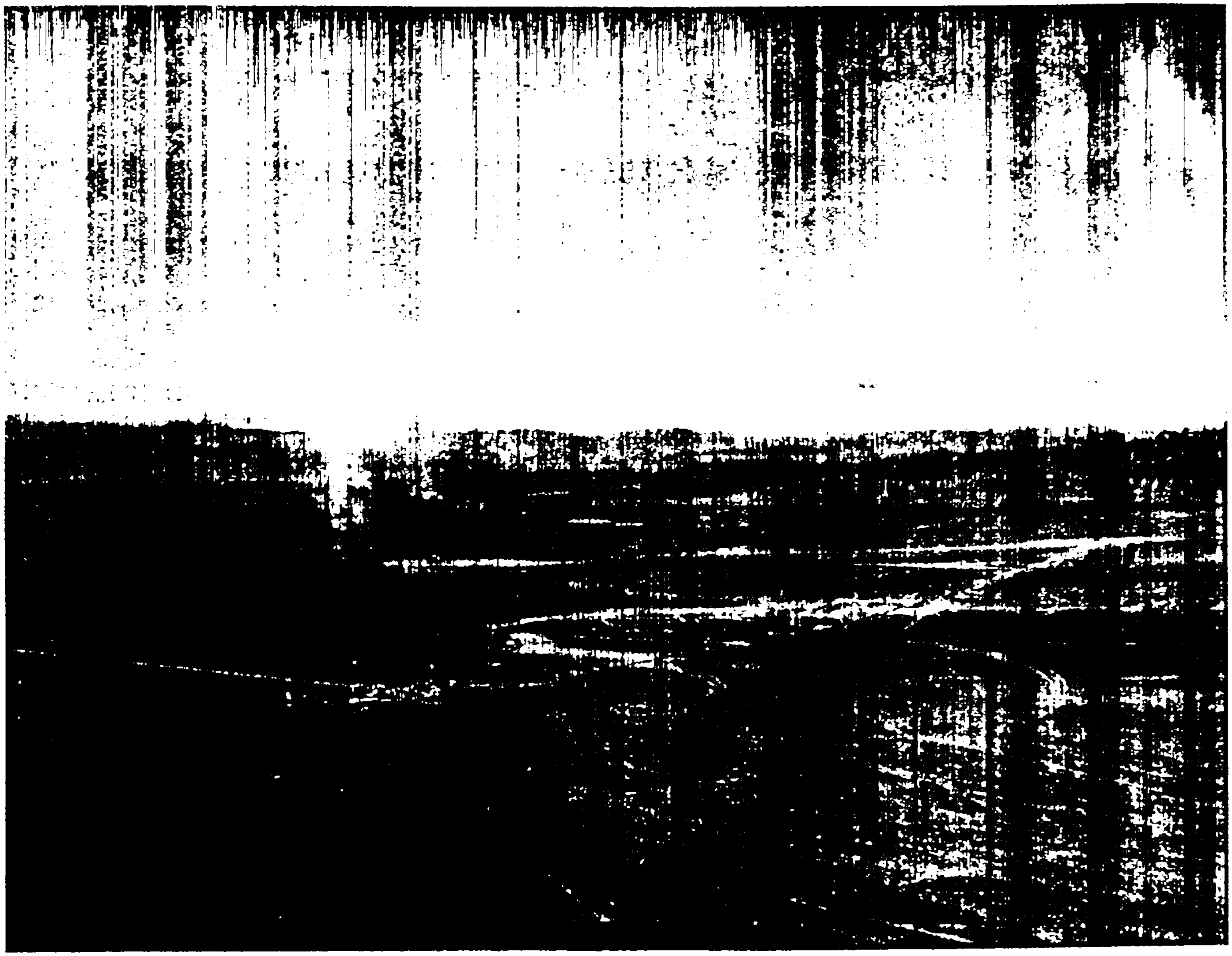

Figure 4-22. Cloud Fromation at About 5 Minutes After Excursion

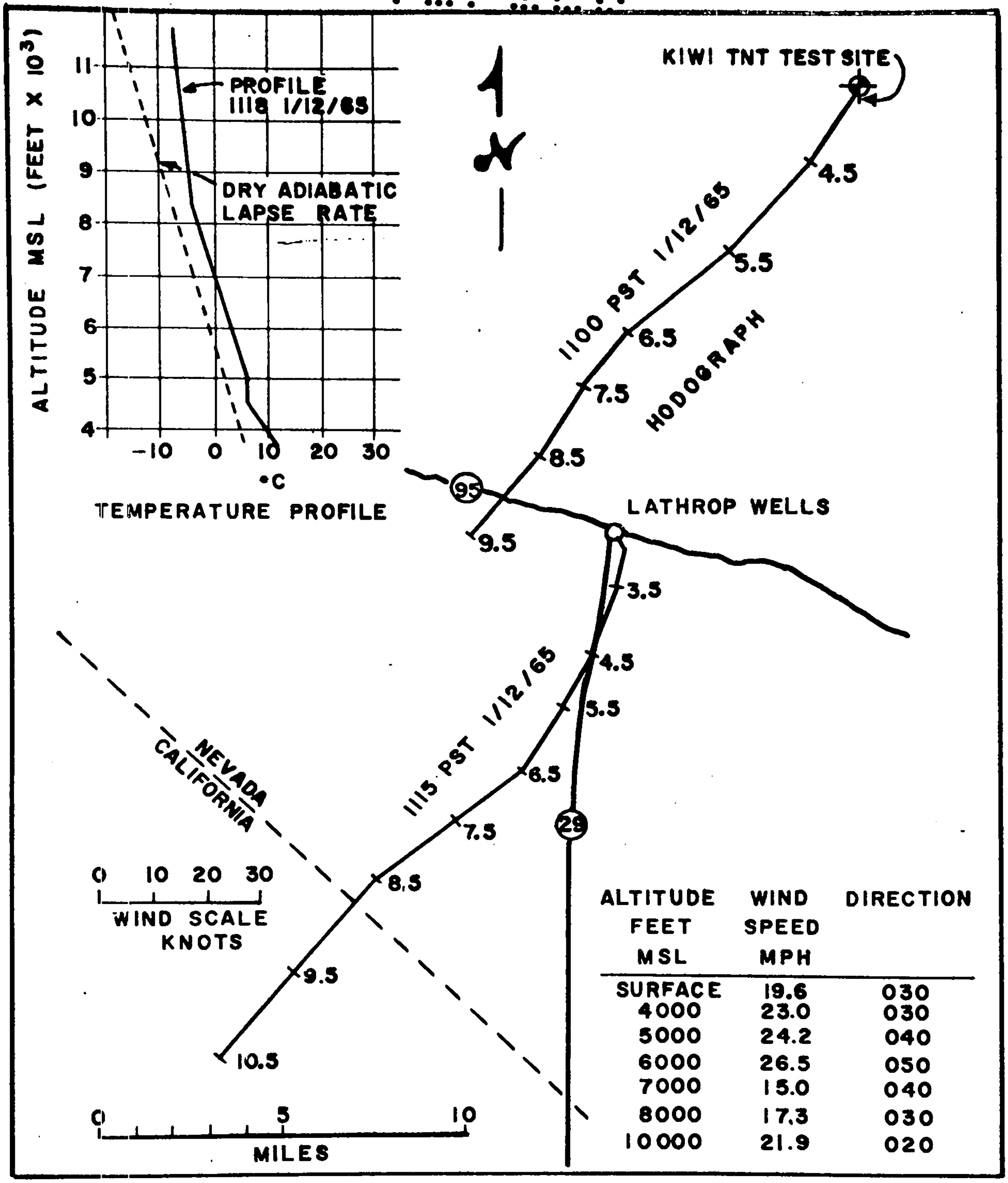

Figure 4-23. Meteorological Information

[redacted]

TABLE 4-4

Results of Analyses of a Sample Collected
From the TNT Cloud by B-57 Sampling Aircraft

Isotope	Ratio to Uranium (fission/gram Oy) (units of 10^{15})	Enrichment Ratio: Ratio to Nd^{147} (fissions/fissions)
Sr^{89}	2.57	1.16
Y^{91}	2.88	1.30
Zr^{95}	2.88	1.30
Mo^{99}	2.22	1.00
Ag^{111}	2.19	0.99
Cd^{115}	2.41	1.09
Sb^{127}	2.87	1.30
I^{131}	--	1.8 - 2.8*
Te^{132}	3.11	1.41
I^{133}	--	1.3 - 1.9*
I^{135}	--	0.6 - 0.8*
Cs^{136}	3.14	1.42
Cs^{137}	2.33	1.05
Ba^{140}	2.88	1.30
Ce^{144}	2.52	1.14
Nd^{147}	2.21	

* Values for I enrichment are qualitative and were obtained by gamma analysis of two pieces of filter paper from the cloud samples.

[redacted]

10. Fragmentation and Particle Study

A considerable effort was expended in evaluating methods and developing technical skills in collecting, sizing, and characterizing particles which resulted from the Kiwi-TNT excursion.

Data on fragment size and distribution were obtained with a wide variety of sampling techniques which included macrotrays, microtrays, resin-coated trays, ground survey, and ground pickup. An evaluation of the collecting techniques and experimental results along with a comparison of the fragment size and distribution with other Rover fuel fragmentation experiments is reported elsewhere.[13]

At least three systems of particles or fragments can be identified from numerous photographs such as shown in Fig. 4-1. The first consisted of the large fragments including particles greater than 0.5 in. The second system of particles are those that were slowly drained from the rising debris, while the third system includes particles adsorbed on the dust and sand which admixed with the debris were deposited downwind.

Six general classes of individual particles were identified in the reactor debris, (1) fuel cores, fuel core shells, and fueled matrix $\leq 3/4$ in. $> 150\ \mu$; (2) fuel core shells and fragments $< 150\ \mu$, fuel cores $< 100\ \mu$; (3) pyrographite pieces with dimpled, flakey surfaces; (4) unloaded graphite 200 μ to 15 in. long; (5) spherical glass balls of fused sand 53 to 2000 μ in diameter; and (6) miscellaneous debris making up 23% by weight of the total sample collected.

The results of these experiments were not expected to be applicable to a deliberate post-operational destruction of a reactor in space due to the large amount of desert debris present and the insufficient magnitude of the excursion for complete fuel fragmentation by uranium bead explosions.

Within a 25,000-ft radius, only about 50% of the core material could be accounted for. The remainder presumably either burned in the air or was so fine as to be carried further downwind in the cloud. The combined distribution data for the material collected is shown in Table 4-5. The average weight in each particle size class was determined experimentally from 100 to 100,000 μ. Fig. 4-24 represents the total weight in each size class for the material that was recovered.

The radioactivity of the larger particles was found to be homogeneous and proportional to the surface area of the particles, presumably due to fuel vapor deposition. The gamma spectrum was essentially the same for all particles except for the case of the glass beads found in the thermally hot cloud which were somewhat enriched within elements in the 140 chain.

[redacted]

TABLE 4-5

Number of Reactor Fragments in Various Size Classes

Size Range Diam, μ			No. of Particles in Size Range	% of Particles in Size Range	% of Particles Smaller Than Upper Size Limit
2.8	-	3.2	7.8×10^{9}	10.44	10.44
3.2	-	6.0	1.2×10^{10}	16.35	26.79
6	-	11	2.4×10^{10}	27.26	54.05
11	-	22	2.1×10^{10}	27.62	81.67
22	-	44	7.6×10^{9}	10.10	91.77
44	-	53	4.0×10^{9}	5.33	97.10
53	-	62	1.0×10^{9}	1.36	98.46
62	-	74	5.2×10^{8}	0.70	99.16
74	-	88	2.6×10^{8}	0.34	99.50
88	-	105	1.3×10^{8}	0.17	99.67
105	-	125	9.4×10^{7}	0.13	99.80
125	-	149	8.5×10^{7}	0.11	99.91
149	-	250	4.8×10^{7}	0.06	99.97
250	-	500	1.1×10^{7}	0.02	99.99
500	-	1000	$1.9\ z\ 10^{7}$		
1000	-	2000	1.1×10^{6}		
2000	-	4000	1.6×10^{5}		
4000	-	8000	6.3×10^{4}		
8000	-	16000	2.6×10^{4}		
16000	-	32000	1.3×10^{4}		
32000	-	64000	6.8×10^{3}		
64000	-	128000	2.8×10^{3}		
		> 128000	1.6×10^{3}		
		Total	7.5×10^{10}		

[redacted]

APPROVED FOR PUBLIC RELEASE

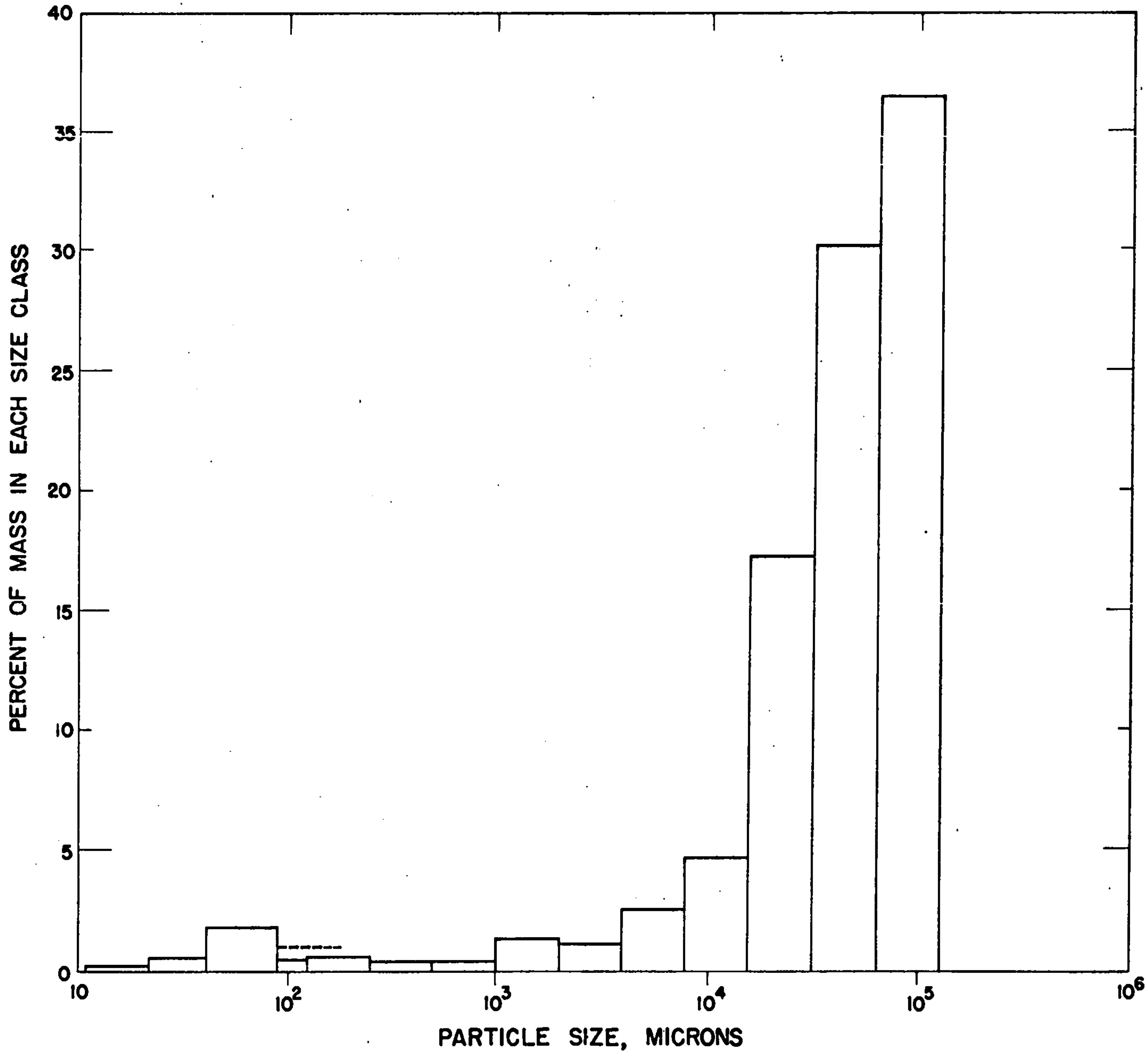

Figure 4-24. Total Weight of Reactor Fragments in Various Size Classes

[redacted]

11. Geographic Distribution of Debris

It is estimated on the basis of the total energy which was produced by the excursion that only 5-15% of the core could have been vaporized. The uncertainty is due to lack of knowledge of the exact isotopic composition of the graphite vapor released under the time-temperature-pressure conditions which existed in the core.

The wind at the time of the experiment affected the geographical distribution of both small and large fragments. A numerical count and geographic location of the larger reactor fragments was obtained. Two categories (fuel elements and unloaded center support elements) were sized and found to fit a normal distribution with a mean value of 0.90 inches and a standard deviation of 1.15 inches. The smallest size was limited to 1/4 inch since this was the smallest fragment that could be easily seen in the field.

For collection purposes of the reactor fragments, the test area was divided into 50 foot, 45° annular sectors from the test point to a 500 foot radius with 250 foot, 45° annular sectors from 500 to 1000 feet. Seven size classes ranging from 1/4 inch to 32 inches were used to categorize the fragments.

Full length fuel elements were nonexistent after the test. The core support plate survived and was the source of identifiable pieces of fuel from the inlet end of the core (Figure 4-25). Most pieces were about 4 inches long. The desert around the test site (Figure 26) was strewn with short pieces of fuel. On many of these pieces a boss, characteristic of the outlet end of the fuel elements, was still visible so that it seems likely that most of these pieces originated from the lower flux region at the upper end of the core.

A large number of graphite support element pieces about 4 inches long were collected as well as fragments of the graphite reflector. Due to the absence of uranium in these fragments, they were not heated to as high a temperature as the fuel or subjected to the internal fragmentation forces produced by the explosion of fuel beads. The fuel plus support element fragments collected accounted for 28% by weight of the initial core material. This included 19% of the initial fuel element material and 74% of the initial support element weight.

For the purpose of debris mapping, the area around the TNT site was divided into seven sections, six 60° sectors plus the area within the TCC perimeter fence. Seven teams were organized to locate, identify, mark, and record the position of reactor debris. Pieces smaller than about three inches in length were not mapped. Position estimates are probably accurate to 5% in overall value. Table 4-6 is the record of debris located in the mapping effort. The position

[redacted]

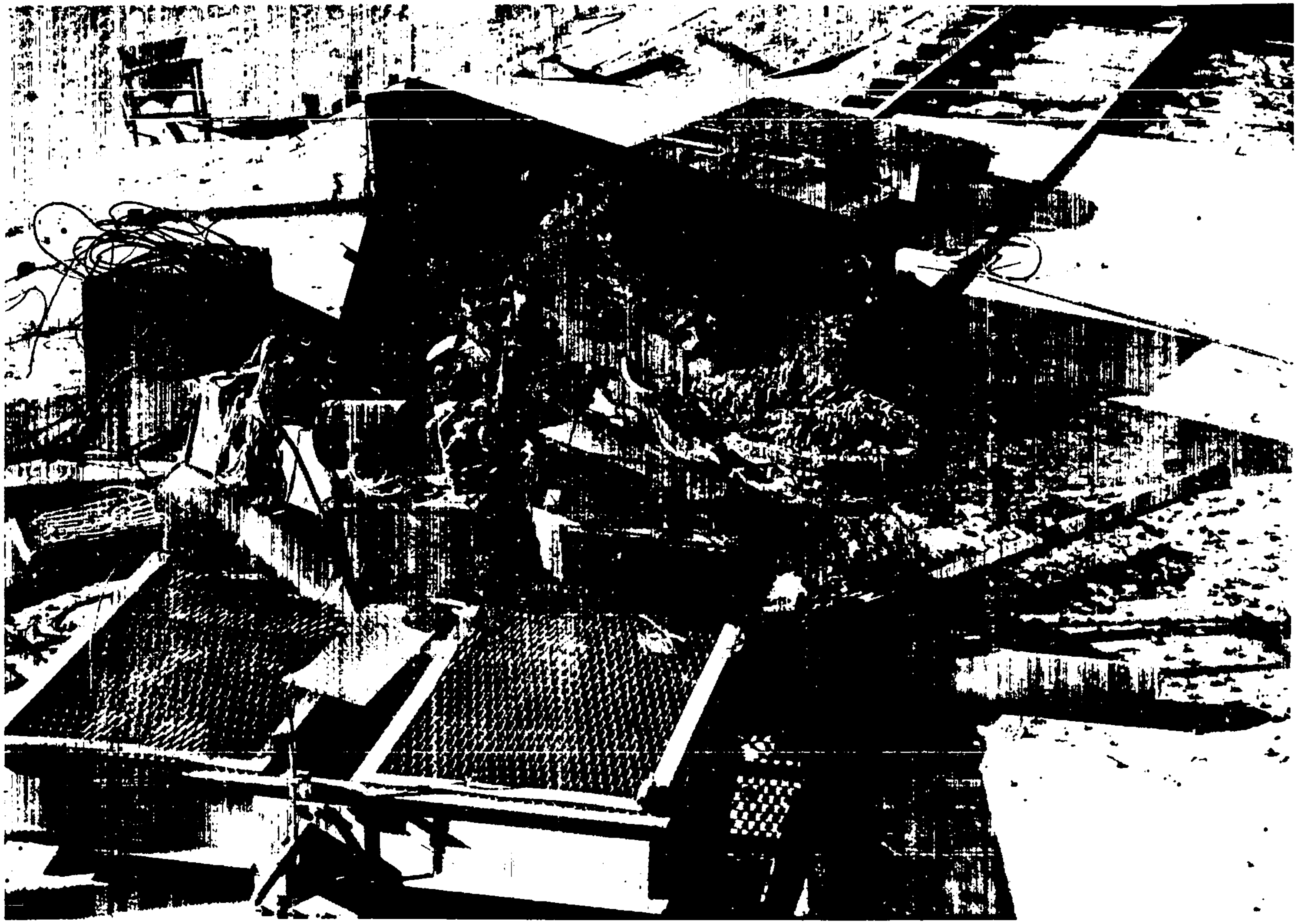

Figure 4-25. View of Test Cart after Excursion

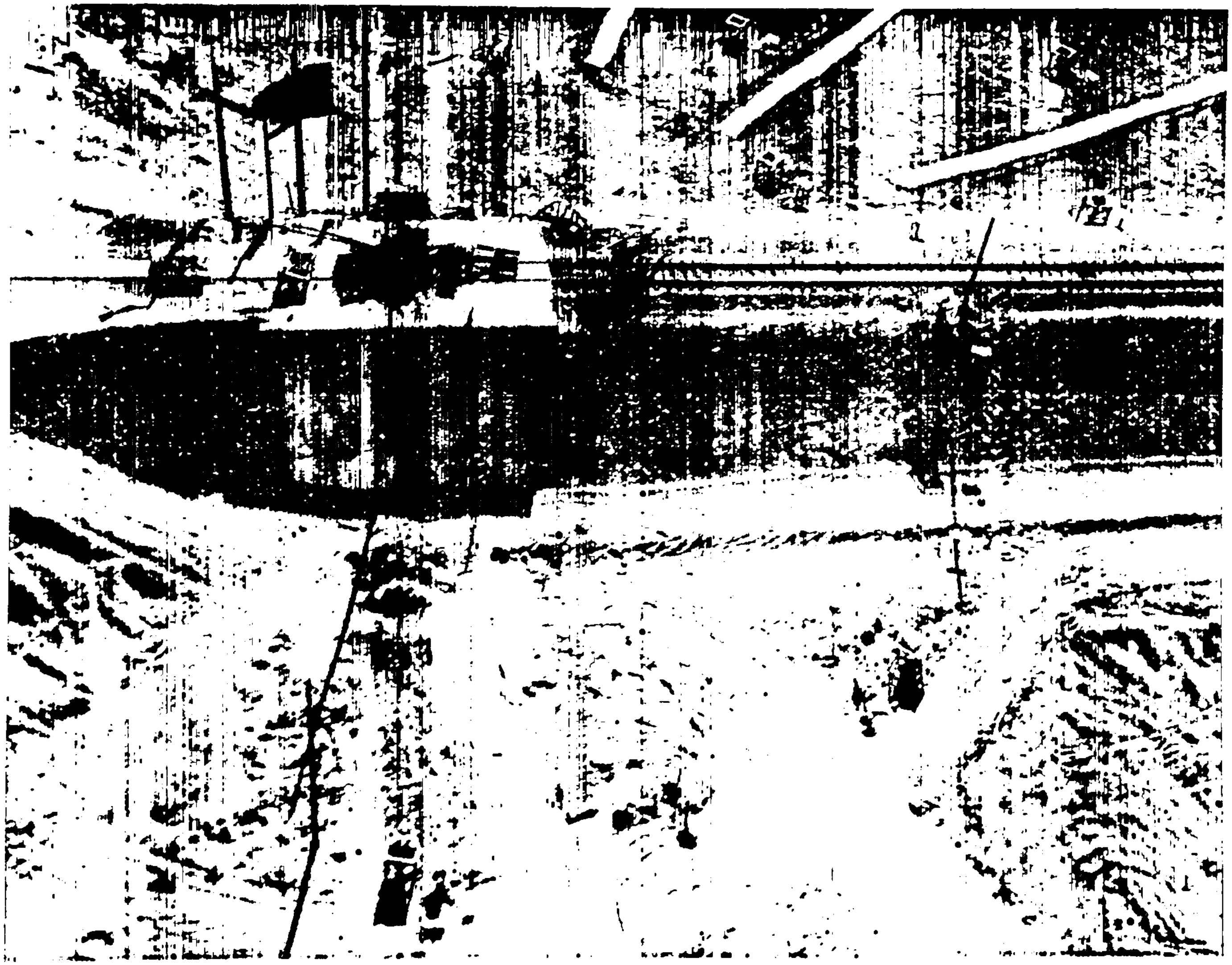

Figure 4-26. View of Test Point Area after Excursion

UNCLASSIFIED
APPROVED FOR PUBLIC RELEASE

TABLE 4-6

Geographic Location of Debris

LOCATION	DESCRIPTION
A-1	Sheet metal with hole
A-2	Mirror mounting plate
A-3	Ring, 4' OD, 3' ID, 3/4" thick
A-4	Pressure vessel section
A-5	Aluminum chunk
A-6	Shim
A-7	Angle
A-8	Angle, 2" x 2"
A-9	Shim, 2' x 3'
A-10	Shim triangle, 4' x 4' x 4' covered with thin aluminum sheet
A-11	Angle 1" x 1" x 3'
A-12	Aluminum, I beam, 1-1/2" x 3/4"
A-13	Aluminum sheet
A-14	Mirror mounting plate
A-15	Bracket with socket screws, 2" x 2" x 30" (Used across top of core to support transducers)
A-16	3' x 3' x 4' with vertical projection
A-17	Aluminum block 4" x 4" x 6"
A-18	Thin metal (Reflector bracket)
A-19	Pressure vessel section, 1' x 2'
A-20	Beryllium reflector sector
A-21	Control rod section, 10" long, 9 lb
A-22	Beryllium reflector sector
A-23	Control rod section 1' long, 9 lb
A-24	Metal piece, 4" x 4" x 6" with 3" hole and cover O-ring (Furnace for fuel sample)
A-25	Graphite reflector cylinder sector 2" x 4" x 6"
A-26	Block, 4" x 4" x 6" with 1-1/2 ft cable attached (Furnace for fuel sample)
A-27	Shiny rod, 1" x 10"
A-28	Block, 4" x 4" x 6" with 3" dia. hole (Furnace for fuel sample)
A-29	Beryllium reflector sector, 2" x 3" x 4"
A-30	Beryllium reflector sector
A-31	Beryllium reflector sector, 2 " x 2" x 8"
A-32	Beryllium reflector sector, 2" x 3" x 3"
E-1	Reflector sector 6" long
E-2	Graphite reflector cylinder sector 3" x 4" x 6"
E-3	Graphite reflector cylinder sector 2" x 3" x 4"
E-4	Flat plate with hole, 6" x 6"
E-5	Reflector sector, 3" cube
E-6	Aluminum pressure vessel section 1/2" x 4" x 6"
E-7	Reflector sector, 1" x 3" x 3"
E-8	Bronze actuator part
E-9	Pressure vessel section, 1/2" x 1" x 6"
E-10	Support block
E-11	Reflector sector, 2" x 3" x 4"
E-12	Reflector sector, 2" x 2" x 3"
E-13	Graphite reflector cylinder sector 2" x 3" x 4"
E-14	Reflector sector, 2" x 3" x 3"
E-15	Reflector sector, 2" x 3" x 3"
E-16	Aluminum actuator parts, 1/4" long x 3" dia.
E-17	Bronze actuator part
E-18	Reflector sector, 2' x 1/2" segment
E-19	Reflector sector, 2" x 2" x 3"
E-20	Reflector sector, 1" x 2" x 2"
E-21	Reflector sector, 1" x 2" x 2"
E-22	Reflector sector, 2" dia.
E-23	Control Rod section, 1' long
E-24	Control rod section, 14" long
E-25	Beryllium reflector sector, 2' x 6"
E-26	Unistrut, 3' long
E-27	Control Rod section, 1' long
E-28	Reflector sector
E-29	Graphite reflector cylinder sector 2" x 2" x 5"
E-30	Channel, 4" x 18" long
E-31	Unistrut, 4' long
E-32	Vane fixture top torus, 3' x 6" wide
E-33	Vane fixture top torus, 3" x 6" wide
E-34	Unistrut, 18" long
E-35	Vane fixture top torus
E-36	Pressure vessel section up from clamp 2' x 2-1/2'
E-37	Aluminum bar, 1' x 1" x 1"
E-38	Sheet metal, 1' x 6"
E-39	Reflector sector, 5" x 5" x 6"
E-40	Aluminum bar, 1' x 1" x 1"
E-41	Aluminum tube, 4' long x 1" dia.
E-42	Metal plate, 3' x 1/4" x 2"
E-43	Top support plate of vane fixture
E-44	Box channel, 3' x 2" x 3" (mirror fixture)
E-45	Ring of vane fixture 90° segment
E-46	Remainder of the top ring of vane fixture
E-47	Aluminum channel, mirror fixture
E-48	Vane fixture pulley and bearing
E-49	Aluminum channel, 4" x 18" long
E-50	Rod drive shaft and bearing
E-51	Sheet metal can, 6" dia.
E-52	Aluminum flash fixture, 3' x 1/8" x 6"
E-53	Actuator parts
E-54	Boral sheet 1' x 1/4" x 8"
E-55	Support block
E-56	Rod drive bearing support
E-57	Vane fixture side support
E-58	Sheet metal, 1' x 2' x 1/16"
E-59	Beryllium reflector sector, 1' x 6"
E-60	Sheet metal, 1/8" x 5" x 8"
E-61	Aluminum sheet, 1' x 1/16" x 8", vane fixture
E-62	Aluminum sheet, 1/16" x 6" x 8", vane fixture
E-63	Mirror mount piece, 8" x 10"
E-64	Reflector sector, 3" x 3" x 4"
E-65	Control rod bearing and shaft
E-66	Upper belt from vane fixture
E-67	Reflector sector, 3' x 6"
E-68	Clamp band segment, 2' long, 17 lb
E-69	1/2 of top hat - mirror fixture
E-70	Boral vane section, 10" x 14"

TABLE 4-6, continued

LOCATION	DESCRIPTION
E-71	Reflector sector, 6" x 10"
E-72	Reflector sector, 6" x 6"
E-73	Reflector sector, 1/2" x 8"
E-74	Slat, 4" long
E-75	Reflector sector, 2" x 3" x 4"
E-76	Reflector sector, 2' x 6"
E-77	Reflector sector, 1/2" x 8", 8 lb
E-78	Graphite reflector cylinder sector, 7" x 8", 3 lb
E-79	Sheet aluminum vane fixture, 1/16" x 8" x 10"
E-80	Graphite reflector cylinder sector, 4" x 7", 3 lb
E-81	Graphite reflector cylinder sector, 4" x 6"
E-82	Reflector sector, 2' x 6", 32 lb
E-83	Sheet aluminum vane fixture, 1/16" x 5" x 8"
F-1	Plate, 1/8" thick, 6" dia. with 12 screws, 3/4" dia. hole in center
F-2	Control rod section, 3" dia. x 1' long 9 lb
F-3	Graphite reflector cylinder sector, 3" x 6"
F-4	Pressure vessel lift ring, 2' long, green
F-5	Plate, 1/8" thick, 8" dia.
F-6	Plate, cylindrical, 1/8" x 3" wide x 8" long
F-7	Graphite reflector cylinder sector, 6" x 18", 29 lb
F-8	Boral sheet, metal, 1/8" x 7" x 16"
F-9	Boral sheet, metal, 1/8" x 6" x 6"
F-10	Boral sheet, metal, 1/8" x 8" x 16"
F-11	Control rod section, 1' x 3" dia., 9 lb
F-12	Wrapper sheet, metal, 1/8" x 7" x 16"
F-13	Control rod part
F-14	Pressure vessel section, 2" x 3" with mounting holes
F-15	Steel rod, 1" dia. x 10" long, No. 881826
F-16	Metal rod, 1' long, 3/8" dia.
F-17	Plate, 1/4" x 6" x 6"
F-18	Pressure vessel section, 5" x 16"
F-19	Pressure vessel band, 5" x 18"
F-20	Control rod section, 1' long x 3" dia., 9 lb
F-21	Plate 1/8" thick, 6" dia. with 12 screws, 3/4" hole in center
F-22	Mirror superstructure
F-23	Unistrut 3'
F-24	Beryllium reflector sector, 1' x 6" x 6", 17 lb
F-25	Pressure vessel band, 16 lb
F-26	Polyurethane piece with sample
F-27	Aluminum channel
F-28	Reflector sector, 7 lbs
F-29	Angle aluminum
F-30	Reflector band
F-31	Bottom piece of pressure vessel, 1' x 3'
F-32	Plate 2' x 6"
F-33	Sheet metal, 2 pieces, one is a clamp
F-34	Part of flash bulb fixture
F-35	Graphite reflector cylinder sector, 6" x 10"
F-36	Instrument box, 2 pieces
F-37	Control rod section, 1' long x 3" dia.
F-38	Plate, 1/8" thick x 6" dia. with 12 screws, 3/4" dia. hole in center
F-39	Poison vane drive motor
F-40	Poison vane fixture
F-41	Pressure vessel section, 2' x 5" x 5"
F-42	Vane assembly, drive screw
F-43	Aluminum strut- channel 4' long
F-44	Sheet metal cover 6" x 10" channel shape
F-45	Sheet metal circle
F-46	Pressure vessel stop net
F-47	Reflector sector
F-48	Plate, 2' x 8"
F-49	Mechanical drive shaft, 1" dia., 2' long
F-50	Angle
F-51	Mechanical rod, 2' long, same as F-49
F-52	Reflector sector, 6" cube
F-53	Plate, 2' x 1/32" x 8"
F-54	Control rod drive part
F-55	Stator and gear box from poison vane
F-56	Pressure vessel, top sector 3-1/2' x 3', green
H-1	Control rod section, 16" long, 9 lb
H-2	Beryllium reflector sector, 6" x 6" x 2', 28 lb
H-3	Control rod section, 14" long, 9 lb
H-4	Control rod section, 12" long, 9 lb
H-5	Beryllium reflector sector, 2' x 6" x 6"
H-6	Beryllium reflector sector, 4" x 5" x 16" 17 lb
H-7	Bracket
H-8	Rod
H-9	Beryllium reflector sector, 5" x 6" x 8" 7 lb
H-10	Ring section 1/2" x 4" x 26"
H-11	Tube, 2" x 8", (A.I. Sample)
H-12	Unistrut and plate, 8' x 1" x 6"
H-13	Plate, 1/16" x 6" x 15"
H-14	Angle, 1" x 1" x 20"
H-15	Drive screw assembly, 6' x 6" x 14"
H-16	Channel, 1' x 2" x 4"
H-17	Channel, 1" x 1" x 16"
H-18	Channel, 2" x 2" x 6"
H-19	Ring section, 1" x 4" x 15"
H-20	Rod, 1-1/2" x 9"
H-21	Bracket, 4" x 7"
H-22	Aluminum chunk, 3" x 3" x 6", 9 lb
H-23	Pressure vessel section, 3" x 1" x 10", red
H-24	Schedule 80 pipe, 4' long, 10" dia. (Gas bottle)
H-25	Pressure vessel band, 4' x 1/2" x 5"
H-26	Boral, 1' x 1/4" x 10"
H-27	Dome ring, 1" x 4" x 18" (clamp band segment)
H-28	Bracket, 3' x 1" x 8" (2, 1-3/4" bolts thru)
H-29	Beryllium reflector sector, 5" x 6" x 14", 19 lb
H-30	Beryllium reflector sector, 6" x 7" x 10"
H-31	Control rod section, 1' long, 9 lb
H-32	Control rod section, 14" long, 9 lb
H-33	Beryllium reflector sector, 3" x 4" x 13", 16 lb
H-34	Pressure vessel section, 3' x 3/4" x 18", red
H-35	Beryllium reflector sector, 6" x 6" x 14", 15 lb

TABLE 4-6, continued

LOCATION	DESCRIPTION
H-36	Gear section, 8 " dia.
H-37	Band, 1" x 3" x 18"
H-38	Unistrut, 5' x 1" x 1-1/2"
H-39	Beryllium reflector sector, 4" x 6" x 6", 8 lb
H-40	Beryllium reflector sector, 4" x 6" x 8", 10 lb
H-41	Pressure vessel section, 3/4" x 14" x 18" 24 lb, red
H-42	Beryllium reflector sector, 6" x 6" x 18", 23 lb
H-43	Control rod section, 12", 9 lb
H-44	Control rod section, 12", 9 lb
H-45	Cylinder, 11" long (AGC sample)
H-46	Beryllium reflector sector, 2' x 4" x 6", 31 lb
H-47	Beryllium reflector sector, 4" x 4" x 10", 9 lb
L-1	Control rod section
L-2	Metal angle
L-3	Rod drive shaft
L-4	Reflector sector, 12 lb
L-5	Metal angle
L-6	Electrical harness
L-7	Electrical gutter
L-8	Grader car (toonerville trolly)
L-9	Grader blade (toonerville trolly "cow catcher")
L-10	Part of grader car
L-11	Pipe, 7" long (A.I. Sample)
L-12	Aluminum angle
L-13	Aluminum angle
L-14	Experiment capsule (AGC sample)
L-15	Metal angle
L-16	Control rod support
L-17	Metal plate
L-18	Metal angle
L-19	Pin
L-20	Experiment cannister (AGC sample)
L-21	Metal angle
L-22	Pipe (A.I. sample)
L-23	Metal angle
L-24	Control rod support
L-25	Experiment cannister (AGC sample)
L-26	Unknown
L-27	Metal angle
L-28	Control rod section, 6 lb
L-29	Control rod section, 10 lb
L-30	Reflector sector sector, 2' x 6"
L-31	Pressure vessel section, 63 lb
L-32	Angle, 4' x 1-1/2"
L-33	Angle
L-34	Clamp band section, 15 lb
L-35	Angle
L-36	Pipe (A.I. Sample)
L-37	Flow separator section, 8 lb
L-38	Reflector sector, 29 lb
L-39	Pressure vessel section, 48 lb
L-40	Control rod section, 9 lb
L-41	Control rod section, 9 lb
L-42	Experiment cannister (AGC sample)
L-43	Pressure vessel section, 22 lb
L-44	Experiment cannister (AGC sample)
L-45	Control rod support, 2 lb
L-46	Reflector segment support
L-47	Reflector sector, 11 lb
L-48	Control rod section, 9 lb
L-49	Reflector sector
L-50	Reflector sector
L-51	Reflector sector, 33 lb
L-52	Experiment sample
L-53	Reflector sector
L-54	Control rod section, 9 lb
N-1	Metal angle, 1" impact damage on fallout collector tray
N-2	Angle, 3/4" x 8" long
N-3	Aluminum retainer plate, clamp, 3' x 1" x 14"
N-4	Aluminum plate, 1' x 1/32" x 8"
N-5	Aluminum angle, 2-1/2' x 1/4" x 1/2" x 1-1/2"
N-6	Aluminum angle, 2' x 1/2" x 2" x 2"
N-7	Aluminum angle, 1/8" x 3/4" x 3/4" x 8"
N-8	Aluminum plate, 1/4" x 6" x 8"
N-9	Aluminum angle, 1/8" x 1-1/4" x 8" long
N-10	Aluminum angle, 1/4" x 1-1/4" x 1-1/4" 10" long, buckled
N-11	Aluminum plate, 1/4" x 8" x 16", mirror mounting plate
N-12	Aluminum plate, 1/4" x 4" x 6", mirror mounting plate
N-13	Aluminum plate, 1/4" x 3" x 6", mirror mounting plate
N-14	Aluminum T 3/8" x 2" x 2-1/2" x 8" long
N-15	Boral piece, 15' long, looks like section of piping opened up
N-16	Piece of foam angle, 18"
N-17	Unistrut, 1" x 2" x 30"
N-18	Large piece of mirror mount consisting of 8" channel, 4" angle, 1" plate, 1/4" webbed plate, 200 lb
N-19	Web plate, 1' x 1/4" x 10", mirror mounting plate
N-20	Web plate, 1/4" x 16" x 20", mirror mounting plate
N-21	Rod drive shaft, 1-1/4" dia. x 6" long
N-22	Angle, 3/4" x 15" long
N-23	Foam, 6" x 14"
N-24	Unistrut, 3' long
N-25	Control rod section, 1' long
N-26	Stainless steel center rod
N-27	Stainless steel center rod
N-28	Reflector segment end plate
N-29	Flash bulb mounting pieces - light sockets and wiring
N-30	Reflector sector, 4" x 6" x 7", 9 lb
N-31	Bolt circle section of pressure vessel, 4" high x 20" long
N-32	Angle, 4' x 3/4"
N-33	Unistrut, 15" long
N-34	Lift bail on pressure vessel, 4" x 20"
N-35	Reflector sector, 1' x 4" x 5", 15 lb
N-36	Reflector sector, 1' x 2" x 5", 6 lb
N-37	Cylinder, 1' long x 1" dia.
N-38	Reflector sector, 4" x 5" x 15", 15 lb
N-39	Reflector sector, 4" x 5" x 18", 32 lb
N-40	Reflector sector, 4" x 5" x 15", 31 lb
N-41	Control rod section, 14" long, 9 lb
N-42	Furnace for fuel sample, 4" x 4" x 7", two cable connectors
T-1	Beryllium piece, 4" x 4" x 18"
T-2	Control rod section, 10 lb
T-3	Beryllium, 1' x 4" x 4"
T-4	Not marked recognizably

TABLE 4-6, continued

LOCATION	DESCRIPTION
T-5	Beryllium piece, 1' x 4" x 4"
T-6	Beryllium piece, 1' x 4" x 4"
T-7	Belly band segment, 6' arc 6' x 1" x 6"
T-8	Aluminum angle, 2-1/2' x 1-1/2" x 1-1/2"
T-9	Aluminum angle, 4' x 1-1/2" x 1-1/2"
T-10	Mirror fixture
T-11	Mirror fixture
T-12	Beryllium piece, 4" x 4" x 8", 9 lb
T-13	Pressure vessel section, 2' x 2'
T-14	Beryllium piece, 1' x 4" x 4"
T-15	Metal angle, 2' x 2" x 4"
T-16	Metal angle, 2' x 2" x 4"
T-17	Belly band segment
T-18	Mirror frame
T-19	Beryllium piece, 2' x 4" x 4", 32 lb
T-20	Band from pressure vessel 2" x 6" x 18" Sixth clamp band segment, 17 lb
T-21	Graphite reflector cylinder sector, 1-1/2 lb
T-22	Beryllium reflector sector, 4" x 4" x 8"
T-23	Beryllium reflector sector, 4" x 4" x 8", 6 lb
T-24	Beryllium reflector sector, 4" x 4" x 8", 6 lb
T-25	Beryllium reflector sector, 4" x 4" x 6"
T-26	Pressure vessel section, 4' x 4', red check with some blue
Z-1	Pressure vessel section, 3' x 8"
Z-2	Slat section, 2" x 10"
Z-3	Control rod section 1' long
Z-4	Lead tube, 6" dia. x 6" long
Z-5	Aluminum tubing, 5" long x 6" dia.
Z-6	Reflector sector, 6" x 6"
Z-7	Graphite reflector sector, 1" x 2" x 8"
Z-8	Steel rod, 2 pieces, 1' long x 1/2" dia.; 1' long x 1" dia.
Z-9	Graphite reflector cylinder sector, 2" x 2" x 8"
Z-10	Pressure vessel section, 1" x 30", green

LOCATION	DESCRIPTION
Z-11	Steel rod, 1/2" dia. x 6" long
Z-12	Control rod section, 1' long
Z-13	Reflector sector, 5" x 6" x 8"
Z-14	Pressure vessel section, 2' x 6", blue
Z-15	Pressure vessel band, 6" x 6" x 10" 6 lb, green
Z-16	Control rod section, 14" long, 9 lb
Z-17	Reflector sector, 6" x 6" x 15" 20 lb
Z-18	Aluminum angle, 1" x 1" x 18" long
Z-19	Aluminum angle, 3' long x 1" x 1"
Z-20	Pressure vessel section, 6" x 6", 1-3/4 lb, green
Z-21	Reflector sector, 1' x 5" x 6"
Z-22	Pressure vessel section, 3' x 3', 148 lb green blue
Z-23	Reflector sector, 5" x 8" x 14", 17 lb
Z-24	Pressure vessel section, 14" x 15", green
Z-25	Reflector sector, 6" x 6" x 20", 21 lb
Z-26	Control rod section, 15" long
Z-27	Reflector sector, 6" x 6" x 15", 28 lb
Z-28	Reflector sector, 5" x 5" x 8", 10 lb
Z-29	Reflector sector, 5" x 5" x 8"
Z-30	Reflector sector, 4" x 4" x 4"
Z-31	Reflector sector, 2' x 6" x 6", 34 lb
Z-32	Control rod section, 1' long, 9 lb
Z-33	Control rod section, 1' long, 9 lb
Z-34	Reflector sector, 1' x 6" x 6", 15 lb
Z-35	Pipe, 2" dia. with cable boss

DEBRIS SAMPLES NOT IDENTIFIED BY NUMBERS

Angle, °	Distance, ft	Description
0	1400	Control drum section, 9 lb
325	700	Control drum section, 9 lb
286	1450	Beryllium reflector sector, 21 lb
	1500	Control drum section, 9 lb
235	2000	Control drum section, 9 lb
310	1300	Beryllium reflector sector, 23 lb
278	1500	Beryllium reflector sector, 33 lb
180-225	1750-2000	Beryllium reflector sector, 32 lb
180-225	1750-2000	Control drum section, 9 lb
225-270	1750-2000	Control drum section, 9 lb
225-270	400-450	Control drum section, 9 lb
225-270	450-500	Control drum section, 9 lb
180-225	1500-1750	Pressure vessel section, 98 lb
90-135	1500	Control drum section, 9 lb
50	1950	Control drum section, 9 lb
120	2300	Control drum section, 9 lb
180-225	1500-1750	Control drum section, 9 lb
322	600	Beryllium reflector sector, 13 lb
30	1350	Beryllium reflector sector, 32 lb
225-270	1500-1756	Control drum section, 9 lb

UNCLASSIFIED

APPROVED FOR PUBLIC RELEASE

is plotted in Figure 4-27 which shows the center of the site; Figures 4-28, 4-29, 4-30, and 4-31 show the surrounding quadrants.

The heaviest piece found was a portion of pressure vessel approximately three feet square and weighing 148 pounds. It was located 750 feet east of the reactor on the railroad track. Another piece of pressure vessel weighing 98 pounds was found between 180° and 225° at 1500 to 1750 feet. A number of pieces weighing a few pounds were found between 2000 and 2500 feet from the reactor. About 90% of the beryllium control drums were found in pieces a foot or so long and weighing approximately nine pounds each. The recovered pressure vessel fragments are shown in Figure 4-32.

Cleanup of the area was performed by segments, and debris picked up was marked to identify the angle and distance of its location. After the activity of the recovered debris had subsided, it was examined to check preliminary identifications, and some of the pieces were weighed. Some external samples which had previously been overlooked were identified.

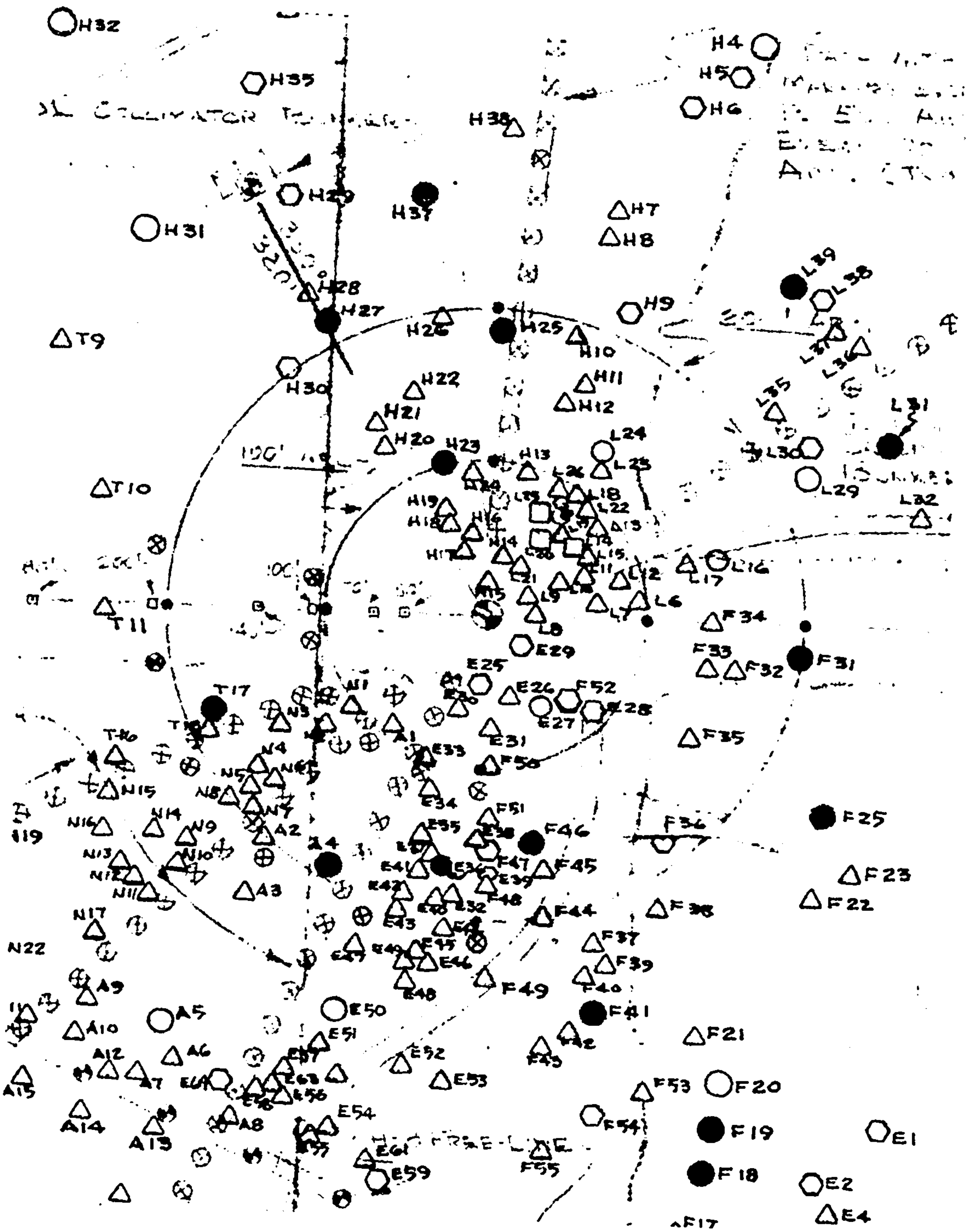

Figure 4-27. Debris Map, Central Area

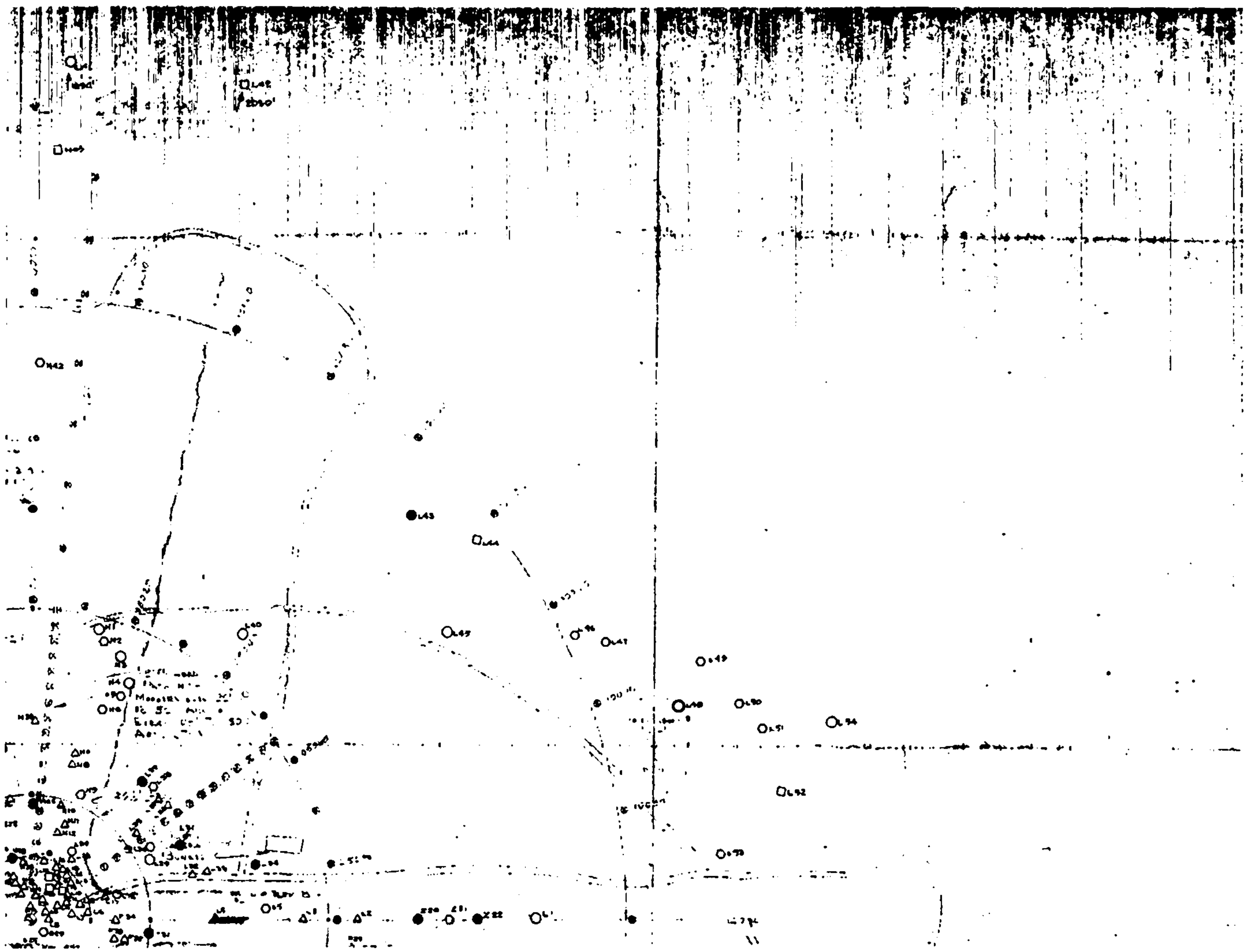

Figure 4-28. Debris Map, First Quadrant

[redacted]

[redacted]

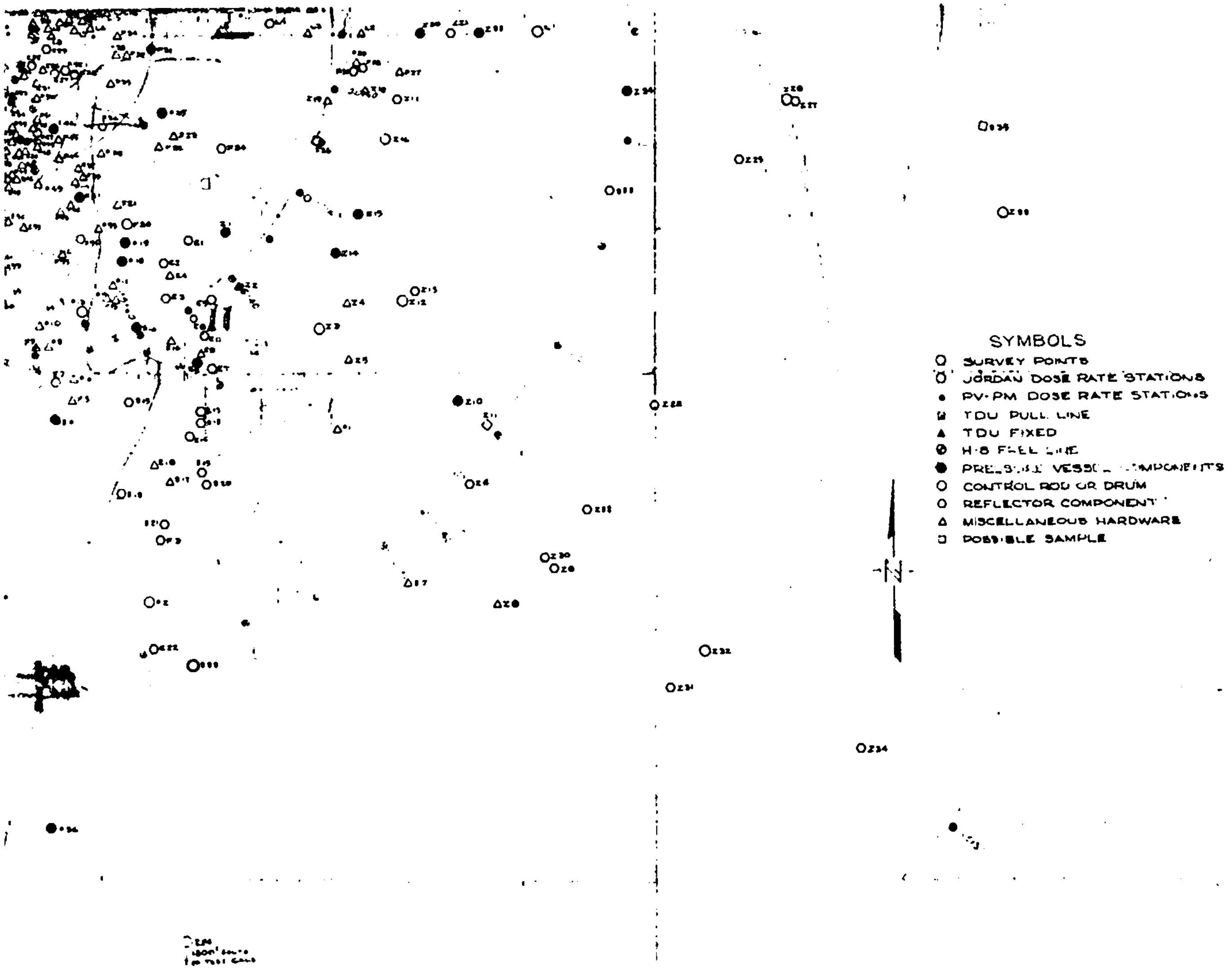

Figure 4-29. Debris Map, Second Quadrant

Figure 4-30. Debris Map, Third Quadrant

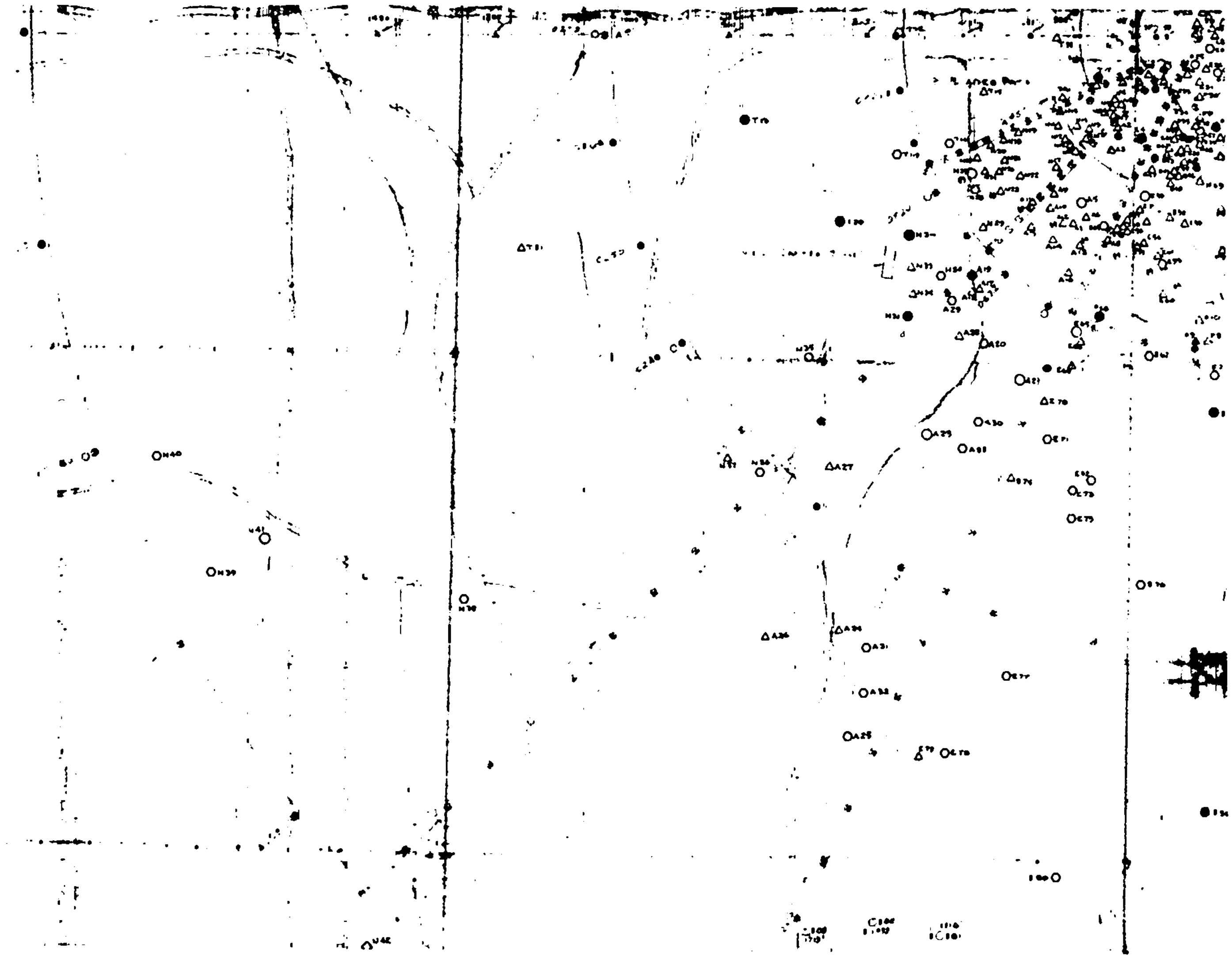

Figure 4-31. Debris Map, Fourth Quadrant

UNCLASSIFIED

APPROVED FOR PUBLIC RELEASE

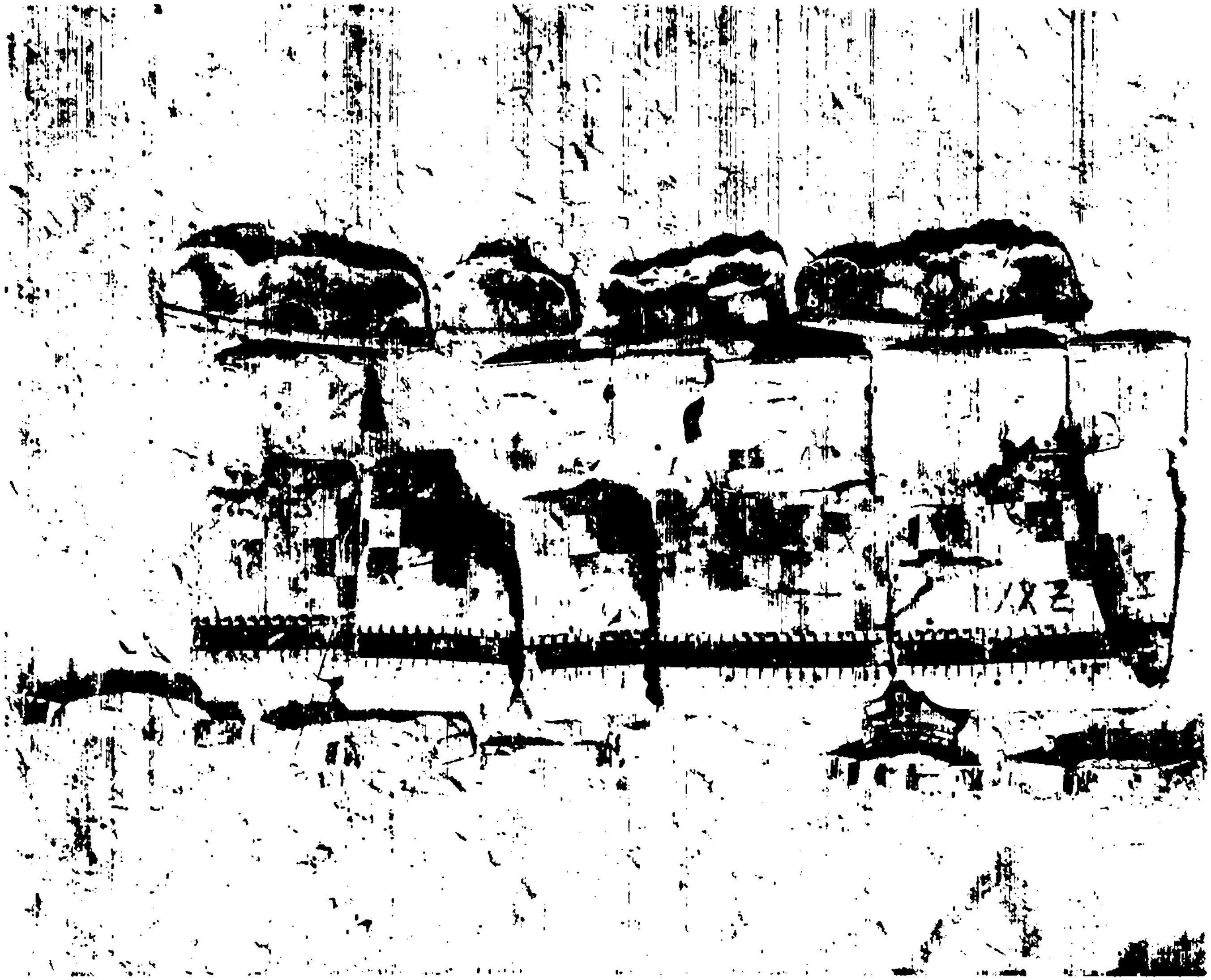

Figure 4-32. Fragments of Pressure Shell

Chapter 5

ADDITIONAL EXTERNAL EXPERIMENTS

A. Why the Auxiliary Experiments?

The Kiwi-TNT experiment was expected to provide an external flux of a magnitude and character which was unobtainable by any other means. It therefore seemed desirable to do a number of experiments which would extend the knowledge of fuel damage into a hitherto unknown region. Many external fuel samples from the LASL and other invited organizations were included.

Since results of the primary Transient Nuclear Test would show only what happens to a specific type of Rover fuel material, it was felt that a better understanding of the mechanism of fuel breakup might be obtained if a number of experiments were carried out which used various fuel modifications.[14] This would not only refine the input data for calculations used in predicting the behavior of nuclear transients in Rover type reactors,[15] but would also contribute to an understanding of the fuel breakup mechanism of interest to ultimate reactor disposal in space.[3]

B. Pre-TNT

In connection with fuel fragmentation studies, there were several preliminary experiments in 1963 and 1964. Small samples of Rover type fuel were irradiated during transients in the following reactors: TREAT (assisted by Argonne National Laboratory at National Reactor Testing Station, Idaho), SPERT-1 and SNAPTRAN 2/10A-3 (assisted by Phillips Petroleum Company at National Reactor Testing Station, Idaho), and TRIGA (a General Atomics reactor, assisted by U. S. Naval Radiological Defense Laboratory). Another irradiation was made during ALVA, an underground bomb test in Nevada.

The first significant result was obtained in the SNAPTRAN 2/10A-3 test. This indicated that there was significant matrix damage if the fuel sample underwent at least 10^{15} fissions per gram U-235 during a transient whose period was about 0.7 millisecond.

C. Preparations for Kiwi-TNT

1. Shock Tests

It had been calculated[16] that velocities of pieces of beryllium reflector and aluminum pressure vessel thrown from the TNT might be like 1000 feet per second, and there was concern about the survivability of samples in capsules. Several tests[17] were performed to study and improve the chance of recovery.

Initially, two proposed capsule designs, with dummy graphite samples, were impacted by an aluminum projectile from a propellant-fired cannon. The capsules were severely damaged and the samples were shattered.

It was then suggested that a foamed Adiprene (a synthetic rubber-like material containing C 63.3 w/o, H 9.3 w/o, N 4/23 w/o, and O 23.17 w/o, of about 20 pounds per cubic foot density) could be used to shock-mount small capsules. The stresses on a capsule were simulated by setting three dummy capsules into a 4-inch-diameter cylinder of the Adiprene, and firing the assembly out of a gun so as to accelerate it to 1000 feet per second in a distance of about 28 inches. The samples survived, and the mounting material was adapted to the Group N-1 and N-2 experiments in the TNT.

2. Flux Calculations and Measurements

Machine calculations[18] gave an average value of the flux expected at the surface of the reactor pressure vessel. Measurements at the Pajarito critical assembly facility indicated the relative drop-off of the flux in air, and the nuclear effect of the Adiprene shock-mounting material.

Figure 5-1 is a plot of flux versus distance from the pressure vessel, adjusted to an excursion of 3.1×10^{20} total fissions. The bar values are those measured by radiochemistry[5] of actual samples (which were mounted in Adiprene) in the TNT. The solid line represents average values for samples mounted in Adiprene. Note that relative to its value in air, the flux is enhanced by the Adiprene at close-in positions (by scattering and thermalization of the neutrons) and farther away it is attenuated. The dashed line represents the value of flux in air, as determined by relative measurements at Pajarito. All these values hold only on a radial line midway between control rods and axially at the core centerline. The TNT samples were positioned this way. There is a large radial

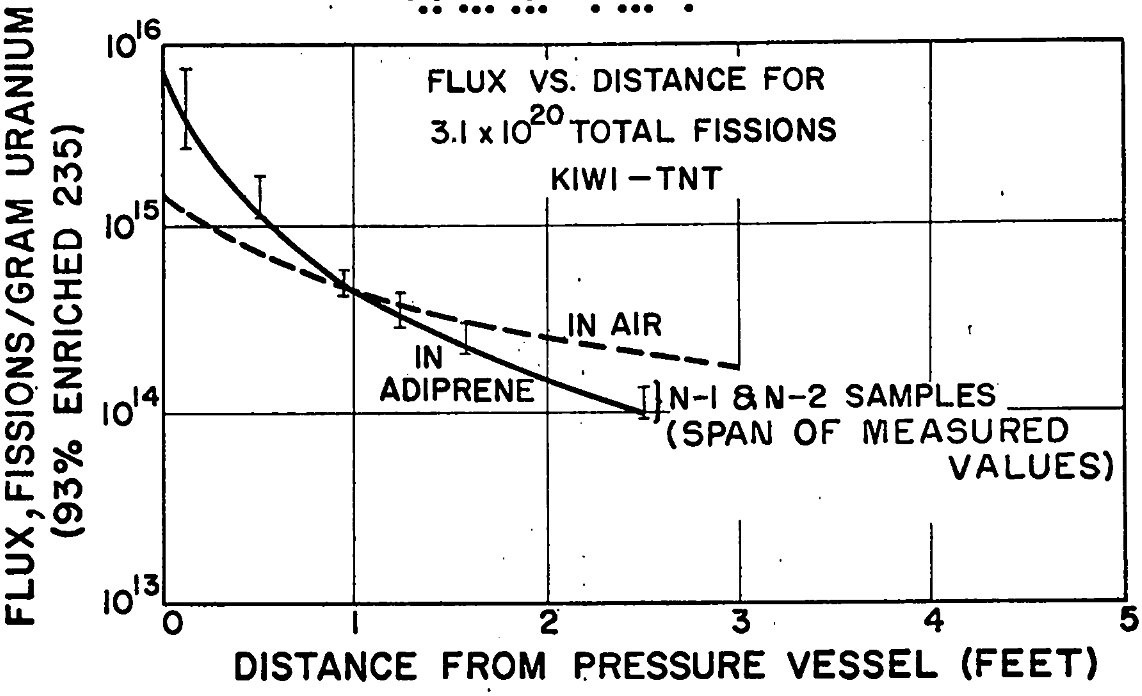

Figure 5-1

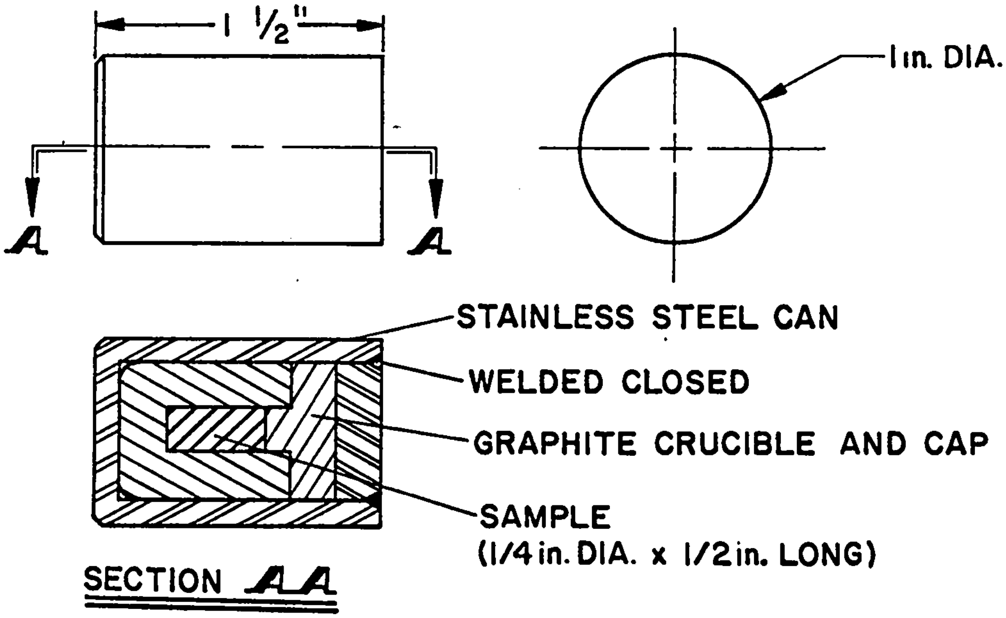

N-2 CAPSULE DESIGN

Figure 5-2

variation (because of shielding by the poison material in the control rods) and a smaller axial variation.

D. Rover-Connected Capsule Experiments

1. General

The Director of Rover Flight Safety asked that the following parameters be studied for their effect on breakup of fuel during the TNT-type transient: bead size, pyrocoat thickness, temperature, and previous irradiation. It was further planned to study the temperature history of individual fuel beads with miniature thermocouples. A positive radiochemical measurement of the reactor fission yield was also needed.

2. The Group N-2 Experiment

The pre-TNT and other preliminary work for the Kiwi-TNT external experiments had been done with the aid of Group N-2. In number of samples, the largest experiment in the TNT was performed by this group. Samples of 20 variations of fuel (Figure 5-5) were placed at each of four general flux positions to cover a range from the maximum available down to a value overlapping with the SNAPTRAN experiment. These fluxes and positions are indicated by the bar values on Figure 5-1.

Figure 5-2 is a drawing of the capsule used. The photograph, Figure 5-3, shows the capsule and a typical block of Adiprene, and Figure 5-4 shows the setup in place next to the reactor.

Detailed results have been reported in several papers. In general, there were the following observations: (1) the most significant parameter was fissions per gram of uranium, (2) at higher fluxes, samples with larger volume percent of particles showed more matrix damage, (3) particles with larger cores are damaged somewhat more easily than those with smaller cores, (4) particles with thicker coatings showed slightly less damage under similar flux conditions, and (5) preirradiation in a full-power, full-duration run (Kiwi-B-4A) caused no observable difference in breakup.

Samples were studied in the following ways: (1) visually at low magnification - to look at gross matrix damage; (2) metallographically - to look at migration of particle core material, coating ruptures, details of matrix ruptures, and resultant expulsion of core material; (3) by microradiography and autoradiography - confirming and extending the information from metallography; and (4) by radiochemistry - for relative gamma activity of all samples, and complete analysis of a few to determine the absolute activity -

[redacted]

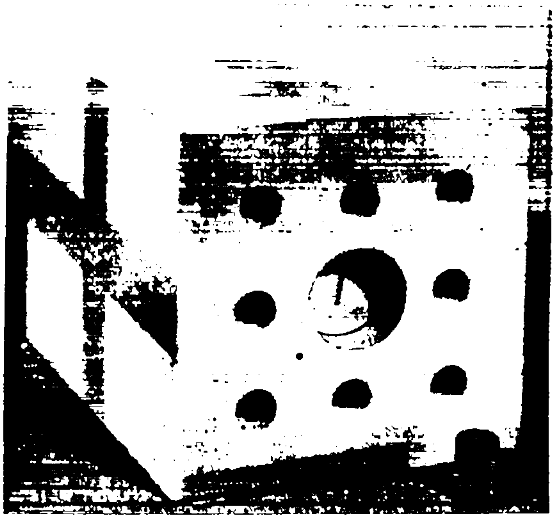

Figure 5-3
Eight N-2 capsules and one Phillips capsule in a typical block of foamed Adiprene

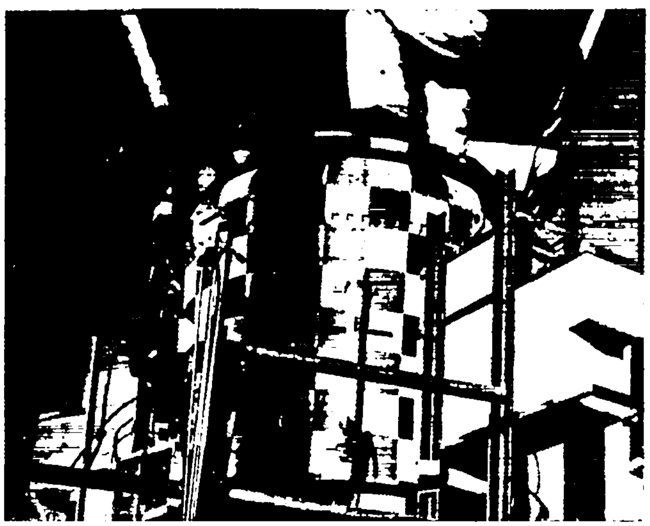

Figure 5-4
Blocks of Adiprene containing the N-2 and Phillips capsules mounted next to the reactor

[redacted]

Sample No.	Core Mat'l / Preparation	Core Dia. (microns)	Coating Thickness (microns)	U-235 Loading mg/cc	Particle Volume Loading %	-1 $5X10^{15}$ Nom. Flux Group f/g U (93% U-235)	-1 Matrix Damage	-1 Particle Damage	-2 $1.5X10^{15}$ Nom. Flux Group f/g U (93% U-235)	-2 Matrix Damage	-2 Particle Damage	-3 $5X10^{14}$ Nom. Flux Group f/g U (93% U-235)	-3 Matrix Damage	-3 Particle Damage	-4 $3X10^{14}$ Nom. Flux Group f/g U (93% U-235)	-4 Matrix Damage	-4 Particle Damage
1	UC_2 Extruded	62-105	50	250	33	$4.0 X 10^{15}$	1	1	$1.3 X 10^{15}$	3	3	$4.9 X 10^{14}$	4	3-4	$3.7 X 10^{14}$	4	5
2	UC_2 Pressed	62-105	100	182	52	$4.5 X 10^{15}$	1	1	$1.2 X 10^{15}$	1	2	$4.7 X 10^{14}$	4	4	$3.1 X 10^{14}$	4	5
3	UC_2 E	105-149	50	259	19	Not Recovered			$1.2 X 10^{15}$	3	2	$4.8 X 10^{14}$	4	3	$3.0 X 10^{14}$	4	4-5
4	UC_2 E	105-149	Duplex 50	250	15	$5.0 X 10^{15}$	1	1	$1.6 X 10^{15}$	2	2	NR			$3.1 X 10^{14}$	4	5
5	UC_2 E	105-149	100	249	47	$4.9 X 10^{15}$	1	1	NR			$4.8 X 10^{14}$	4	5	$3.1 X 10^{14}$	4	5
6	UC_2 E	210-297	25	262	4.8	$4.2 X 10^{15}$	1	1	$1.7 X 10^{15}$	2	1-2	$6.2 X 10^{14}$	4	3	NR		
7	UC_2 E	210-297	50	261	7.3	$4.6 X 10^{15}$	2	1	$1.8 X 10^{15}$	2	1-2	$6.2 X 10^{14}$	3	3	$3.2 X 10^{14}$	3	3-4
8	UO_2 E	210-297	100	256	16.9	NR			$1.7 X 10^{15}$	2	1-2	$5.7 X 10^{14}$	3	3	$3.0 X 10^{14}$	3	3-4
9	UC_2 E	50-150	25	254	8.9	$5.9 X 10^{15}$	1	(Dissolved for radch)	NR			$6.0 X 10^{14}$	3	3	$3.00 X 10^{14}$ Dissolved for Radiochemistry		
10	D-38 E	50-150	25	253	8.1	NR			NR			—	4	6	—	4	6
11	UC_2 E	50-150	25	256	7.1	$5.0 X 10^{15}$	1	1	$1.6 X 10^{15}$	3	2	$5.7 X 10^{14}$	3	3-4	$2.73 X 10^{14}$ Dissolved for Radiochemistry		
12	UC_2 E	50-150	Duplex 25	254	11.5	NR			NR			NR			$2.6 X 10^{14}$	4	5
13	UC_2 E	100-150	Duplex 25	253	8.6	$4.2 X 10^{15}$	1	1	NR			$4.0 X 10^{14}$	3	3-4	NR		
14	UC_2 E	50-150	25	253	8.5	NR			$1.7 X 10^{15}$	3	2	NR			$2.2 X 10^{14}$	4	5
15	UC_2 E	20-30	34	27	14.1	$7.4 X 10^{15}$	4	3	$2.0 X 10^{15}$	4	4	NR			$2.2 X 10^{14}$	4	5-6
16	UO_2 E	127	40	261	13.5	No Sample			NS			$4.7 X 10^{14}$	3	3	$1.3 X 10^{14}$	4	5
17	UO_2 E	125	24	258	7.7	NS			NS			$4.2 X 10^{14}$	3	3	$1.1 X 10^{14}$	4	5
18	UO_2 E	125	41	260	12.1	NS			NS			$3.3 X 10^{14}$	3	3	$1.0 X 10^{14}$	4	5
19	UO_2 E	125	57	257	19.0	NS			NS			$3.0 X 10^{14}$	3	3	$1.0 X 10^{14}$	4	5
20	UC_2 E	50-150	25	258	8.5	$5.0 X 10^{15}$	1	1	NR			NR			$3.0 X 10^{14}$	4	5 "lost"

N-2 SAMPLES IN Kiwi-TNT

Figure 5-5. N-2 Samples in Kiwi-TNT

(adjusted for loss of fission products to the steel container) - stated in terms of fissions per gram of uranium (93% enriched U-235).

Figure 5-5 consolidates all these data. All samples were 0.25 inch in diameter x 0.50 inch long, with 0.1 inch diameter hole. All were extruded except type 2. The particle volume loading is the percent of total volume of material occupied by particles (core plus coating). In the block for each sample is given the value of flux (fissions per gram uranium (93% enriched U-235)) as determined by gamma count and radiochemical analysis.

The sketch at the left of each block pictures the condition of sample <u>matrix</u> as removed from its capsule. Photographs in Figure 5-6 show four typical matrix damage categories; sample porous or powdered, major cracks, minor cracks, and like new.

The sketch at the right of each block pictures the condition of <u>particles</u> as examined by metallography, micro- and autoradiography. Photographs in Figure 5-7 show six typical particle damage categories: (1) particles completely destroyed, uranium distributed, matrix shattered, (2) particles all broken, associated matrix cracks, uranium distributed, (3) particles cracked, associated matrix cracks, uranium along cracks, (4) no macroscopic matrix damage, broken particles, most uranium in particles, (5) no macroscopic or microscopic matrix damage, some coating remained, cores melted, and (6) no observable change in matrix or particles.

3. The Group N-1 Experiment

In order to study the effect on fuel breakup of a temperature, representing "after-heat" in an orbiting reactor, N-1 was asked to prepare samples which would be at elevated temperatures at the time of the transient. Miniature shock-mounted furnaces powered by automotive-type batteries were used. Figure 5-8 is a photograph of a furnace, and Figure 5-9 shows six of them mounted next to the reactor. Two furnaces (one heated just prior to the excursion to 2100°C and one to 2400°C) were placed at each of three different flux regions. The samples themselves were identical to one of the types in the N-2 experiment, and post-test examinations were conducted together.

The conclusion was that there is no significant change in damage due to an initial temperature of the sample[19] that is higher than ambient. The heated samples appeared to suffer only slightly more damage under similar flux conditions. Detailed results are included in References 3 and 14.

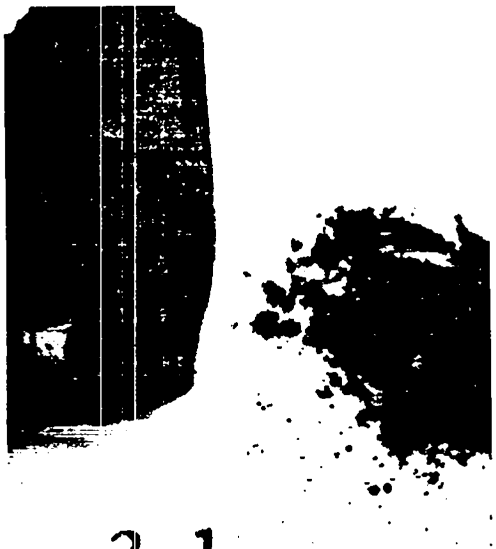

1. Powdered or Porous

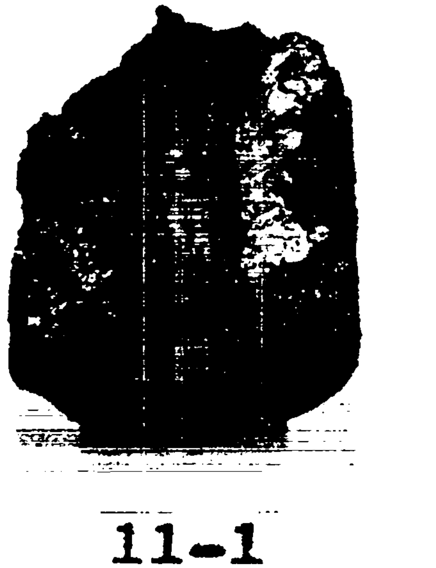

2. Major Cracks

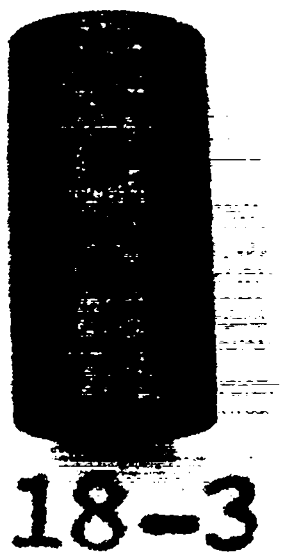

3. Minor Cracks

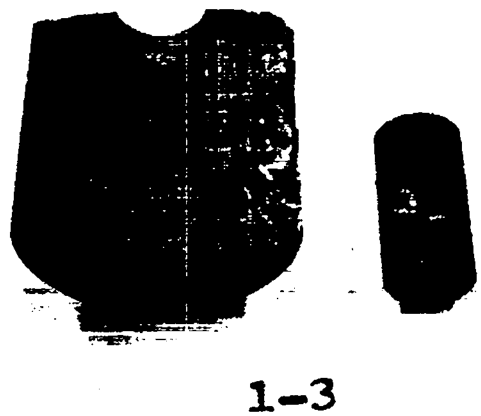

4. Like New

Figure 5-6. Typical Matrix Damage Categories

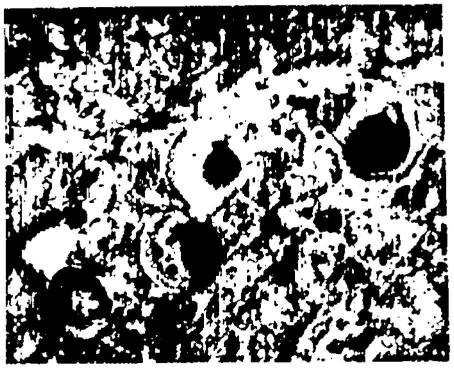

1. Completely destroyed

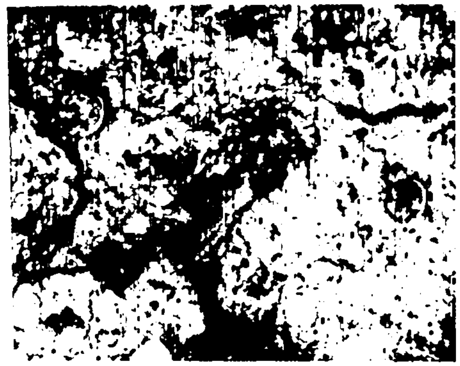

2. All broken

3. Badly cracked

4. Cracked

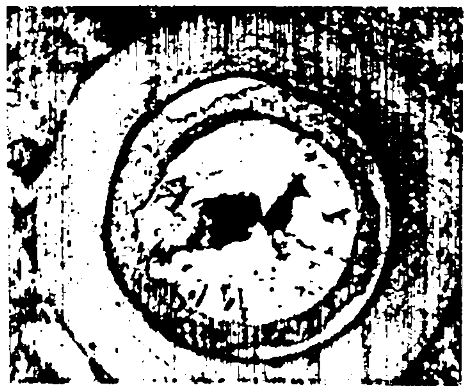

5. Cores melted

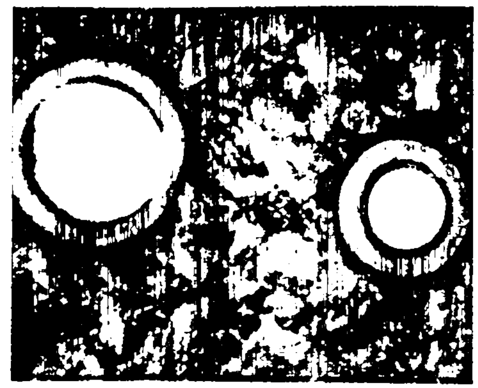

6. No change

Figure 5-7. Typical Particle Damage Categories

UNCLASSIFIED

APPROVED FOR PUBLIC RELEASE

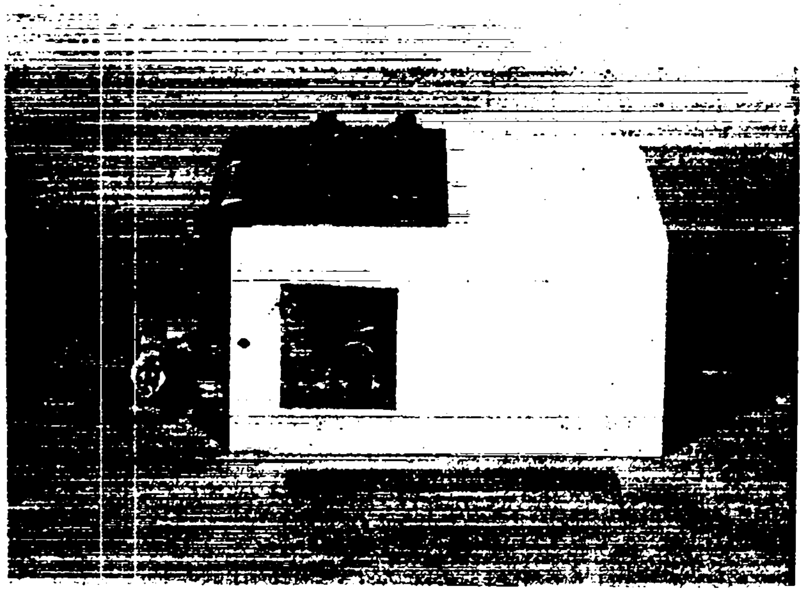

Figure 5-8
The N-1
Miniature Furnace

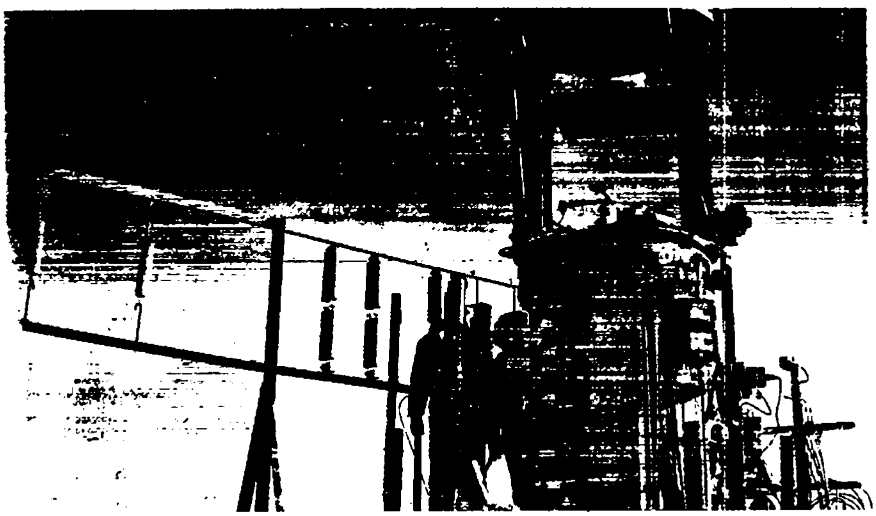

Figure 5-9

At right, six N-1 furnaces in Adiprene blocks mounted next to the reactor

At left, 24 Argonne capsules spaced out on hangers to provide wide range of flux

[redacted]

4. The Group J-8 Experiment[20]

Tiny thermocouples were placed on several individual beads with different coating thicknesses for the purpose of describing the time lag required for the heat generated in the core to travel through the pyrolytic-graphite coating. This information is to be used in refining calculations intended to understand and describe the detailed physical processes involved in deliberate and accidental nuclear excursions.

5. The Group J-11 Experiment

Three identical capsules containing depleted uranium foils were placed in the same position as similar detectors on previous Kiwi power runs. The analysis by radiochemistry of these foils assisted in evaluating the total yield of the Kiwi-TNT excursion,[5] 3.1 (±0.3) $\times 10^{20}$ fissions.

E. Non-Rover Experiments

1. General

The TNT excursion provided a unique source of neutrons which was utilized by several other groups within the LASL and other organizations. The wide distribution of participants is indicated on the map in Figure 5-10. The possibility of interference with the primary experiment, however, dictated that these be kept to a manageable number.

2. The Group K-4 Experiment

Samples of fuel for the UHTREX reactor were irradiated. The flux positions chosen for their four capsules were much lower than those in the Kiwi-type samples, but higher than those expected in a maximum credible accident in the UHTREX. Fuel damage and other observations have been reported.[21]

3. The Group J-12 Experiment

In cooperation with the U. S. Nuclear Defense Laboratory, Edgewood Arsenal, Maryland; Harry Diamond Laboratory, Washington, D. C.; and ELRDL, Fort Monmouth, N. J.; this group conducted neutron and gamma spectral and flux measurements.[22]

4. The Aerojet General Corporation Experiment

Eighteen capsules, each containing 3.6 gram samples of high explosive or propellant considered for use on the NERVA destruct

[redacted]

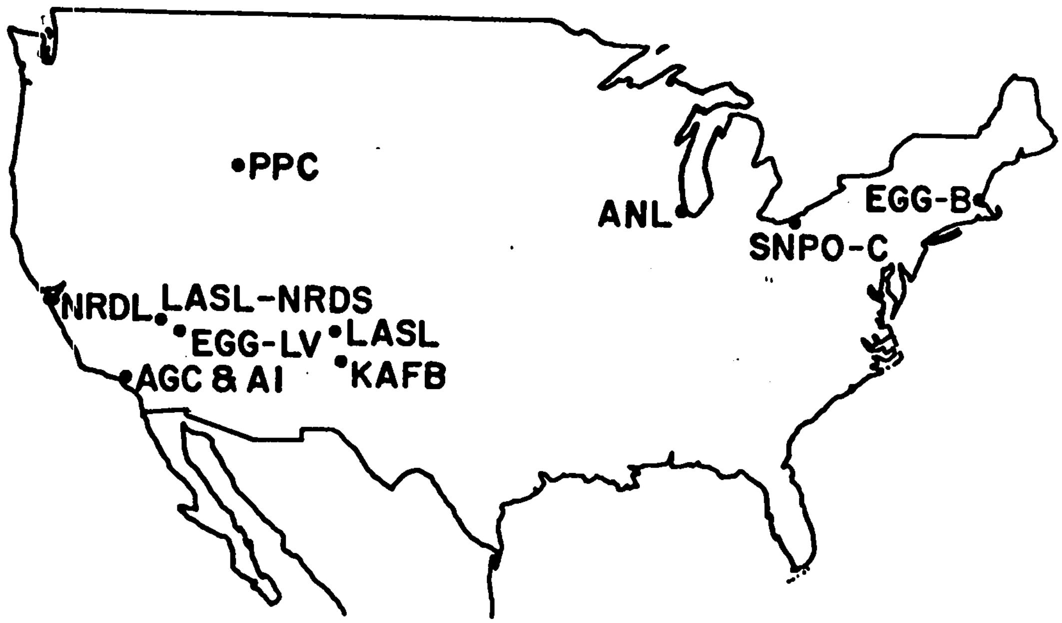

LASL GROUPS (EXPERIMENTERS)
- N-1
- N-2
- K-4
- J-8
- J-11
- J-12
- J-18

LASL (SERVICE GROUPS)
- H-3
- H-8
- GMX-1
- GMX-3
- GMX-6
- J-9
- J-17

OTHER EXPERIMENTERS

AGC-AZUSA, CALIF.
DOWNEY, CALIF.
SNPO-CLEVELAND, O.

ANL-ARGONNE, ILL.

AI-CANOGA PARK, CALIF.
EGG-BOSTON, MASS.
LAS VEGAS, NEV.

KAFB-ALBUQUERQUE, N.M.

PPC-IDAHO FALLS, IDAHO

US NRDL-SAN FRANCISCO, CALIF.

Figure 5-10. Kiwi-TNT Auxiliary External Experiments

[redacted]

system, were irradiated; and those samples recovered were tested for radiation effects. No significant changes were noted.[23]

5. The Argonne National Laboratory Experiment

Fuels from four typical power reactors were irradiated in an extension of a large evaluation program of that Laboratory. The transient meltdown behavior in water of typical reactor fuels is being investigated as part of a program on nuclear reactor safety. The fuel types were: (1) Zr-2 clad UO_2 core pellets, (2) SS-304 clad UO_2 core pellets, (3) uranium-zirconium alloy pins, and (4) aluminum-uranium alloy plates. Results have been described in a paper[24] presented at the ANS Gatlinburg Meeting.

The recovery record (23 out of 24) for these capsules was good. Figure 5-9 shows them installed around the reactor.

6. The Atomics International Experiment

The SNAPTRAN program was supplemented by an irradiation of 32 fuel samples from the SNAP-10 reactor. Edgerton, Germeshausen & Grier assisted in this program. Results were reported at the ANS Gatlinburg Meeting.[25]

7. The Kirtland Air Force Base Experiment

The Air Force Weapons Laboratory (Biophysics Branch) conducted an experiment to evaluate collection and radiochemistry characteristics of a newly developed filter medium consisting of a rayon prefilter, for particulate collection, backed by carbon fibers for iodine retention.

Fourteen filters were mounted on Staplex air samplers and exposed approximately 4,000 feet downwind from the excursion site. Eight of these were new filter material, four were MSA 1106B fiberglass filters, and two were BM 2133 carbon-impregnated cellulose dust filters. Analyses were performed at Kirtland Air Force Base.[26]

8. The Phillips Petroleum Company Experiment

Samples of fuel for a proposed Power Burst Facility were irradiated at and beyond the flux expected in that reactor. The pressure generated by vaporizing fuel was evaluated for inclusion in their Safety Analysis Report.[27] All four of their capsules (2-1/2 inches in diameter x 9 inches long), which were shock-mounted, were recovered.

UNCLASSIFIED

[redacted]

APPROVED FOR PUBLIC RELEASE

[redacted]

9. <u>The U. S. Naval Radiological Defense Laboratory Experiment</u>

Under a contract with the Atomic Energy Commission, this Laboratory is studying the chemical reaction between fission products and sea water.[28] Beaded Rover type fuel was used. Probably due to the very large size, their capsules were severely damaged, reducing the amount of data gathered. One of three capsules was not found.

F. <u>Test Operations</u>

1. <u>Installation</u>

The arrangement of capsules around the Kiwi-TNT reactor has been described in many phrases, from "Christmas tree ornaments" to "a motley array of test objects." (See photo, Figure 5-9).

Several considerations suggested the final installation. Among them were: (1) to obtain maximum possible flux, capsules were placed on radial lines between control rods; (2) the beryllium reflector was segmented on these same lines, so it was believed the location likely to give smallest damage by flying reflector and pressure vessel pieces; (3) all experimenters desired to have capsules at various flux levels; (4) the profile view seen by each camera bunker should be kept clear, so that movement of the pressure vessel might be observed; and (5) flimsy supports would allow capsules to be thrown away from the reactor with a minimum of damage.

The location of capsules is shown in Figure 5-11. Test site personnel fabricated the hanging equipment and placed the capsules around the reactor. Because there were freezing temperatures during the night, some capsules which contained water were installed the morning of the test.

2. <u>Recovery</u>

Since speculation about the condition of the reactor and the location of capsules after the test was so varied, it was essentially impossible to plan recovery operations in any detail. Recovery was done this way: (1) special early recovery teams entered the area within a few hours to bring out the Aerojet General capsules (project personnel believed that meaningful data required analysis within 24 hours), (2) routine recovery of all other capsules was carried out by reentry teams during the following week, and finally, (3) there was a complete cleanup of the area.

Test site personnel performed most of the recovery. They were furnished with a Recovery Notebook which included photos,

[redacted]

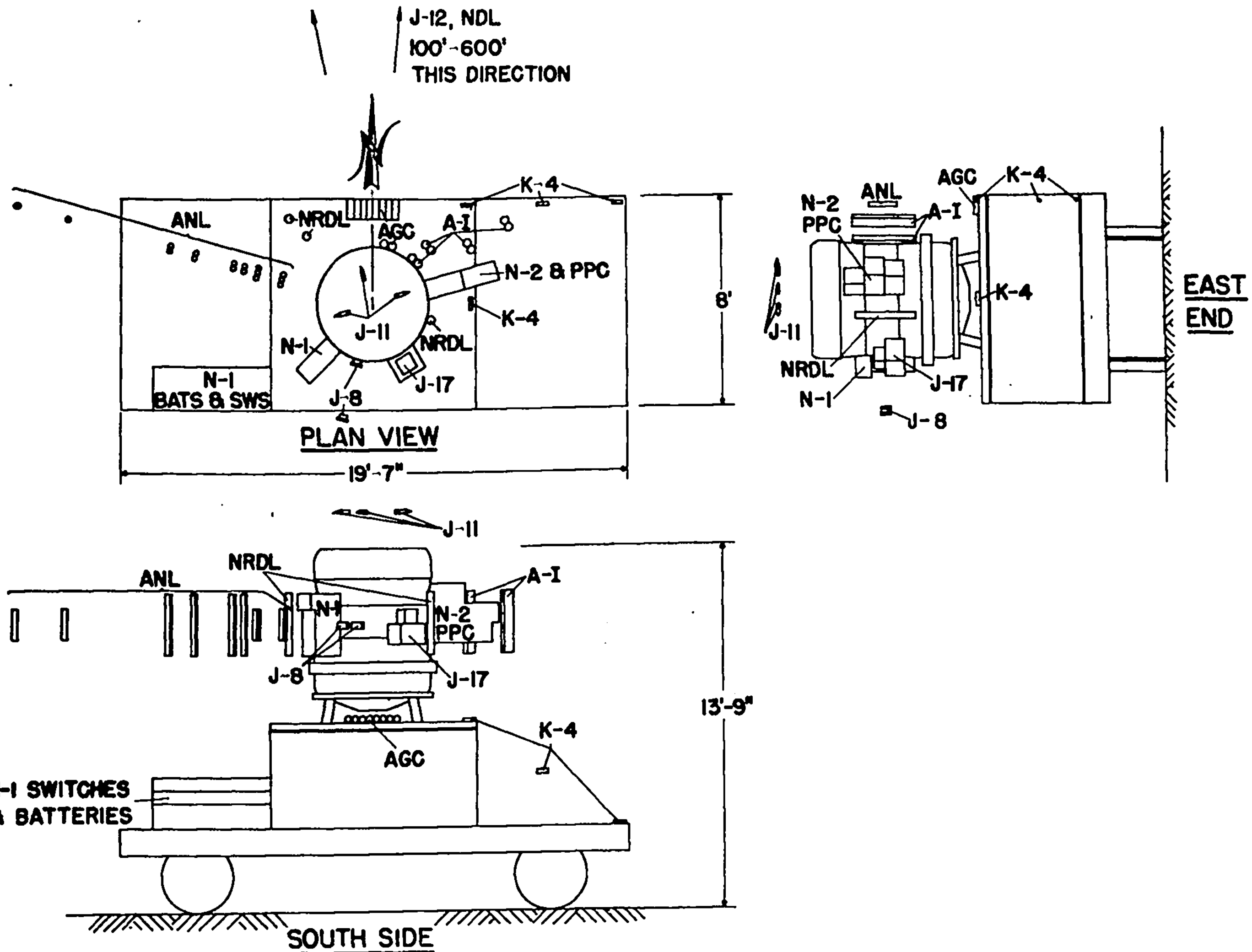

Figure 5-11. Location of Capsules

dimensional drawings, and a prediction as to the direction each group of capsules would be thrown.

After recovery from the test area, the capsules were decontaminated and shipped to their owners. Particularly, as the shipment of radioactive, contaminated material via commercial truck lines is not easy, assistance from test site personnel was invaluable.

A final tally of recovered capsules shows the following: N-2, 54 out of 72; N-1, 6 out of 6; J-8, not recoverable; J-11, 3 out of 3; K-4, 2 out of 4; J-12, all material recovered; Aerojet, 17 out of 18; Argonne, 23 out of 24; Atomics International, 24 out of 32; Kirtland, all material recovered; Phillips, 4 out of 4; and NRDL, 2 out of 3.

G. Suggestions for Possible Future Similar Tests

The N-2 capsules were so small that they were hard to find on the desert. (Most of them were torn from the Adiprene - possibly because it was shared with some much heavier capsules.) NRDL's were so large that they suffered excessive damage. The recovery record indicated clearly that an intermediate size of about 2-1/2 inches in diameter x 10 inches long, with 1/4 inch thick steel walls (similar to those used by Argonne, Phillips, and J-11), is better.

Although there is no conclusive evidence except that based on the sample shattering in the gun tests, it is felt that the shock-mounting was helpful.

The bright colors did not help in all cases. Most things were blackened by graphite deposits or burned by high temperature gases and fragments.

Mounting equipment should be kept as light as practical.

Since most of the rupture lines of the pressure vessel were between control rods, this appears to have been a good choice for the radial location.

It was believed necessary to keep a clear profile view of the reactor for the cameras, thus making some areas unavailable for locating capsules. However, since incandescent material streamed out of the pressure vessel fissures obscuring the camera's view of the profile, it seems that this restriction is no longer needed.

Anticipating that all large pieces thrown from the reactor would again be mapped as to their location in the field, it is suggested that external experiment capsules be included in this mapping.

[redacted]

Early recovery (the day of the test) should be discouraged, in favor of a more efficient, routine effort. One member of each re-entry team might have the duty of recording the location of all items retrieved.

Advance coordination with the road block operations and the decontamination facility is important.

It is desirable to have a representative at the site from each agency involved in the test who can make all arrangements for the return of radioactive materials to his own agency.

A pre-arranged schedule for the handling and examination of multiple samples after their return is advantageous.

[redacted]

References

1. AIAA Bulletin, May 1965 - Propulsion Joint Specialist Conference, June 14-18, 1965, "Kiwi Transient Nuclear Test," by C. A. Fenstermacher, L. D. P. King, and W. R. Stratton; and "Analysis of the Kiwi-TNT Experiment," by W. R. Stratton, C. A. Fenstermacher, and L. D. P. King, LASL.

2. Transactions American Nuclear Society, Vol. 8, #1, June 21-25, 1965.

   "Description of the Kiwi-TNT Excursion," by L. D. P. King, LASL.

   "Analysis of the Kiwi-TNT Experiment," by W. R. Stratton and D. M. Peterson, LASL.

   "Kiwi-TNT Evaluation of Environmental Effects," by H. S. Jordan, R. V. Fultyn, and R. W. Henderson, LASL.

   "Pin Technique for Displacement Measurements in Kiwi-TNT," by B. Washburn, LASL, and C. Hudson, EG&G.

3. LA-3535-MS, "The Self Destruct Concept for Post Operational Rover Reactor Disposal," by L. D. P. King, LASL.

4. LA-3358-MS, "Safety Neutronics for Rover Reactors," by L. D. P. King, LASL.

5. LA-3290, "Radiochemical Measurements on Kiwi-TNT," by E. A. Bryant, J. E. Sattizahn, and G. F. Wagner, LASL.

6. Report No. B-2991, "Brightness and Temperature Data on Rover/Nerva Transient Nuclear Test," by B. J. Constantine, EG&G.

7. Internal Laboratory document, "Analysis of Optical Records of Kiwi Transient Nuclear Test of January 12, 1965," by Kenneth B. Mitchell and Dale Sappenfield.

8. LA-3388-MS, "Pin Techniques for Displacement Measurements in Kiwi-TNT," by B. Washburn and C. E. Hudson; "Pin Technique for Displacement Measurements in Kiwi-TNT," Transactions of ANS Meeting, Gatlinburg, Tennessee, June 21-25, 1965.

[redacted]

9. LA-3304, "Integral Gamma and Neutron Measurements on Kiwi-TNT," by P. K. Lee and F. C. V. Worman, LASL.

10. LA-3446, "Gamma Dose Measurements - Kiwi Transient Nuclear Test," by Fred W. Sanders, LASL.

11. LA-3395-MS, "Radiation Measurements of the Effluent from the Kiwi-TNT Experiment," by R. W. Henderson and R. V. Fultyn, LASL.

12. LA-3449, "Environmental Effects of the Kiwi-TNT Effluent," by R. V. Fultyn, LASL.

13. LA-3337-MS, "Kiwi-TNT Particle Study," by Evan E. Campbell, LASL.

14. LA-3367, "The Behavior of Coated Particles in a Large Nuclear Transient (Kiwi-TNT)," by W. U. Geer, C. G. Hoffman, and J. F. Kerrisk, LASL.

15. LA-3115-MS, "NECKLACE, A Computer Program Concerning the Transient Temperature of Fissioning Spheres Imbedded in Graphite," by C. G. Chezem and W. R. Stratton, LASL.

    LAMS-2920, "RAC, A Computer Program for Reactor Accident Calculations," by C. G. Chezem and W. R. Stratton, LASL.

16. Internal Laboratory memo, "The Kiwi-TNT Experiment, Some Expected Results," L. D. P. King from W. R. Stratton, June 24, 1964.

17. Private communications, J. W. Taylor to W. U. Geer, LASL.

18. Internal Laboratory memo, "Neutron Fluxes Outside the Kiwi-TNT Reactor," L. D. P. King from G. A. Graves, June 26, 1964.

19. Private communications about work done by E. A. Bryant, LASL.

20. LA-3313-MS and Transactions American Nuclear Society, Vol. 8, #1, "Application of Miniature Intrinsic Thermocouples for Reactor-Transient Diagnostics," by Roderick G. Morrison; and LA-3470-MS, "Fission-Couples Applied Toward Reactor Diagnostics and Safety," by R. G. Morrison and D. B. Stillman, LASL.

21. Internal Laboratory report, "UHTREX Fuel Element Samples in Kiwi-TNT," by D. W. McEachern.

22. Reports POR-6100 through 6107, Defense Atomic Support Agency (DASA).

23. RN-S-0218, "Preliminary Test Report for Phase I-D (Kiwi-TNT) of the Countermeasures Radiation Effects Program," by W. D. Stinnet, REON Division of AGC.

[redacted]

24. Transactions American Nuclear Society, Vol. 8, #1, pp. 131-132, "Metal-Water Reactions Initiated by a Short-Period Nuclear Reactor Excursion (Kiwi-TNT)," by R. C. Liimatainen, Richard O. Ivins, and Frank J. Testa, ANL.

ANL-7055, "Argonne National Laboratory Chemical Engineering Division Semiannual Report," January-June 1965.

25. Transactions American Nuclear Society, Vol. 8, #1, pp. 130-131, "Measurements of Properties of Uranium-Zirconium Hydride Fuel in a Large Nuclear Transient (Kiwi-TNT)," by L. I. Moss and R. E. Forrester, AI, and W. T. Foreman, EG&G.

26. WL TDR 65-50, "Improvement of Medium Flow-Rate Filters," June 1965. (Describes the new filter and presents results of laboratory evaluations. For field-test results, contact the Biophysics Branch of AFWL, Kirtland AFB.)

27. IDO-technical report, "Quarterly Technical Report; Spert Project; April, May, June, 1965."

28. "Radionuclide Release from Aero-Space Nuclear Reactor Fuels. V. Phase Two: Pulsed Neutron Irradiation of Fuel in Water," by L. W. Weisbecker et al., to be published as U. S. Naval Radiological Defense Laboratory Technical Report.

29. LAMS-2710, Revised, "Project Rover Primary Radiological Safety Guide and Safety Analysis Report," January 31, 1964.